

Wavelet Score-Based Generative Modeling

Florentin Guth, Simon Coste, Valentin de Bortoli, Stéphane Mallat

▶ **To cite this version:**

Florentin Guth, Simon Coste, Valentin de Bortoli, Stéphane Mallat. Wavelet Score-Based Generative Modeling. 36th Conference on Neural Information Processing Systems (NeurIPS 2022)., Nov 2022, New Orleans (Louisiana), United States. hal-03959112

HAL Id: hal-03959112
https://hal.science/hal-03959112

Submitted on 27 Jan 2023

HAL is a multi-disciplinary open access archive for the deposit and dissemination of scientific research documents, whether they are published or not. The documents may come from teaching and research institutions in France or abroad, or from public or private research centers.

L'archive ouverte pluridisciplinaire **HAL**, est destinée au dépôt et à la diffusion de documents scientifiques de niveau recherche, publiés ou non, émanant des établissements d'enseignement et de recherche français ou étrangers, des laboratoires publics ou privés.



Distributed under a Creative Commons Attribution - NonCommercial - NoDerivatives 4.0 International License

Wavelet Score-Based Generative Modeling

Florentin Guth
Computer Science Department,
ENS, CNRS, PSL University

Simon Coste
Computer Science Department,
ENS, CNRS, PSL University

Valentin De Bortoli
Computer Science Department,
ENS, CNRS, PSL University

Stéphane Mallat
Collège de France, Paris, France
Flatiron Institute, New York, USA

Abstract

Score-based generative models (SGMs) synthesize new data samples from Gaussian white noise by running a time-reversed Stochastic Differential Equation (SDE) whose drift coefficient depends on some probabilistic score. The discretization of such SDEs typically requires a large number of time steps and hence a high computational cost. This is because of ill-conditioning properties of the score that we analyze mathematically. Previous approaches have relied on multiscale generation to considerably accelerate SGMs. We explain how this acceleration results from an implicit factorization of the data distribution into a product of conditional probabilities of wavelet coefficients across scales. The resulting Wavelet Score-based Generative Model (WSGM) synthesizes wavelet coefficients with the same number of time steps at all scales, and its time complexity therefore grows linearly with the image size. This is proved mathematically for Gaussian distributions, and shown numerically for physical processes at phase transition and natural image datasets.

1 Introduction

Score-based Generative Models (SGMs) have obtained remarkable results to learn and sample probability distributions of image and audio signals [44, 3, 24, 38, 39, 6]. They proceed as follows: the data distribution is mapped to a Gaussian white distribution by evolving along a Stochastic Differential Equation (SDE), which progressively adds noise to the data. The generation is implemented using the time-reversed SDE, which transforms a Gaussian white noise into a data sample. At each time step, it pushes samples along the gradient of the log probability, also called *score function*. This score is estimated by leveraging tools from score-matching and deep neural networks [13, 47]. At sampling time, the computational complexity is therefore proportional to the number of time steps, i.e., the number of forward network evaluations. Early SGMs in [44, 46, 11] used thousands of time steps, and hence had a limited applicability.

Diffusion models map a Gaussian white distribution into a highly complex data distribution. We thus expect that this process will require a large number of time steps. It then comes as a surprise that recent approaches have drastically reduced this time complexity. This is achieved by optimizing the discretization schedule or by modifying the original SGM formulation [18, 17, 27, 53, 42, 37, 43, 23, 11, 29, 41, 51]. High-quality score-based generative models have also been improved by cascading multiscale image generations [40, 12, 6] or with subspace decompositions [16]. We make explicit the reason of this improvement, which provably accelerates the sampling of SGMs.

A key idea is that typical high-dimensional probability distributions coming from physics or natural images have complex multiscale properties. They can be simplified by factorizing them as a product of conditional probabilities of normalized wavelet coefficients across scales, as shown in [33].

36th Conference on Neural Information Processing Systems (NeurIPS 2022).

These conditional probabilities are more similar to Gaussian white noise than the original image distribution, and can thus be sampled more efficiently. On the physics side, this observation is rooted in the renormalization group decomposition in statistical physics [49], and has been used to estimate physical energies from data [33]. In image processing, it relies on statistical observations of wavelet coefficient properties [48]. A Wavelet Score-based Generative Model (WSGM) generates normalized wavelet coefficients from coarse to fine scales, as illustrated in Figure 1. The conditional distribution of each set of wavelet coefficients, given coarse scale coefficients, is sampled with its own (conditional) SGM. The main result is that a normalization of wavelet coefficients allows fixing the same discretization schedule at all scales. Remarkably, and as opposed to existing algorithms, it implies that the total number of sampling iterations per image pixel does not depend on the image size.

After reviewing score-based generation models, Section 2 studies the mathematical properties of its time discretization, with a focus on Gaussian models and multiscale processes. Images and many physical processes are typically non-Gaussian, but do have a singular covariance with long- and short-range correlations. In Section 3, we review how to factorize these processes into probability distributions which capture interactions across scales by introducing orthogonal wavelet transforms. We shall prove that it allows considering SGMs with the same time schedule at all scales, independently of the image size. In Section 4, we present numerical results on Gaussian distributions, the φ^4 physical model at phase transition, and the CelebA-HQ image dataset [19]. The main contributions of the paper are as follows:

- A Wavelet Score-based Generative Model (WSGM) which generates samples from the conditional distribution of normalized wavelet coefficients, with the same discretization schedule at all scales. The number of time steps per image pixel does not need to depend upon the image size to reach a fixed error level.
- Theorems controlling errors of time discretizations of SGMs, proving accelerations obtained by scale separation with wavelets. These results are empirically verified by showing that WSGM provides an acceleration for the synthesis of physical processes at phase transition and natural image datasets.

2 Sampling and Discretization of Score-Based Generative Models

2.1 Score-Based Generative Models

Diffusions and time reversal A Score-based Generative Model (SGM) [44, 46, 11] progressively maps the distribution of data x into the normal distribution, with a forward Stochastic Differential Equation (SDE) which iteratively adds Gaussian white noise. It is associated with a *noising process* $(x_t)_t$, with x_0 distributed according to the data distribution p, and satisfying:

$$\mathrm{d}x_t = -x_t \mathrm{d}t + \sqrt{2}\mathrm{d}w_t, \tag{1}$$

where $(w_t)_t$ is a Brownian motion. The solution is an Ornstein-Uhlenbeck process which admits the following representation for any $t \geq 0$:

$$x_t = \mathrm{e}^{-t} x_0 + \sqrt{1 - \mathrm{e}^{-2t}} z, \qquad z \sim \mathcal{N}(0, \mathrm{Id}). \tag{2}$$

The process $(x_t)_t$ is therefore an interpolation between a data sample x_0 and Gaussian white noise. The *generative process* inverts (1). Under mild assumptions on p [2, 9], for any $T \geq 0$, the reverse-time process x_{T-t} satisfies:

$$\mathrm{d}x_{T-t} = \{x_{T-t} + 2\nabla \log p_{T-t}(x_{T-t})\}\, \mathrm{d}t + \sqrt{2}\, \mathrm{d}w_t, \tag{3}$$

where p_t is the probability density of x_t, and $\nabla \log p_t$ is called the *Stein score*. Since x_T is close to a white Gaussian random variable, one can approximately sample from x_T by sampling from the normal distribution. We can generate x_0 from x_T by solving this time-reversed SDE, if we can estimate an accurate approximation of the score $\nabla \log p_t$ at each time t, and if we can discretize the SDE without introducing large errors.

Efficient approximations of the Stein scores are the workhorse of SGM. [13] shows that the score $\nabla \log p_t$ can be approximated with parametric functions s_θ which minimize the so-called implicit

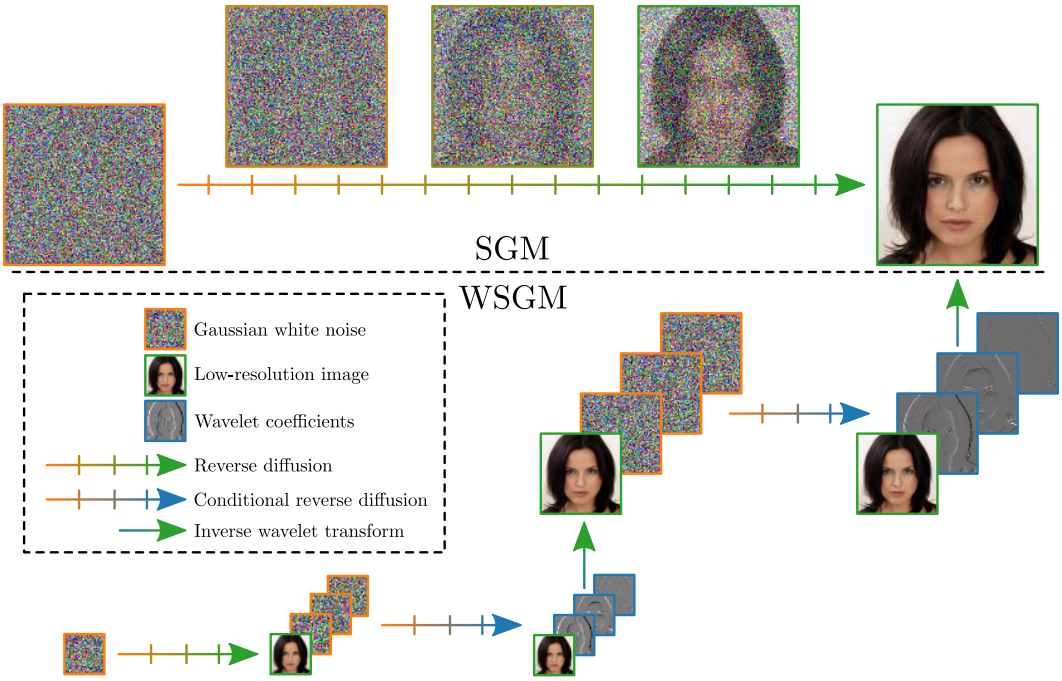


Figure 1: An SGM generates images by discretizing a reverse diffusion, which progressively transforms white Gaussian noise into a natural image. A WSGM generates increasingly higher-resolution images by discretizing reverse diffusions on wavelet coefficients at each scale. It begins by generating a first low-resolution image. Renormalized wavelet coefficients are then generated conditionally to this low-resolution image. A fast inverse wavelet transform reconstructs a higher-resolution image from these wavelet coefficients. This process is repeated at each scale. The number of steps is the same at each scale, and can be orders of magnitude smaller than for SGM.

score matching loss:

$$s_t = \arg\min_\theta \mathbb{E}_{p_t}\left[\frac{1}{2}\|s_\theta(x_t)\|^2 + \mathrm{div}(s_\theta)(x_t)\right], \tag{4}$$

or, equivalently, the denoising score matching loss:

$$s_t = \arg\min_\theta \mathbb{E}_{p_0,\mathcal{N}(0,\mathrm{Id})}\left[\|s_\theta(\mathrm{e}^{-t}x_0 + \sqrt{1-\mathrm{e}^{-2t}}z) + \frac{z}{\sqrt{1-\mathrm{e}^{-2t}}}\|^2\right]. \tag{5}$$

For image generation, s_θ is calculated by a neural network parameterized by θ. In statistical physics problems where the energy can be linearly expanded with coupling parameters, we obtain linear models $s_\theta(x) = \theta^\top \nabla U(x)$. This is the case for Gaussian processes where $U(x) = xx^\top$; it also applies to non-Gaussian processes, using non-quadratic terms in $U(x)$.

Time discretization of generation An approximation of the generative process (3) is computed by approximating $\nabla \log p_t$ by s_t and discretizing time. It amounts to approximating the time-reversed SDE by a Markov chain which is initialised by $\tilde{x}_T \sim \mathcal{N}(0, \mathrm{Id})$, and computed over times t_k which decrease from $t_N = T$ to $t_0 = 0$, at intervals $\delta_k = t_k - t_{k-1}$:

$$\tilde{x}_{t_{k-1}} = \tilde{x}_{t_k} + \delta_k\{\tilde{x}_{t_k} + 2s_{t_k}(\tilde{x}_{t_k})\} + \sqrt{2\delta_k}z_k, \qquad z_k \overset{\text{i.i.d.}}{\sim} \mathcal{N}(0, \mathrm{Id}). \tag{6}$$

Ignoring the error due to the score model, the minimum number of time steps is limited by the Lipschitz regularity of the score $\nabla \log p_t$, see [5, Theorem 1]. The overall complexity of this generation is N evaluations of the score $s_t(x)$.

2.2 Discretization of SGM and Score Regularity

We now study how the regularity of the score $\nabla \log p$ affects the discretization of (6). Assuming that the score is known, i.e., that $s_t = \nabla \log p_t$, we prove that for Gaussian processes, the number of time steps to reach a fixed error ε depends on the condition number of its covariance. This result is generalized to non-Gaussian processes by relating this error to the regularity of $\nabla \log p_t$.

Gaussian distributions Suppose that the data distribution is a Gaussian $p = \mathcal{N}(0, \Sigma)$ with covariance matrix Σ, in dimension d. Let p_t be the distribution of x_t. Using (2), we have:

$$\nabla \log p_t(x) = -(\mathrm{Id} + (\Sigma - \mathrm{Id})\mathrm{e}^{-2t})^{-1} x.$$

Let $\tilde{p}_t$ be the distribution of $\tilde{x}_t$ obtained by the time discretization (6). The approximation error between the distribution $\tilde{p}_0$ obtained with the time-reversed SDE and the data distribution p stems from (i) the mismatch between the distributions of x_T and $\tilde{x}_T$, and (ii) the time discretization. The following theorem relates these two errors to the covariance Σ of x in the particular case of a uniform time sampling at intervals $\delta_k = \delta$. We normalize the signal energy by imposing that $\mathrm{Tr}(\Sigma) = d$, and we write κ the condition number of Σ, which is the ratio between its largest and smallest eigenvalues.

Theorem 1. *If the data distribution $p = \mathcal{N}(0, \Sigma)$, the distribution $\tilde{p}_0$ of $\tilde{x}_0$ in (6) with a uniform discretization $\delta_k = \delta$ satisfies $\mathrm{KL}(p \| \tilde{p}_0) \leq E_T + E_\delta + E_{T,\delta}$, with :*

$$E_T = f(\mathrm{e}^{-4T} |\mathrm{Tr}((\Sigma - \mathrm{Id})\Sigma))|), \tag{7}$$

$$E_\delta = f(\delta |\mathrm{Tr}(\Sigma^{-1} - \Sigma(\Sigma - \mathrm{Id})^{-1} \log(\Sigma)/2 + (\mathrm{Id} - \Sigma^{-1})/3))|), \tag{8}$$

where $f(t) = t - \log(1 + t)$ and $E_{T,\delta}$ is a higher-order term with $E_{T,\delta} = o(\delta + \mathrm{e}^{-4T})$ when $\delta \to 0$ and $T \to +\infty$. Furthermore, for any $\varepsilon > 0$, there exists $T, \delta \geq 0$ such that:

$$(1/d)(E_T + E_\delta) \leq \varepsilon \quad \text{and} \quad N = T/\delta \leq C\varepsilon^{-2}\kappa^3. \tag{9}$$

with $C \geq 0$ a universal constant and κ the conditioning number of Σ.

This theorem specifies the dependence of the Kullback-Leibler error on the covariance matrix. It computes an upper bound on the number of time steps $N = T/\delta$ to reach an error ε as a function of the condition number κ of Σ. As expected, it indicates that the number of time steps should increase with the condition number of the covariance. This theorem is proved in a more general case in Appendix S5, which includes the case where p has a non-zero mean. An exact expansion of the Kullback-Leibler divergence is also given.

For stationary processes of images, the covariance eigenvalues are given by the power spectrum, which typically decays like $|\omega|^{-1}$ at a frequency ω. It results that κ is proportional to a power of the image size. Many physical phenomena produce such stationary images with a power spectrum having a power law decay. In these typical cases, the number of time steps must increase with the image size. This is indeed what is observed in numerical SGM experiments, as seen in Section 3.

General processes Theorem 1 can be extended to non-Gaussian processes. The number of time steps then depends on the regularity of the score $\nabla \log p_t$.

Theorem 2. *Assume that $\nabla \log p_t(x)$ is $\mathscr{C}^2$ in both t and x, and that:*

$$\sup_{x,t} \|\nabla^2 \log p_t(x)\| \leq K \quad \text{and} \quad \|\partial_t \nabla \log p_t(x)\| \leq M\, \mathrm{e}^{-\alpha t} \|x\|. \tag{10}$$

for some $K, M, \alpha > 0$. Then $\|p - \tilde{p}_0\|_{\mathrm{TV}} \leq E_T + E_\delta + E_{T,\delta}$, where:

$$E_T = \sqrt{2}\mathrm{e}^{-T} \mathrm{KL}(p \| \mathcal{N}(0, \mathrm{Id}))^{1/2}, \tag{11}$$

$$E_\delta = 6\sqrt{\delta}\,[1 + \mathbb{E}_p(\|x\|^4)^{1/4}]\,[1 + K + M(1 + 1/(2\alpha)^{1/2})], \tag{12}$$

and $E_{\delta,T}$ is a higher order term with $E_{T,\delta} = o(\sqrt{\delta} + \mathrm{e}^{-T})$ when $\delta \to 0$ and $T \to +\infty$.

The proof of Theorem 2 is postponed to Appendix S5 and we show that the result can be strengthened by providing a quantitative upper bound on $\|p - \tilde{p}_0\|_{\mathrm{TV}}$. Theorem 2 improves on [5, Theorem 1] by proving explicit bounds exhibiting the dependencies on the regularity constants K and M of the

score and by eliminating an exponential growth term in T in the upper bound. Theorem 2 is much more general but not as tight as Theorem 1.

The first error term (11) is due to the fact that T is chosen to be finite. The second error term (12) controls the error depending upon the discretization time step δ. Since p_t is obtained from p through a high-dimensional convolution with a Gaussian convolution of variance proportional to t, the regularity of $\nabla \log p_t(x)$ typically increases with t so $\|\nabla^2 \log p_t(x)\|$ and $\|\partial_t \nabla \log p_t(x)\|$ rather decrease when t increases. This qualitatively explains why a *quadratic* discretization schedule with non-uniform time steps $\delta_k \propto k$ are usually chosen in numerical implementations of SGMs [38, 45]. For simplicity, we focus on the uniform discretization schedule, but our result could be adapted to non-uniform time steps with no major difficulties. This remark also explains that it is mainly the regularity of the score at time $t = 0$ $\nabla \log p$ which determines the error decay (12).

While Theorem 2 is more general than Theorem 1, the Gaussian case provides intuition about the speed of the error decay (12) through the value of the constants K and M. If p is Gaussian, then the Hessian $\nabla^2 \log p$ is the negative inverse of the covariance matrix. We verify in Appendix S5 that in this case, the assumptions of Theorem 2 are satisfied. Furthermore, the constants K and M, and hence the number of discretization steps, are controlled using the condition number of Σ. We thus conjecture that non-Gaussian processes with an ill-conditioned covariance matrix will require many discretization steps to have a small error. This will be verified numerically. As we now explain, such processes are ubiquitous in physics and natural image datasets.

Multiscale processes Most images have variations on a wide range of scales. They require to use many time steps to sample using an SGM, because their score is not well-conditioned. This is also true for a wide range of phenomena encountered in physics, biology, or economics [22, 32]. We define a *multiscale process* as a stationary process whose power spectrum has a power law decay. The stationarity implies that its covariance is diagonalized in a Fourier basis. Its eigenvalues, which then coincide with its power spectrum, have a power law decay defined by:

$$P(\omega) \sim (\xi^\eta + |\omega|^\eta)^{-1}, \tag{13}$$

where $\eta > 0$ and $2\pi/\xi$ is the maximum correlation length. Physical processes near phase transitions have such a power-law decay, but it is also the case of many disordered systems such as fluid and gas turbulence. Natural images also typically define stationary processes. Their power spectrum satisfy this property with $\eta = 2$ and $2\pi/\xi \approx L$ for images of size $L \times L$. To efficiently synthesize images and more general multiscale signals, we must eliminate the ill-conditioning properties of the score. This is done by applying a wavelet transform.

3 Wavelet Score-Based Generative Model

The numerical complexity of the SGM algorithm depends on the number of time steps, which itself depends upon the regularity of the score. We show that an important acceleration is obtained by factorizing the data distribution into normalized wavelet conditional probability distributions, which are closer to a white Gaussian distribution, and so whose score is better-conditioned.

3.1 Wavelet Whitening and Cascaded SGMs

Normalized orthogonal wavelet coefficients Let x be the input signal of width L and dimension $d = L^n$, with $n = 2$ for images. We write x_j its low-frequency approximation subsampled at intervals 2^j, of size $(2^{-j}L)^n$, with $x_0 = x$. At each scale $2^{j-1} \geq 1$, a fast wavelet orthogonal transform decomposes x_{j-1} into $(\bar{x}_j, x_j)$ where $\bar{x}_j$ are the wavelet coefficient which carries the higher frequency information over $2^n - 1$ signals of size $(2^{-j}L)^n$ [30]. They are calculated with convolutional and subsampling operators G and $\bar{G}$ specified in Appendix S3:

$$x_j = \gamma_j^{-1} G\, x_{j-1} \quad \text{and} \quad \bar{x}_j = \gamma_j^{-1} \bar{G}\, x_{j-1}\,. \tag{14}$$

The normalization factor γ_j guarantees that $\mathbb{E}[\|\bar{x}_j\|^2] = (2^n - 1)(2^{-j}L)^n$. We consider wavelet orthonormal filters where $(G, \bar{G})$ is a unitary operator, i.e.:

$$\bar{G}G^\top = G\bar{G}^\top = 0 \quad \text{and} \quad G^\top G + \bar{G}^\top \bar{G} = \mathrm{Id}\,.$$

It results that x_{j-1} is recovered from $(\bar{x}_j, x_j)$ with:

$$x_{j-1} = \gamma_j \, G^\top x_j + \gamma_j \, \bar{G}^\top \bar{x}_j .$$

The wavelet transform is computed over $J \approx \log_2 L$ scales by iterating J times on (14). The last x_J has a size $(2^{-J} L)^n \approx 1$. Appendix S3 contains a more detailed introduction to the wavelet transform. The choice of wavelet filters G and $\bar{G}$ specifies the properties of the wavelet transform and the number of vanishing moments of the wavelet, as explained in Appendix S4.

Renormalized probability distribution A conditional wavelet renormalization factorizes the distribution $p(x)$ of signals x into conditional probabilities over wavelet coefficients:

$$p(x) = \alpha \prod_{j=1}^{J} \bar{p}_j(\bar{x}_j | x_j) \, p_J(x_J) \, . \tag{15}$$

where α (the Jacobian) depends upon all γ_j.

Although $p(x)$ is typically highly non-Gaussian, the factorization (15) involves distributions that are closer to Gaussians. The largest scale distribution p_J is usually close to a Gaussian when the image has independent structures, because x_J is an averaging of x over large domains of size 2^J. In images, the wavelet coefficients $\bar{x}_j$ are usually sparse and thus have a highly non-Gaussian distribution; however, it has been observed [48] that their conditional distributions $\bar{p}_j(\bar{x}_j | x_j)$ become much more Gaussian, due to dependencies of wavelet coefficients across scales. Furthermore, because of the renormalization, the normalized wavelet coefficients $\bar{x}_j$ have a white spectrum, as opposed to a power-law decay for x_j, which implies they are closer to a white Gaussian distribution. In statistical physics, the analysis of high frequencies conditioned by lower frequencies have been studied in [50]. More recently, normalized wavelet factorizations (15) have been introduced in physics to implement renormalization group calculations, and model probability distributions with maximum likelihood estimators near phase transitions [33].

Wavelet Score-based Generative Model Instead of computing a Score-based Generative Model (SGM) of the distribution $p(x)$, a Wavelet Score-based Generative Model (WSGM) applies an SGM at the coarsest scale $p_J(x_J)$ and then on each conditional distribution $\bar{p}_j(\bar{x}_j | x_j)$ for $j \leq J$. It is thus a cascaded SGM, similarly to [12, 40], but calculated on $\bar{p}_j(\bar{x}_j | x_j)$ instead of $p_j(x_{j-1} | x_j)$. The normalization of wavelet coefficients $\bar{x}_j$ effectively produces a whitening which can considerably accelerate the algorithm by reducing the number of time steps. This is not possible on x_{j-1} because its covariance is ill-conditioned. It will be proved for Gaussian processes.

A forward noising process is computed on each $\bar{x}_j$ for $j \leq J$ and x_J:

$$\mathrm{d}\bar{x}_{j,t} = -\bar{x}_{j,t} \, \mathrm{d}t + \sqrt{2} \mathrm{d}\bar{w}_{j,t} \;\text{ and }\; \mathrm{d}x_{J,t} = -x_{J,t} \, \mathrm{d}t + \sqrt{2} \mathrm{d}w_{J,t},$$

where the $\bar{w}_{j,t}, w_{J,t}$ are Brownian motions. Since $\bar{x}_j$ is nearly white and has Gaussian properties, this diffusion converges much more quickly than if applied directly on x. Using (4) or (5), we compute a score function $s_{J,t}(x_{J,t})$ which approximates the score $\nabla \log p_{J,t}(x_{J,t})$. For each $j \leq J$ we also compute the conditional score $\bar{s}_{j,t}(\bar{x}_{j,t} | x_j)$ which approximates $\nabla \log \bar{p}_{j,t}(\bar{x}_{j,t} | x_j)$.

The inverse generative process is computed from coarse to fine scales as follows. At the largest scale 2^J, we sample the low-dimensional x_J by discretizing the inverse SDE. Similarly to (6), the generative process is given by:

$$x_{J,t_{k+1}} = x_{J,t_k} + \delta_k \{ x_{J,t_k} + 2 s_{J,t_k}(x_{J,t_k}) \} + \sqrt{2\delta_k} z_{J,k}, \qquad z_{J,k} \overset{\text{i.i.d.}}{\sim} \mathcal{N}(0, \mathrm{Id}). \tag{16}$$

For j going from J to 1, we then generate the wavelet coefficients $\bar{x}_j$ conditionally to the previously calculated x_j, by keeping the same time discretization schedule at all scales:

$$\bar{x}_{j,t_{k+1}} = \bar{x}_{j,t_k} + \delta_k \{ \bar{x}_{j,t_k} + 2 \bar{s}_{j,t_k}(\bar{x}_{j,t_k} | x_j) \} + \sqrt{2\delta_k} \, z_{j,k}, \qquad z_{j,k} \overset{\text{i.i.d.}}{\sim} \mathcal{N}(0, \mathrm{Id}). \tag{17}$$

The inverse wavelet transform then approximately computes a sample of x_{j-1} from $(\bar{x}_{j,0}, x_j)$:

$$\tilde{x}_{j-1} = \gamma_j \, G^\top x_j + \gamma_j \, \bar{G}^\top \bar{x}_{j,0}. \tag{18}$$

The generative process is illustrated in Figure 1 and its pseudocode is given in Algorithm 1 in Appendix S2. The appendix also verifies that if x is of size d then the numerical complexity of the generation is $O(Nd)$, where N is the number of time steps, which is the same at each scale. For multiscale processes, we shall see that the number of time steps N does not depend upon d to reach a fixed error measured with a KL divergence.

Related work Multi-scale representations, based on wavelets or not, have been incorporated in many generative modeling approaches in order to increase generation quality and sampling efficiency. Specifically, they have been shown to improve results for auto-encoders [4], GANs [7] and normalizing flows [26]. Closer in spirit to our work, [52] introduces Wavelet Flow, a normalizing flow with a cascade of layers generating wavelet coefficients conditionally on lower-scales, then aggregating them with an inverse wavelet transform. This method yields training time acceleration and high-resolution (1024×1024) generation.

WSGM is closely related to other cascading diffusion algorithms, such as the ones introduced in [12, 40, 6]. The main difference lies in that earlier works on cascaded SGMs do not model the *wavelet coefficients* $\{\bar{x}_j\}_{j=1}^J$ but the *low-frequency* coefficients $\{x_j\}_{j=1}^J$. As a result, cascaded models do not explicitly exploit the whitening properties of the wavelet transform, nor the fact that conditional wavelet distributions are often nearly Gaussian, and the mechanisms behind the acceleration remain implicit. We also point out the recent work of [16] which, while not using the cascading framework, drop subspaces from the noising process at different times. This allows using only one SDE to sample approximately from the data distribution. However, the reconstruction is still computed with respect to $\{x_j\}_{j=1}^J$ instead of the wavelet coefficients.

Finally, we highlight that our work could be combined with other acceleration techniques such as the ones of [17, 27, 53, 42, 37, 43, 11, 23, 29, 41, 51] in order to improve the empirical results of WSGM.

3.2 Discretization and Accuracy for Gaussian Processes

We now illustrate Theorem 1 and the effectiveness of WSGM on Gaussian multiscale processes. We use the whitening properties of the wavelet transform to show that the time complexity required in order to reach a given error is linear in the image dimension.

The following result proves that the normalization of wavelet coefficients performs a preconditioning of the covariance, whose eigenvalues then remain of the order of 1. This is a consequence of a theorem proved by [34] on the representation of classes of singular operators in wavelet bases, see Appendix S4. As a result, the number of iterations $N = T/\delta$ required to reach an error ε is independent of the dimension.

Theorem 3. *Let x be a Gaussian stationary process of power spectrum $P(\omega) = c\,(\xi^\eta + |\omega|^\eta)^{-1}$ with $\eta > 0$ and $\xi > 0$. If the wavelet has a compact support, $q \geq \eta$ vanishing moments and is $\mathscr{C}^q$, then the first-order terms E_T and E_δ in the sampling error of WSGM $\mathrm{KL}(p\|\tilde{p}_0)$ are such that for any $\varepsilon > 0$, there exists $C > 0$ such that for any δ, T:*

$$(1/d)(E_T + E_\delta) \leq \varepsilon \;\; \textit{and} \;\; N = T/\delta \leq C\varepsilon^{-2}. \tag{19}$$

To prove this result, we show that the conditioning number of the covariance matrix of the renormalized wavelet coefficients does not depend on the dimension, by using Sobolev norm equivalences [15, 34]. We conclude upon combining this result, the cascading property of the Kullback-Leibler divergence and an extension of Theorem 1 to the setting with non-zero mean. The detailed proof is postponed to Appendix S6.

Numerical results We illustrate Theorem 3 on a Gaussian field x, whose power spectrum P has a power law decay (13). In Figure 2, we display the sup-norm between P and the power spectrum $\hat{P}$ of the samples obtained using either vanilla SGM or WSGM with uniform stepsize $\delta_k = \delta$. In the case of vanilla SGM, the number $N(\varepsilon)$ of time steps needed to reach a small error $\|P - \hat{P}\| = \varepsilon$ increases with the size of the image L (Fig. 2, right). Equation (9) suggests that $N(\varepsilon)$ scales like a power of the conditioning number κ of Σ, which is for multiscale Gaussian processes $\kappa \sim L^\eta$, for images of size $L \times L$. In the WSGM case, we sample from the conditional distributions $\bar{p}_j$ of wavelet coefficients $\bar{x}_j$ given low frequencies x_j. At a scale j, the conditioning numbers $\bar{\kappa}_j$ of the conditional covariance become dimension-independent (Appendix S4), removing the dependency of $N(\varepsilon)$ on the image size L as suggested by (19).

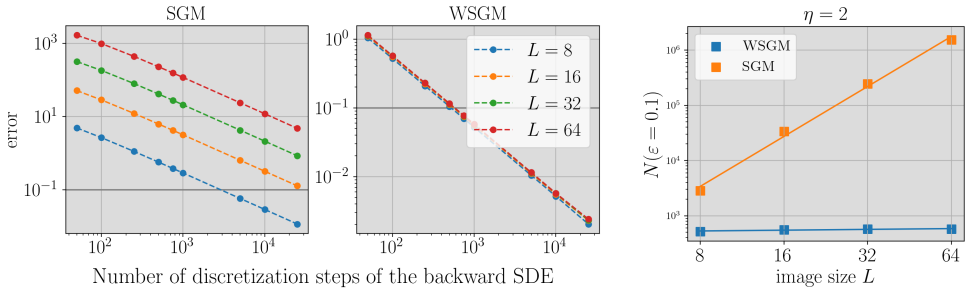


Figure 2: **Left and middle:** evolution of the error on the estimated covariance matrix using either SGM or WSGM w.r.t. the number of stepsizes used in the model ($T = 10$ is fixed). **Right:** number $N(\varepsilon)$ of discretization steps required to reach a given error $\varepsilon = 0.1$ using either SGM or WSGM.

4 Acceleration with WSGM: Numerical Results

For multiscale Gaussian processes, we proved that with WSGMs, the number of time steps $N(\varepsilon)$ to reach a fixed error ε does not depend on the signal size, as opposed to SGMs. This section shows that this result applies to non-Gaussian multiscale processes. We consider a physical process near a phase transition and images from the CelebA-HQ database [19].

4.1 Physical Processes with Scalar Potentials

Gaussian stationary processes are maximum entropy processes conditioned by second order moments defined by a circulant matrix. More complex physical processes are modeled by imposing a constraint on their marginal distribution, with a so-called scalar potential. The marginal distribution of x is the probability distribution of an image pixel $x(u)$, which does not depend upon u if x is stationary. Maximum entropy processes conditioned by second order moments and marginal distributions have a probability density which is a Gibbs distribution $p(x) = Z^{-1}\,\mathrm{e}^{-E(x)}$ with:

$$E(x) = \tfrac{1}{2} x^\top C x + \textstyle\sum_u V(x(u)) \;\;, \tag{20}$$

where C is a circulant matrix and $V : \mathbb{R} \to \mathbb{R}$ is a scalar potential. Appendix S8 explains how to parameterize V as a linear combination of a family of fixed elementary functions. The φ^4 model is a particular example where $C = -\Delta$ is the negative Laplacian and V is a fourth-order polynomial, adjusted in order to impose that $x(u) \approx \pm 1$ with high probability. For so-called critical values of these parameters, the resulting process becomes multiscale with long range interactions and a power law spectrum, see Figure 3-(c).

We train SGMs and WSGMs on critical φ^4 processes of different sizes; for the score model s_θ, we use a simple linear parameterization detailed in Appendix S8.2. To evaluate the quality of the generated samples, it is sufficient to verify that these samples have the same second order moment and marginals as φ^4. We define the error metric as the sum of the L^2 error on the power spectrum and the total-variation distance between marginal distributions. Figure 3-(a) shows the decay of this error as a function of the number of time steps used in an SGM and WSGM with a uniform discretization. With vanilla SGM, the loss has a strong dependency in L, but becomes almost independent of L for WSGM. This empirically verifies the claim that an ill-conditioned covariance matrix leads to slow sampling of SGM, and that WSGM is unaffected by this issue by working with the conditional distributions of normalized wavelet coefficients.

4.2 Scale-Wise Time Reduction in Natural Images

Images are highly non-Gaussian multiscale processes whose power spectrum has a power law decay. We now show that WSGM also provides an acceleration over SGM in this case, by being independent of the image size.

We focus on the CelebA-HQ dataset [28] at the 128×128 resolution. Its power spectrum has a power law decay, as shown in Figure 4, and it thus suffers from ill-conditioning, even though it is a

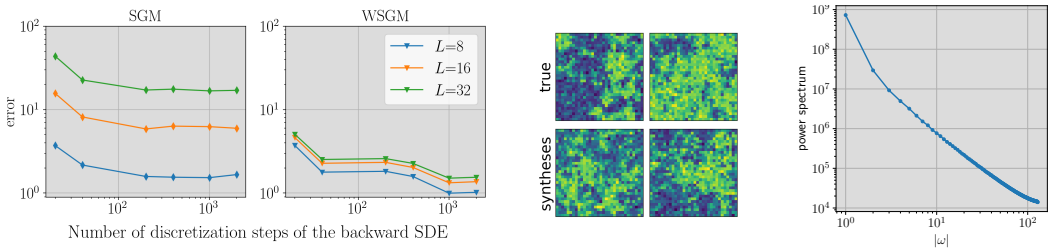


Figure 3: **Left:** error between ground-truth φ^4 datasets in various dimensions L, and the synthetized datasets with SGM and WSGM, for various number of discretization steps. **Middle:** realizations of φ^4 (top) and WSGM samples (bottom). **Right:** power spectrum of φ^4 for $L = 256$.

non-stationary process. We compare SGM [11] samples at the 128×128 resolution with WSGM samples which start from the 32×32 resolution. Though smaller, the 32×32 resolution still suffers from a power law decay of its spectrum over several orders of magnitude. The reason why we limit this coarsest resolution is because border effects become dominant at lower image sizes. To simplify the handling of border conditions, we use Haar wavelets.

Following [38], the global scores $s_\theta(x)$ are parameterized by a neural network with a U-Net architecture. It has 3 residual blocks at each scale, and includes multi-head attention layers at lower scales. The conditional scores $s_\theta(\bar{x}_j|x_j)$ are parameterized in the same way, and the conditioning on the low frequencies x_j is done with a simple input concatenation along channels [38, 40]. The details of the architecture are in Appendix S9. We use a uniform discretization of the backward SDE to stay in the setting of Theorem 2, and show that WSGM still obtains satisfactory results in this case.

The generation results are given in Figure 4. With the same computational budget of 16 discretizations steps at the largest scale (iterations at smaller scales having a negligible cost due to the exponential decrease in image size), WSGM achieves a much better perceptual generation quality. Notably, SGM generates noisy images due to discretization errors. This is confirmed quantitatively with the Fréchet Inception Distance (FID) [10]. The FID of the WSGM generations decreases with the number of steps, until it plateaus. This plateau is reached with at least 2 orders of magnitude less steps for WSGM than SGM. This number of steps is also independent of the image size for WSGM, thus confirming the intuition given in the Gaussian case by Theorems 1 and 3. Our results confirm that vanilla SGM on a wide range of multiscale processes, including natural images, suffers from ill-conditioning, in the sense that the number of discretization steps grows with the image size. WSGM, on the contrary, leads to uniform discretization schemes whose number of steps at each scale does not depend on the image size.

We also stress that there exists many techniques [18, 17, 27, 53, 42, 37, 43, 23, 11, 29, 41, 51] to accelerate the sampling of vanilla SGMs, with sometimes better FID-time complexity tradeoff curves. Notably, the FID plateaus at a relatively high value of 20 because the coarsest resolution 32×32 is still ill-conditioned, and thus requires thousands of steps with a non-uniform discretization schedule to achieve FIDs less than 10 with vanilla SGM [38]. Such improvements (including proper handling of border conditions) are beyond of the scope of this paper. The contribution of WSGM is rather to show the reason behind this sampling inefficiency and mathematically prove in the Gaussian setting that wavelet decompositions of the probability distribution allows solving this problem. Extending this theoretical result to a wider class of non-Gaussian multiscale processes, and combining WSGM with other sampling accelerations, are interesting research directions.

5 Discussion

This paper introduces a Wavelet Score-based Generative Model (WSGM) which applies an SGM to normalized wavelet coefficients conditioned by lower frequencies. We prove that the number of steps in SGMs is controlled by the regularity of the score of the target distribution. For multiscale processes such as images, it requires a considerable number of time steps to achieve a good accuracy, which increases quickly with the image size. We show that a WSGM eliminates ill-conditioning issues by normalizing wavelet coefficients. As a result, the number of steps in WSGM does not increase with

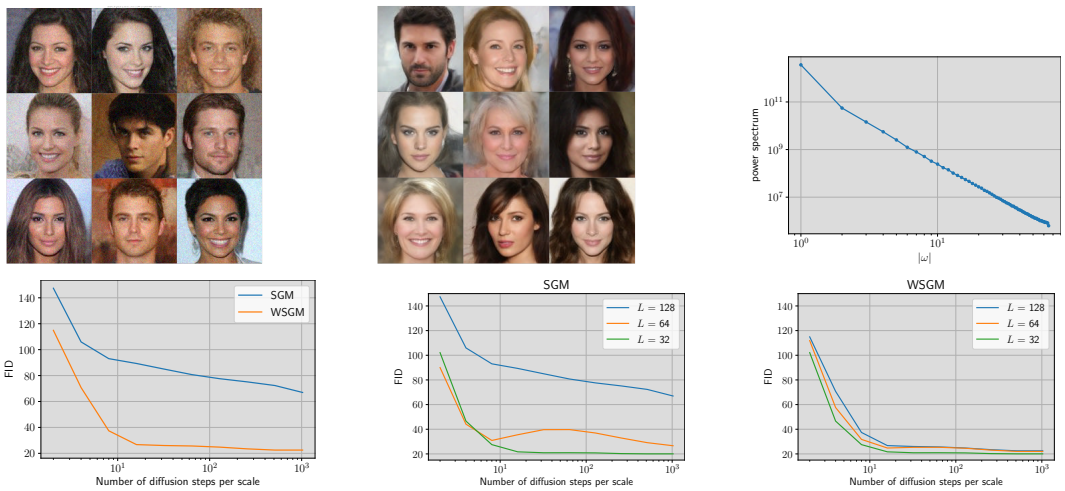


Figure 4: **Top.** (a): Generations from SGM with 16 discretization steps. (b): Generations from WSGM with 16 discretization steps at each scale. (c): Power spectrum of CelebA-HQ. **Bottom.** (a): Evolution of the FID w.r.t. the number of diffusion steps for SGM and WSGM with $L = 128$. (b): Evolution of the FID w.r.t. the number of diffusion steps for SGM at several image sizes L. (c) Evolution of the FID w.r.t. the number of diffusion steps for WSGM at several image sizes L.

the image size. We illustrated our results on Gaussian distributions, physical processes and image datasets.

One of the main limitations of WSGM is that it is limited to multiscale processes for which the conditional wavelet probabilities are nearly white. A promising direction for future work is to combine WSGM with other acceleration techniques such as adaptive time discretizations to handle such cases. In another direction, one could strengthen the theoretical study of SGM and extend our results beyond the Gaussian setting, in order to fully describe SGM on physical processes that can be seen as perturbations of Gaussian distributions.

Acknowledgments

This work was supported by a grant from the PRAIRIE 3IA Institute of the French ANR-19-P3IA-0001 program. We would like to thank the Scientific Computing Core at the Flatiron Institute for the use of their computing resources.

References

[1] D. Bakry, I. Gentil, and M. Ledoux. *Analysis and Geometry of Markov Diffusion Operators*, volume 348. Springer, 2014.

[2] Patrick Cattiaux, Giovanni Conforti, Ivan Gentil, and Christian Léonard. Time reversal of diffusion processes under a finite entropy condition. *arXiv preprint arXiv:2104.07708*, 2021.

[3] Nanxin Chen, Yu Zhang, Heiga Zen, Ron J Weiss, Mohammad Norouzi, and William Chan. Wavegrad: Estimating gradients for waveform generation. *International Conference on Learning Representations*, 2021.

[4] Tianshui Chen, Liang Lin, Wangmeng Zuo, Xiaonan Luo, and Lei Zhang. Learning a wavelet-like auto-encoder to accelerate deep neural networks. In *Proceedings of the AAAI Conference on Artificial Intelligence*, volume 32, 2018.

[5] Valentin De Bortoli, James Thornton, Jeremy Heng, and Arnaud Doucet. Diffusion schrödinger bridge with applications to score-based generative modeling. *Advances in Neural Information Processing Systems*, 34, 2021.

[6] Prafulla Dhariwal and Alex Nichol. Diffusion models beat GAN on image synthesis. *arXiv preprint arXiv:2105.05233*, 2021.

[7] Rinon Gal, Dana Cohen Hochberg, Amit Bermano, and Daniel Cohen-Or. Swagan: A style-based wavelet-driven generative model. *ACM Transactions on Graphics (TOG)*, 40(4):1–11, 2021.

[8] Leonard Gross. Logarithmic sobolev inequalities. *American Journal of Mathematics*, 97(4):1061–1083, 1975.

[9] Ulrich G Haussmann and Etienne Pardoux. Time reversal of diffusions. *The Annals of Probability*, 14(4):1188–1205, 1986.

[10] Martin Heusel, Hubert Ramsauer, Thomas Unterthiner, Bernhard Nessler, Günter Klambauer, and Sepp Hochreiter. Gans trained by a two time-scale update rule converge to a nash equilibrium. *CoRR*, abs/1706.08500, 2017.

[11] Jonathan Ho, Ajay Jain, and Pieter Abbeel. Denoising diffusion probabilistic models. *Advances in Neural Information Processing Systems*, 2020.

[12] Jonathan Ho, Chitwan Saharia, William Chan, David J Fleet, Mohammad Norouzi, and Tim Salimans. Cascaded diffusion models for high fidelity image generation. *Journal of Machine Learning Research*, 23(47):1–33, 2022.

[13] Aapo Hyvärinen and Peter Dayan. Estimation of non-normalized statistical models by score matching. *Journal of Machine Learning Research*, 6(4), 2005.

[14] Nobuyuki Ikeda and Shinzo Watanabe. *Stochastic Differential Equations and Diffusion Processes*, volume 24 of *North-Holland Mathematical Library*. North-Holland Publishing Co., Amsterdam; Kodansha, Ltd., Tokyo, second edition, 1989.

[15] S. Jaffard. Wavelelt methods for fast resolution elliptic problems. *SIAM Journal on Numerical Analysis*, 29(5):965–986, 1992.

[16] Bowen Jing, Gabriele Corso, Renato Berlinghieri, and Tommi Jaakkola. Subspace diffusion generative models, 2022.

[17] Alexia Jolicoeur-Martineau, Ke Li, Rémi Piché-Taillefer, Tal Kachman, and Ioannis Mitliagkas. Gotta go fast when generating data with score-based models. *arXiv preprint arXiv:2105.14080*, 2021.

[18] Zahra Kadkhodaie and Eero P Simoncelli. Solving linear inverse problems using the prior implicit in a denoiser. *arXiv preprint arXiv:2007.13640*, 2020.

[19] Tero Karras, Timo Aila, Samuli Laine, and Jaakko Lehtinen. Progressive growing of gans for improved quality, stability, and variation. arxiv 2017. *arXiv preprint arXiv:1710.10196*, pages 1–26, 2018.

[20] J Kaupuvzs, RVN Melnik, and J Rimvsāns. Corrections to finite-size scaling in the φ 4 model on square lattices. *International Journal of Modern Physics C*, 27(09):1650108, 2016.

[21] D. P Kingma and J. Ba. Adam: A method for stochastic optimization. *arXiv preprint arXiv:1412.6980*, 2014.

[22] A. N. Kolmogorov. A refinement of previous hypotheses concerning the local structure of turbulence in a viscous incompressible fluid at high reynolds number. *Journal of Fluid Mechanics*, 13(1):82–85, 1962.

[23] Zhifeng Kong and Wei Ping. On fast sampling of diffusion probabilistic models. *arXiv preprint arXiv:2106.00132*, 2021.

[24] Zhifeng Kong, Wei Ping, Jiaji Huang, Kexin Zhao, and Bryan Catanzaro. Diffwave: A versatile diffusion model for audio synthesis. *International Conference on Learning Representations*, 2021.

[25] Christian Léonard. Some properties of path measures. In *Séminaire de Probabilités XLVI*, pages 207–230. Springer, 2014.

[26] Shuo-Hui Li. Learning non-linear wavelet transformation via normalizing flow. *arXiv preprint arXiv:2101.11306*, 2021.

[27] Luping Liu, Yi Ren, Zhijie Lin, and Zhou Zhao. Pseudo numerical methods for diffusion models on manifolds, 2022.

[28] Ziwei Liu, Ping Luo, Xiaogang Wang, and Xiaoou Tang. Deep learning face attributes in the wild. In *International Conference on Computer Vision*, December 2015.

[29] Eric Luhman and Troy Luhman. Knowledge distillation in iterative generative models for improved sampling speed. *arXiv preprint arXiv:2101.02388*, 2021.

[30] S. Mallat. A theory for multiresolution signal decomposition: the wavelet representation. 11(7):674–693, July 1989.

[31] Stéphane Mallat. *A wavelet tour of signal processing: the sparse way*. Academic Press, 2009.

[32] BB Mandelbrot. The fractal geometry of nature/revised and enlarged edition. *New York*, 1983.

[33] Tanguy Marchand, Misaki Ozawa, Giulio Biroli, and Stéphane Mallat. Wavelet conditional renormalization group. *arXiv preprint arXiv:2207.04941*, 2022.

[34] Y. Meyer. *Wavelets and Operators*. Advanced mathematics. Cambridge university press, 1992.

[35] Sean P. Meyn and R. L. Tweedie. Stability of Markovian processes. III. Foster-Lyapunov criteria for continuous-time processes. *Advances in Applied Probability*, 25(3):518–548, 1993.

[36] A Milchev, DW Heermann, and K Binder. Finite-size scaling analysis of the $\varphi 4$ field theory on the square lattice. *Journal of statistical physics*, 44(5):749–784, 1986.

[37] Eliya Nachmani, Robin San Roman, and Lior Wolf. Non gaussian denoising diffusion models. *arXiv preprint arXiv:2106.07582*, 2021.

[38] Alex Nichol and Prafulla Dhariwal. Improved denoising diffusion probabilistic models. *arXiv preprint arXiv:2102.09672*, 2021.

[39] Vadim Popov, Ivan Vovk, Vladimir Gogoryan, Tasnima Sadekova, and Mikhail Kudinov. Grad-tts: A diffusion probabilistic model for text-to-speech. *arXiv preprint arXiV:2105.06337*, 2021.

[40] Chitwan Saharia, Jonathan Ho, William Chan, Tim Salimans, David J Fleet, and Mohammad Norouzi. Image super-resolution via iterative refinement. *arXiv preprint arXiv:2104.07636*, 2021.

[41] Tim Salimans and Jonathan Ho. Progressive distillation for fast sampling of diffusion models. *arXiv preprint arXiv:2202.00512*, 2022.

[42] Robin San-Roman, Eliya Nachmani, and Lior Wolf. Noise estimation for generative diffusion models. *arXiv preprint arXiv:2104.02600*, 2021.

[43] Jiaming Song, Chenlin Meng, and Stefano Ermon. Denoising diffusion implicit models. *arXiv preprint arXiv:2010.02502*, 2020.

[44] Yang Song and Stefano Ermon. Generative modeling by estimating gradients of the data distribution. In *Advances in Neural Information Processing Systems*, 2019.

[45] Yang Song and Stefano Ermon. Improved techniques for training score-based generative models. In *Advances in Neural Information Processing Systems*, 2020.

[46] Yang Song, Jascha Sohl-Dickstein, Diederik P. Kingma, Abhishek Kumar, Stefano Ermon, and Ben Poole. Score-based generative modeling through stochastic differential equations. In *International Conference on Learning Representations*, 2021.

[47] Pascal Vincent. A connection between score matching and denoising autoencoders. *Neural Computation*, 23(7):1661–1674, 2011.

[48] Martin J Wainwright and Eero Simoncelli. Scale mixtures of gaussians and the statistics of natural images. *Advances in neural information processing systems*, 12, 1999.

[49] Kenneth G Wilson. Renormalization group and critical phenomena. ii. phase-space cell analysis of critical behavior. *Physical Review B*, 4(9):3184, 1971.

[50] Kenneth G Wilson. The renormalization group and critical phenomena. *Reviews of Modern Physics*, 55(3):583, 1983.

[51] Zhisheng Xiao, Karsten Kreis, and Arash Vahdat. Tackling the generative learning trilemma with denoising diffusion gans. *arXiv preprint arXiv:2112.07804*, 2021.

[52] Jason J Yu, Konstantinos G Derpanis, and Marcus A Brubaker. Wavelet flow: Fast training of high resolution normalizing flows. *Advances in Neural Information Processing Systems*, 33:6184–6196, 2020.

[53] Qinsheng Zhang and Yongxin Chen. Fast sampling of diffusion models with exponential integrator, 2022.

Checklist

1. For all authors...
   (a) Do the main claims made in the abstract and introduction accurately reflect the paper's contributions and scope? [Yes]
   (b) Did you describe the limitations of your work? [Yes] See the end of Section 4
   (c) Did you discuss any potential negative societal impacts of your work? [No] Like all generative models, WCRG can reproduce or amplify biases present in the data, or could be used to generate deceptive content. We stress that this work is theoretical in nature and should not be used for practical applications without a careful consideration of the aforementioned issues.
   (d) Have you read the ethics review guidelines and ensured that your paper conforms to them? [Yes]
2. If you are including theoretical results...
   (a) Did you state the full set of assumptions of all theoretical results? [Yes] Assumptions are stated in the respective theorems.
   (b) Did you include complete proofs of all theoretical results? [Yes] See Appendices S5 and S6.
3. If you ran experiments...
   (a) Did you include the code, data, and instructions needed to reproduce the main experimental results (either in the supplemental material or as a URL)? [Yes] All the code needed to reproduce the experiments is provided in the supplemental material.
   (b) Did you specify all the training details (e.g., data splits, hyperparameters, how they were chosen)? [Yes] See Appendix S9.
   (c) Did you report error bars (e.g., with respect to the random seed after running experiments multiple times)? [No] Standard errors are negligible for the comparisons we perform.
   (d) Did you include the total amount of compute and the type of resources used (e.g., type of GPUs, internal cluster, or cloud provider)? [No] We estimate the total amount of compute used during the preparation of this paper, including preliminary experiments, at around 10k hours of NVIDIA A100 GPUs.
4. If you are using existing assets (e.g., code, data, models) or curating/releasing new assets...
   (a) If your work uses existing assets, did you cite the creators? [Yes]
   (b) Did you mention the license of the assets? [No]
   (c) Did you include any new assets either in the supplemental material or as a URL? [No]
   (d) Did you discuss whether and how consent was obtained from people whose data you're using/curating? [No]

(e) Did you discuss whether the data you are using/curating contains personally identifiable information or offensive content? [No]

5. If you used crowdsourcing or conducted research with human subjects...
   (a) Did you include the full text of instructions given to participants and screenshots, if applicable? [N/A]
   (b) Did you describe any potential participant risks, with links to Institutional Review Board (IRB) approvals, if applicable? [N/A]
   (c) Did you include the estimated hourly wage paid to participants and the total amount spent on participant compensation? [N/A]

S1 Organization of the Supplementary Material

We provide the pseudocode for the WSGM algorithm in Appendix S2. Appendix S3 contains an introduction to wavelet transforms, and their whitening properties are presented in Appendix S4. The proofs of Section 2 and Section 3 are gathered Appendix S5 and Appendix S6 respectively. Details about the Gaussian model and the φ^4 model are given in Appendix S7 and Appendix S8 respectively. Finally, experimental details and additional experiments are described in Appendix S9.

S2 WSGM Algorithm

In Algorithm 1, we provide the pseudocode for WSGM. Notice that the training of score models at each scale can be done in parallel, while the sampling is done sequentially one scale after the next.

Algorithm 1 Wavelet Score-based Generative Model

Require: J, N_{iter}, N, T,$\{\bar\theta_{j,0}, \theta_{J,0}\}_{j=0}^{J}$, $\{x_0^m\}_{m=1}^M$
/// WAVELET TRANSFORM ///
for $j \in \{1, \dots, J\}$ **do**
  for $m \in \{1, \dots, M\}$ **do**
    $x_j^m = \gamma_j^{-1} G x_{j-1}^m$, $\bar x_j^m = \gamma_j^{-1} \bar G x_{j-1}^m$ ▷ Wavelet transform of the dataset
  end for
end for
/// TRAINING ///
Train score network $s_{\theta_J^\star}$ at scale J with dataset $\{x_J^m\}_{m=0}^M$ ▷ Unconditional SGM training
for $j \in \{J, \dots, 1\}$ **do** ▷ Can be run in parallel
  for $n \in \{0, \dots, N_{\text{iter}} - 1\}$ **do**
    Sample $(\bar x_{j,0}, x_j)$ from $\{\bar x_j^m, x_j^m\}_{m=1}^M$
    Sample t in $[0, T]$ and $\bar Z \sim \mathrm{N}(0, \mathrm{Id})$
    $\bar x_{j,t} = \mathrm{e}^{-t} \bar x_{j,0} + (1 - \mathrm{e}^{-2t})^{1/2} \bar Z$
    $\ell(\bar\theta_{j,n}) = \| (\mathrm{e}^{-t} \bar x_{j,0} - \bar x_{j,t}) - (1 - \mathrm{e}^{-2t})^{1/2} \bar s_{\bar\theta_{j,n}}(t, \bar x_{j,t} | x_j) \|^2$
    $\bar\theta_{j,n+1} = \texttt{optimizer_update}(\bar\theta_{j,n}, \ell(\bar\theta_{j,n}))$ ▷ ADAM optimizer step
  end for
  $\bar\theta_j^\star = \bar\theta_{j, N_{\text{iter}}}$
end for
/// SAMPLING ///
$x_J = \texttt{EulerMaruyama}(T, N, s_{\theta_J^\star})$ ▷ Euler-Maruyama recursion following (16)
for $j \in \{J, \dots, 1\}$ **do**
  $\bar x_j = \texttt{EulerMaruyama}(T, N, \bar s_{\bar\theta_j^\star}(\cdot, \cdot | x_j))$ ▷ Euler-Maruyama recursion following (17)
  $x_{j-1} = \gamma_j G^\top x_j + \gamma_j \bar G^\top \bar x_j$ ▷ Wavelet reconstruction
end for
return $\{\bar\theta_j^\star, \theta_J^\star\}_{j=1}^J, x_0$ ▷ Returns learned parameters and generated samples

S3 Introduction to the Fast Orthogonal Wavelet Transform

This section introduces the fast orthogonal wavelet transform introduced in [30]. It is computed with convolutional operators G and $\bar G$. In this section, we deal with the non-normalized wavelet transform, which is obtained by setting $\gamma_j = 1$. To avoid confusion with normalized wavelet coefficients $(x_j, \bar x_j)$, we denote the non-normalized wavelet coefficients with a w exponent: $(x_j^w, \bar x_j^w)$.

Let x_0^w be a signal. The index u in $x_0^w(u)$ belongs to an n-dimensional grid of linear size L and hence with L^n sites, with $n = 2$ for images. Let us denote x_j^w the coarse-grained version of x_0^w at a scale 2^j defined over a coarser grid with intervals 2^j and hence $(2^{-j} L)^n$ sites. The coarser signal x_j^w is iteratively computed from x_{j-1}^w by applying a coarse-graining operator, which acts as a scaling filter G which eliminates high frequencies and subsamples the grid:

$$(G x_{j-1}^w)(u) = \sum_{u'} x_{j-1}^w(u')\, G(2u - u') \ . \tag{S1}$$

The index u on the left-hand side runs on the coarser grid, whereas u' runs on the finer one.

The degrees of freedom of x^w_{j-1} that are not in x^w_j are encoded in orthogonal wavelet coefficients $\bar{x}^w_j$. The representation $(x^w_j, \bar{x}^w_j)$ is an orthogonal change of basis calculated from x^w_{j-1}. The coarse signal x^w_j is calculated in (S1) with a low-pass scaling filter G and a subsampling. In dimension n, the wavelet coefficients $\bar{x}^w_j$ have $2^n - 1$ channels computed with a convolution and subsampling operator $\bar{G}$. We thus have:

$$x^w_j = G\, x^w_{j-1} \text{ and } \bar{x}^w_j = \bar{G}\, x^w_{j-1}. \tag{S2}$$

The wavelet filter $\bar{G}$ computes $2^n - 1$ wavelet coefficients $\bar{x}^w_j(u,k)$ indexed by $1 \leq k \leq 2^n - 1$, with separable high-pass filters $\bar{G}_k(u)$:

$$\bar{x}^w_j(u,k) = \sum_{u'} x^w_{j-1}(u')\, \bar{G}_k(2u - u').$$

As an example, the Haar wavelet leads to a block averaging filter G. In dimension $n = 1$

$$x^w_j(u) = \frac{x^w_{j-1}(2u) + x^w_{j-1}(2u+1)}{\sqrt{2}},$$

and there is a single wavelet channel in $\bar{x}^w_j$. The corresponding wavelet filter $\bar{G}$ computes the wavelet coefficients with increments divided by $\sqrt{2}$:

$$\bar{x}^w_j(u) = \frac{x^w_{j-1}(2u) - x^w_{j-1}(2u+1)}{\sqrt{2}}.$$

If $n = 2$, then there are $2^n - 1 = 3$ wavelet channels as shown in Figure 1.

The fast wavelet transform cascades (S2) for $1 \leq j \leq J$ to compute the decomposition of the high-resolution signal x^w_0 into its orthogonal wavelet representation over J scales:

$$\left\{x^w_J\,,\, \bar{x}^w_j\right\}_{1 \leq j \leq J}. \tag{S3}$$

The wavelet orthonormal filters G and $\bar{G}$ define a unitary transformation, which satisfies:

$$\bar{G}G^\top = G\bar{G}^\top = 0 \text{ and } G^\top G + \bar{G}^T\bar{G} = \mathrm{Id}\,,$$

where Id is the identity. Conjugate mirror conditions are given in [30] on the Fourier transforms of G and $\bar{G}$ to build such unitary filters. The filtering equations (S2) can then be inverted with the adjoint operators:

$$x^w_{j-1} = G^\top x^w_j + \bar{G}^\top \bar{x}^w_j\,. \tag{S4}$$

The adjoint $G^\top$ enlarge the grid size of x^w_j by inserting a zero between each coefficients, and then filters the output:

$$(G^\top x^w_j)(u) = \sum_{u'} x^w_j(u')\, G(2u' - u).$$

The adjoint of $\bar{G}$ performs the same operations over the $2^n - 1$ channels and adds them:

$$(\bar{G}^\top \bar{x}^w_j)(u) = \sum_{k=1}^{2^n-1} \sum_{u'} \bar{x}^w_j(u',k)\, \bar{G}_k(2u' - u).$$

The fast inverse wavelet transform [30] recovers x^w_0 from its wavelet representation (S3) by progressively recovering x^w_{j-1} from x^w_j and $\bar{x}^w_j$ with (S4), for j going from J to 1.

S4 Orthogonal Wavelet Bases and Preconditioning of Operators

This appendix relates the fast discrete wavelet transform to decomposition of finite energy functions in orthonormal bases of $\mathbf{L^2}([0,1]^n)$. Although the covariance of normalized wavelet coefficients of multiscale processes are badly conditioned, after normalisation these covariance matrices become well conditioned because the normalisation acts as a preconditioning operator [15]. This is a central result to prove Theorem 3. The results of this appendix are based on the multiresolution theory [30, 31] and the representation of elliptic singular operators in wavelet orthonormal bases [34].

Orthonormal wavelet bases From an input discrete signal $x_0(u) = x(u)$ defined over an n-dimensional grid of width L, we introduced in (14) a normalized wavelet transform which computes wavelet coefficients $\bar{x}_j(u,k)$ having $2^n - 1$ channels $1 \leq k < 2^n$. The orthonormal wavelet transform without renormalization is obtained by setting $\gamma_j = 1$ and has been introduced in appendix S3. We write $\bar{x}^w = (\bar{x}^w_j, x^w_J)_{j \leq J}$ the vector of non-normalized wavelet coefficients.

The multiresolution wavelet theory [31, 34] proves that the coefficients of $\bar{x}^w$ can also be written as the decomposition coefficients of a finite energy function, in a wavelet orthonormal basis of the space $\mathbf{L^2}(\mathbb{R}^n)$ of finite energy functions. These wavelets arise from the cascade of the convolutional filters G and $\bar{G}$ in (**??**) when we iterate on j [31]. This wavelet orthonormal basis is thus entirely specified by the choice of the filters G and $\bar{G}$. A wavelet orthonormal basis is defined by a *scaling function* $\psi^0(v)$ for $v \in \mathbb{R}^n$ which has a unit integral $\int \psi^0(v)\,\mathrm{d}v = 1$, and $2^n - 1$ *wavelets* which have a zero integral $\int \psi^k(v)\,\mathrm{d}v = 0$ for $1 \leq k < 2^n$. Each of these functions are dilated and translated by $u \in \mathbb{Z}^n$, for $1 \leq k < 2^n$ and $j \in \mathbb{Z}$:

$$\psi^k_{j,u}(v) = 2^{-nj/2}\,\psi^k(2^{-j}v - u).$$

The main result proved in [31, 34], is that for appropriate filters G and $\bar{G}$ such that $(G, \bar{G})$ is unitary, the family of translated and dilated wavelets up to the scale 2^J:

$$\{\psi^0_{J,u}\,,\ \psi^k_{j,u}\}_{1 \leq k < 2^n\,,\, j \leq J\,,\, u \in \mathbb{Z}^n}$$

is an orthonormal basis of $\mathbf{L^2}(\mathbb{R}^n)$. A periodic wavelet basis of $\mathbf{L^2}([0,1]^n)$ is defined by replacing each wavelet $\psi^k_{j,u}$ by the periodic function $\sum_{r \in \mathbb{Z}^n} \psi^k_{j,u}(v - r)$ which we shall still write $\psi^k_{j,u}$.

The properties of the wavelets $\psi^k_{j,u}$ depend upon the choice of the filters G and $\bar{G}$. If these filters have a compact support then one can verify [31] that all wavelets $\psi^k_{j,u}$ have a compact support of size proportional to 2^j. With an appropriate choice of filters, one can also define wavelets having q vanishing moments, which means that they are orthogonal to any polynomial $Q(v)$ of degree strictly smaller than q:

$$\int_{[0,1]^n} Q(v)\,\psi^k_{j,u}(v)\,\mathrm{d}v = 0.$$

One can also ensure that wavelet are q times continuously differentiable. Daubechies wavelets [31] are examples of orthonormal wavelets which can have q vanishing moments and be $\mathbf{C}^q$ for any q.

The relation between the fast wavelet transform and these wavelet orthonormal bases proves [31] that any discrete signal $x_0(u)$ of width L can be written as a discrete approximation at a scale $2^\ell = L^{-1}$ ($\ell < 0$) of a (non-unique) function $f \in \mathbf{L^2}([0,1]^n)$. The support of f is normalized whereas the approximation scale 2^ℓ decreases as the number of samples L increases. The coefficients $x_0(u)$ are inner products of f with the orthogonal family of scaling functions at the scale 2^ℓ for all $u \in \mathbb{Z}^n$ and $2^\ell u \in [0,1]^n$:

$$x_0(u) = \int_{[0,1]^n} f(v)\,\psi^0_{\ell,u}(v)\,\mathrm{d}v = \langle f, \psi^0_{\ell,u} \rangle.$$

Let V_ℓ be the space generated by the orthonormal family of scaling functions $\{\psi^0_{\ell,u}\}_{2^\ell u \in [0,1]^n}$, and $P_{V_\ell} f$ be the orthogonal projection of f in V_ℓ. The signal x_0 gives the orthogonal decomposition coefficients of $P_{V_\ell} f$ in this family of scaling functions. One can prove [31] that the non-normalized wavelet coefficients $\bar{x}^w_j$ of x_0 computed with a fast wavelet transform are equal to the orthogonal wavelet coefficients of f at the scale $2^{j+\ell}$, for all $u \in \mathbb{Z}^n$ and $2^{j+\ell} u \in [0,1]^n$:

$$\bar{x}^w_j(u,k) = \int_{[0,1]^n} f(v)\,\psi^k_{j+\ell,u}(v)\,\mathrm{d}v = \langle f, \psi^k_{j+\ell,u} \rangle.$$

and at the largest scale 2^J

$$x^w_J(u,k) = \int_{[0,1]^n} f(v)\,\psi^0_{J+\ell,u}(v)\,\mathrm{d}v = \langle f, \psi^k_{j+J,u} \rangle.$$

Normalized covariances We now consider a periodic stationary multiscale random process $x(u)$ of width L. It covariance is diagonalised in a Fourier basis and its power spectrum (eigenvalues) has a power-law decay $P(\omega) = c(\xi^\eta + |\omega|^\eta)^{-1}$, for frequencies $\omega = 2\pi m/L$ with $m \in \{0, \ldots, L-1\}^n$. The following lemma proves that the covariance matrix $\bar{\Sigma}$ of the normalized wavelet coefficients $\bar{x}$ of x is well conditioned, with a condition number which does not depend upon L. It relies on an equivalence between Sobolev norms and weighted norms in a wavelet orthonormal basis.

Lemma S4. *For a wavelet transform corresponding to wavelets having $q > \eta$ vanishing moments, which have a compact support and are q times continuously differentiable, there exists $C_2 \geq C_1 > 0$ such that for any L the covariance $\bar{\Sigma}$ of $\bar{x} = (\bar{x}_j, x_J)_{j \leq J}$ satisfies:*

$$C_1 \ \mathrm{Id} \leq \bar{\Sigma} \leq C_2 \ \mathrm{Id}\,. \tag{S5}$$

The remaining of the appendix is a proof of this lemma. Without loss of generality, we shall suppose that $\mathbb{E}[x] = 0$. Let $\sigma^2_{j,k}$ be the variance of $\bar{x}^w_j(u,k)$, and D be the diagonal matrix whose diagonal values are $\sigma^{-1}_{j,k}$. The vector of normalized wavelet coefficients $\bar{x} = (\bar{x}_j, x_J)_{j \leq J}$ are related to the non-normalized wavelet coefficients $\bar{x}^w$ by a multiplication by D:

$$\bar{x} = D\,\bar{x}^w.$$

Let $\bar{\Sigma}_w$ be the covariance of $\bar{x}^w$. It results from this equation that the covariance $\bar{\Sigma}$ of $\bar{x}$ and the covariance $\bar{\Sigma}_w$ of $\bar{x}^w$ satisfy:

$$\bar{\Sigma} = D\bar{\Sigma}_w D.$$

The diagonal normalization D is adjusted so that the variance of each coefficient of $\bar{x}$ is equal to 1, which implies that the diagonal of $\bar{\Sigma}$ is the identity. We must now prove that $\bar{\Sigma}$ satisfies (S5), which is equivalent to prove that there exists C_1 and C_2 such that:

$$C_1 \ \mathrm{Id} \leq D\bar{\Sigma}_w D \leq C_2 \ \mathrm{Id}\,. \tag{S6}$$

To prove (S6), we relate it to Sobolev norm equivalences that have been proved in harmonic analysis. We begin by stating the result on Sobolev inequalities and then prove that it implies (S6) for appropriate constants C_1 and C_2.

Let Σ_∞ be the singular self-adjoint convolutional operator over $\mathbf{L^2}(\mathbb{R}^n)$ defined in the Fourier domain for all $\omega \in \mathbb{R}^n$:

$$\widehat{\Sigma_\infty f}(\omega) = \hat{f}(\omega)\,(\xi^\eta + |\omega|^\eta).$$

Observe that:

$$\langle \Sigma_\infty f, f\rangle = \tfrac{1}{(2\pi)^n} \int_{\mathbb{R}^n} |\hat{f}(\omega)|^2\,(\xi^\eta + |\omega|^\eta)\,\mathrm{d}\omega$$

is a Sobolev norm of exponent η. Such Sobolev norms are equivalent to weighted norms in wavelet bases, as proved in Theorem 4, Chapter 3 in [34]. To take into account the constant ξ, we introduce a maximum scale $2^{J'} = \xi^{-1}$. For all $f \in \mathbf{L^2}(\mathbb{R}^n)$, there exists $B \geq A > 0$ such that:

$$\begin{aligned} A\,\langle \Sigma_\infty f, f\rangle \leq \textstyle\sum_{u \in \mathbb{Z}^n} 2^{-J\eta} |\langle f, \psi^0_{J',u}\rangle|^2 \\ + \textstyle\sum_{j=-\infty}^{J'} \sum_{u \in \mathbb{Z}^n} \sum_{k=1}^{2^n-1} 2^{-j\eta}\,|\langle f, \psi^k_{j,u}\rangle|^2 \leq B\,\langle \Sigma_\infty f, f\rangle. \end{aligned} \tag{S7}$$

The remaining of the proof shows that these inequalities imply similar inequalities over the covariance of discrete wavelet coefficients. This is done by first restricting it to a finite support and then using the correspondence between the orthonormal wavelet coefficients of f and the discrete wavelet coefficients $\bar{x}^w$ of x_0.

One can verify that the equivalence (S7) remains valid for functions $f \in \mathbf{L^2}([0,1]^n)$ decomposed over periodic wavelet bases, because functions in $\mathbf{L^2}([0,1]^n)$ can be written $f(v) = \sum_{r \in \mathbb{Z}^n} \tilde{f}(v-r)$ with $\tilde{f} \in \mathbf{L^2}(\mathbb{R}^n)$:

$$\begin{aligned} A\,\langle \Sigma_\infty f, f\rangle \leq \textstyle\sum_{2^{J'}u \in [0,1]^n} 2^{-J'\eta} |\langle f, \psi^0_{J',u}\rangle|^2 \\ + \textstyle\sum_{j=-\infty}^{J'} \sum_{2^j u \in [0,1]^n} \sum_{k=1}^{2^n-1} 2^{-j\eta}\,|\langle f, \psi^k_{j,u}\rangle|^2 \leq B\,\langle \Sigma_\infty f, f\rangle. \end{aligned}$$

Applying this result to $f \in V_\ell$ is equivalent to restricting Σ_∞ to V_ℓ, which proves that $\Sigma_\ell = P_{V_\ell}\Sigma_\infty P_{V_\ell}$ satisfies:

$$\begin{aligned} A\,\langle \Sigma_\ell f, f\rangle \leq \textstyle\sum_{2^{J'}u \in [0,1]^n} 2^{-J'\eta} |\langle f, \psi^0_{J',u}\rangle|^2 \\ + \textstyle\sum_{j=\ell+1}^{J'} \sum_{2^j u \in [0,1]^n} \sum_{k=1}^{2^n-1} 2^{-j\eta}\,|\langle f, \psi^k_{j,u}\rangle|^2 \leq B\,\langle \Sigma_\ell f, f\rangle. \end{aligned} \tag{S8}$$

The operator $\Sigma_\ell = P_{V_\ell}\,\Sigma_\infty\,P_{V_\ell}$ is covariant with respect to shifts by any $m2^\ell$ for $m \in \mathbb{Z}^n$ because P_{V_ℓ} and Σ_∞ are covariant to such shifts. Its representation in the basis of scaling functions

$\{\psi^0_{\ell,u}\}_{2^\ell u\in[0,1]^n}$ is thus a Toeplitz matrix which is diagonalized by a Fourier transform. There exists $0 < A_1 \leq B_1$ such that for all $\ell < 0$ and all $\omega \in [-2^{-\ell}\pi, 2^{-\ell}\pi]^n$,

$$A_1\,(\xi^\eta + |\omega|^\eta) \leq P_\ell(\omega) \leq B_1\,(\xi^\eta + |\omega|^\eta). \tag{S9}$$

Indeed, the spectrum of Σ_∞ is $c\,(\xi^\eta + |\omega|^\eta)$ for $\omega \in \mathbb{R}^n$ and P_{V_ℓ} performs a filtering with the scaling function ψ^0_ℓ whose support is essentially restricted to the frequency interval $[-\pi 2^{-\ell}, \pi 2^{-\ell}]$ so that the spectrum of $P_{V_\ell}\,\Sigma_\infty\,P_{V_\ell}$ is equivalent to the spectrum of Σ_∞ restricted to this interval.

The lemma hypothesis supposes that the covariance $\widetilde{\Sigma}$ of x_0 has a spectrum equal to $c\,(\xi^\eta + |\omega|^\eta)^{-1}$ and hence that the spectrum of $\widetilde{\Sigma}^{-1}$ is $c^{-1}\,(\xi^\eta + |\omega|^\eta)$. Since x_0 are decomposition coefficients of $f \in V_\ell$ in the basis of scaling functions, equation (S9) can be rewritten for any $f \in V_\ell$:

$$A_1\,c\,\langle\widetilde{\Sigma}^{-1}x_0, x_0\rangle \leq \langle\Sigma_\ell f, f\rangle \leq B_1\,c\,\langle\widetilde{\Sigma}^{-1}x_0, x_0\rangle. \tag{S10}$$

Since the orthogonal wavelet coefficients $\bar{x}^w$ defines an orthonormal representation of x_0, the covariance $\bar{\Sigma}_w$ of $\bar{x}^w$ satisfies $\langle\bar{\Sigma}_w^{-1}\bar{x}^w, \bar{x}^w\rangle = \langle\widetilde{\Sigma}^{-1}x_0, x_0\rangle$. Moreover, we saw that that the wavelet coefficients $\bar{x}^w$ of x_0 satisfy $\bar{x}^w_j(u,k) = \langle f, \psi^k_{j+\ell,u}\rangle$ and at the largest scale $\bar{x}^w_J(u,k) = \langle f, \psi^0_{J+\ell,u}\rangle$. Hence for $J + \ell = J'$, we derive from (S8) and (S10) that:

$$\begin{aligned} A\,A_1\,c\,\langle\bar{\Sigma}_w^{-1}\bar{x}^w, \bar{x}^w\rangle &\leq \textstyle\sum_{2^J u\in[0,1]^n} 2^{-(J+\ell)\eta}\,|x^w_J(u)|^2 \\ &\quad + \textstyle\sum_{j=1}^J \sum_{2^j u\in[0,1]^n} \sum_{k=1}^{2^n-1} 2^{-(j+\ell)\eta}\,|\bar{x}^w_j(u,k)|^2 \leq B\,B_1\,c\,\langle\bar{\Sigma}_w^{-1}\bar{x}^w, \bar{x}^w\rangle. \end{aligned}$$

It results that for $A_2 = A\,A_1\,c$ and $B_2 = B\,B_1\,c$ we have:

$$A_2\,\langle\bar{\Sigma}_w^{-1}\bar{x}^w, \bar{x}^w\rangle \leq 2^{-(J+\ell)\eta}\,\|x^w_J\|^2 + \sum_{j=1}^J 2^{-(j+\ell)\eta}\,\|\bar{x}^w_j\|^2 \leq B_2\,\langle\bar{\Sigma}_w^{-1}\bar{x}^w, \bar{x}^w\rangle.$$

Let $\tilde{D}$ be the diagonal operator over the wavelet coefficients $\bar{x}^w$, whose diagonal values are $2^{-\eta(j+\ell)/2}$ at all scales 2^j. These inequalities can be rewritten as operator inequalities:

$$A_2\,\bar{\Sigma}_w^{-1} \leq \tilde{D}^2 \leq B_2\,\bar{\Sigma}_w^{-1},$$

and hence:

$$A_2\,\mathrm{Id} \leq \tilde{D}\bar{\Sigma}_w\tilde{D} \leq B_2\,\mathrm{Id}\,. \tag{S11}$$

Since D^{-2} is the diagonal of $\bar{\Sigma}_w$, we derive from (S11) that:

$$A_2\,\tilde{D}^{-2} \leq D^{-2} \leq B_2\,\tilde{D}^{-2}.$$

Inserting this equation in (S11) proves that:

$$A_2\,B_2^{-1}\,\mathrm{Id} \leq D\,\bar{\Sigma}_w\,D \leq B_2\,A_2^{-1}\,\mathrm{Id},$$

and since $\bar{\Sigma} = D\,\bar{\Sigma}_w\,D$ it proves the lemma result (S6), with $C_1 = A_2B_2^{-1}$ and $C_2 = B_2A_2^{-1}$.

S5 Proof of Theorems 1 and 2

In this section, we first present the continuous-time framework in a Gaussian setting in Appendix S5.1. The general outline of the proof of Theorem 1 is presented in Appendix S5.2. Technical lemmas are gathered in Appendix S5.3. The proof of Theorem 2 is presented in Appendix S5.4.

S5.1 Gaussian setting

In what follows we present the Gaussian setting used in the proof of Theorem 1. We assume that $p_0 = \mathrm{N}(0, \Sigma)$ with $\Sigma \in \mathbb{S}_d(\mathbb{R})_+$. Let $\mathrm{D} \in \mathcal{M}_d(\mathbb{R})_+$ a diagonal positive matrix such that $\Sigma = \mathrm{P}^\top\mathrm{D}\mathrm{P}$ with P an orthonormal matrix. We consider the following forward dynamics

$$\mathrm{d}x_t = -x_t\mathrm{d}t + \sqrt{2}\mathrm{d}w_t,$$

with $\mathcal{L}(x_0) = p_0$. We also consider the backward dynamics given by

$$\mathrm{d}y_t = \{y_t + 2\nabla \log p_{T-t}(y_t)\}\mathrm{d}t + \sqrt{2}\mathrm{d}w_t,$$

with $\mathcal{L}(y_0) = p_\infty = \mathrm{N}(0, \mathrm{Id})$. Note that since for any $t \in [0,T]$ and $x \in \mathbb{R}^d$, $\nabla \log p_t(x) = -\Sigma_t^{-1} x$ with $\Sigma_t = \exp[-2t]\Sigma + (1 - \exp[-2t])\,\mathrm{Id}$, we have that $(y_t)_{t\in[0,T]}$ is a Gaussian process. In particular, we can compute the mean and the covariance matrix of y_t in a closed form for any $t \in [0,T]$. The results of Proposition S5 will not be used to prove Theorem 1. However, they provide some insights regarding the evolution of the mean and covariance of the backward process.

Proposition S5. *For any $t \in [0,T]$, we have that $\mathcal{L}(y_t) = \mathrm{N}(0, \bar{\Sigma}_t)$ with*

$$\bar{\Sigma}_t = \mathrm{P}^\top((1 - \exp[-2t])\bar{\mathrm{D}}_t + \exp[-2t]\bar{\mathrm{D}}_t^2)\mathrm{P},$$

and

$$\bar{\mathrm{D}}_t = (\mathrm{Id} + (\mathrm{D} - \mathrm{Id})\exp[-2(T-t)]) \oslash (\mathrm{Id} + (\mathrm{D} - \mathrm{Id})\exp[-2T])\,.$$

Note that $\bar{\mathrm{D}}_0 = \mathrm{Id}$ and $\bar{\mathrm{D}}_T = \mathrm{D} \oslash (\mathrm{Id} + (\mathrm{D} - \mathrm{Id})\exp[-2T]) \approx \mathrm{D}$. Hence, we have $\bar{\Sigma}_T \approx \Sigma$ and therefore $\mathcal{L}(y_T) \approx p_0$.

Proof. First, note that for any $t \in [0,T]$ we have that

$$y_t = y_0 + \int_0^t (\mathrm{Id} - 2\Sigma_{T-t}^{-1})y_t + \sqrt{2}w_t = y_0 + \int_0^t (\mathrm{Id} - 2\mathrm{P}^\top D_{T-t}^{-1}\mathrm{P})y_t + \sqrt{2}w_t,$$

with $\mathrm{D}_{T-t} = \exp[-2(T-t)]\mathrm{D} + (1 - \exp[-2(T-t)])\,\mathrm{Id}$. Denote $\{y_t^{\mathrm{P}}\}_{t\in[0,T]} = \{\mathrm{P}y_t\}_{t\in[0,T]}$. Using that $\mathrm{P}^\top\mathrm{P} = \mathrm{Id}$, we have that for any $t \in [0,T]$

$$y_t^{\mathrm{P}} = y_0^{\mathrm{P}} + \int_0^t (\mathrm{Id} - 2D_{T-t}^{-1})y_t^{\mathrm{P}} + \sqrt{2}w_t^{\mathrm{P}},$$

where $\{w_t^{\mathrm{P}}\}_{t\in[0,T]} = \{\mathrm{P}w_t\}_{t\in[0,T]}$. Note that since P is orthonormal, $\{w_t^{\mathrm{P}}\}_{t\in[0,T]}$ is also a d-dimensional Brownian motion. We also have that $\mathcal{L}(y_0^{\mathrm{P}}) = \mathrm{N}(0, \mathrm{Id})$. Hence for any $\{\{y_t^{\mathrm{P},i}\}_{t\in[0,T]}\}_{i=1}^d$ is a collection of d independent Gaussian processes, where for any $i \in \{1,\dots,d\}$ and $t \in [0,T]$, $y_t^{\mathrm{P},i} = \langle y_t^{\mathrm{P}}, e_i\rangle$ and $\{e_i\}_{i=1}^d$ is the canonical basis of $\mathbb{R}^d$. Let $i \in \{1,\dots,d\}$ and for any $t \in [0,T]$ denote $u_t^i = \mathbb{E}[y_t^{\mathrm{P},i}]$ and $v_t^i = \mathbb{E}[(y_t^{\mathrm{P},i})^2]$. We have that for any $t \in [0,T]$, $\partial_t u_t^i = (1 - 1/\mathrm{D}_t^i)u_t^i$ with $u_0 = 0$ and $\mathrm{D}_t^i = \exp[-2t]\mathrm{D}_i + 1 - \exp[-2t]$. Hence, we get that for any $t \in [0,T]$, $u_t^i = 0$. Using Itô's lemma we have that

$$\partial v_t^i = \{2 - 4/\mathrm{D}_{T-t}^i\}v_t^i + 2, \tag{S12}$$

with $v_0^i = 1$. Denote $\alpha_T^i = (\mathrm{D}^i - 1)\exp[-2T]$, we have that for any $t \in [0,T]$, $\mathrm{D}_{T-t}^i = 1 + \alpha_T^i \exp[2t]$. Therefore, we get that for any $t \in [0,T]$

$$2 - 4/\mathrm{D}_{T-t}^i = -2 + 2 \times (2\alpha_T^i)\exp[2t]/(1 + \alpha_T^i \exp[2t]) = -2 + 2\partial_t \log(1 + \alpha_T^i \exp[2t]).$$

Hence, we have that for any $t \in [0,T]$

$$\int_0^t 2 - 4/\mathrm{D}_{T-s}^i \mathrm{d}s = -2t + \log((1 + \alpha_T^i \exp[2t])^2/(1 + \alpha_T^i)^2).$$

Hence, there exists $C_t^i \in \mathrm{C}^1([0,T],\mathbb{R})$ such that for any $t \in [0,T]$, $v_t^i = C_t^i \exp[-2t](1 + \alpha_T^i \exp[2t])^2/(1 + \alpha_T^i)^2$. Using (S12), we have that for any $t \in [0,T]$

$$\partial_t C_t^i = 2\exp[2t]((1 + \alpha_T^i \exp[2t])/(1 + \alpha_T^i))^{-2} = -(1/\alpha_T^i)(1 + \alpha_T^i)^2 \partial_t (1 + \alpha_T^i \exp[2t])^{-1}.$$

Hence, we have that for any $t \in [0,T]$

$$C_t^i = (1/\alpha_T^i)(1 + \alpha_T^i)^2[(1 + \alpha_T^i)^{-1} - (1 + \alpha_T^i \exp[2t])^{-1}] + A,$$

with $A \geq 0$. Hence, we get that for any $t \in [0,T]$

$$\begin{aligned} v_t^i = (1/\alpha_T^i)\exp[-2t](1 + \alpha_T^i \exp[2t])[(1 + \alpha_T^i \exp[2t])/(1 + \alpha_T^i) - 1] \\ + A\exp[-2t](1 + \alpha_T^i \exp[2t])^2/(1 + \alpha_T^i)^2. \end{aligned}$$

In addition, we have that $v_0^i = 1$ and therefore $A = 1$. Therefore, for any $t \in [0,T]$ we have

$$\begin{aligned} v_t^i &= (1/\alpha_T^i)\exp[-2t](1 + \alpha_T^i \exp[2t])[(1 + \alpha_T^i \exp[2t])/(1 + \alpha_T^i) - 1] \\ &\quad + \exp[-2t](1 + \alpha_T^i \exp[2t])^2/(1 + \alpha_T^i)^2 \\ &= (1 - \exp[-2t])(1 + \alpha_T^i \exp[2t])/(1 + \alpha_T^i) + \exp[-2t](1 + \alpha_T^i \exp[2t])^2/(1 + \alpha_T^i)^2, \end{aligned}$$

which concludes the proof. □

S5.2 Convergence results for the discretization

In what follows, we denote $(Y_k)_{k\in\{0,\dots,N-1\}} = (\bar{x}_{t_k})_{k\in\{0,\dots,N-1\}}$, the sequence given by (6). The following result gives an expansion of the covariance matrix and the mean of Y_N, i.e. the output of SGM, in the case where $p = \mathrm{N}(\mu, \Sigma)$.

Theorem S6. *Let $N \in \mathbb{N}$, $\delta > 0$ and $T = N\delta$. Then, we have that $\bar{x}_{t_N} \sim \mathrm{N}(\hat{\mu}_N, \hat{\Sigma}_N)$ with*

$$\hat{\Sigma}_N = \Sigma + \exp[-4T]\hat{\Sigma}_T + \delta\hat{\mathrm{E}}_T + \delta^2 \mathrm{R}_{T,\delta} \;, \qquad \hat{\mu}_N = \mu + \exp[-2T]\hat{\mu}_T + \delta\hat{e}_T + \delta^2 r_{T,\delta} \;,$$

where $\hat{\Sigma}_T, \hat{\mathrm{E}}_T, \mathrm{R}_{T,\delta} \in \mathbb{R}^{d\times d}$, $\hat{\mu}_T, \hat{e}_T, r_{T,\delta} \in \mathbb{R}^d$ and $\|\mathrm{R}_{T,\delta}\| + \|r_{T,\delta}\| \leq R$ not dependent on $T \geq 0$ and $\delta > 0$. We have that

$$\begin{aligned}
\hat{\Sigma}_T &= -(\Sigma - \mathrm{Id})(\Sigma\Sigma_T^{-1})^2 \;, \\
\hat{\mathrm{E}}_T &= \mathrm{Id} - (1/2)\Sigma^2(\Sigma - \mathrm{Id})^{-1}\log(\Sigma) + \exp[-2T]\tilde{\mathrm{E}}_T \;.
\end{aligned} \tag{S13}$$

In addition, we have

$$\begin{aligned}
\hat{\mu}_T &= -\Sigma_T^{-1}\Sigma\mu \;, \\
\hat{e}_T &= \{-2\Sigma^{-1} - (1/4)\Sigma(\Sigma - \mathrm{Id})^{-1}\log(\Sigma)\}\mu + \exp[-2T]\tilde{\mu}_T \;,
\end{aligned}$$

with $\tilde{\mathrm{E}}_T, \tilde{\mu}_T$ bounded and not dependent on T.

Before turning to the proof of Theorem S6, we state a few consequences of this result.

Corollary S7. *Let $\{\bar{x}_{t_k}\}_{k=0}^N$ the sequence defined by (6). We have that $\bar{x}_{t_N} \sim \mathrm{N}(\mu_N, \Sigma_N)$ with*

$$\begin{aligned}
\Sigma_N &= \Sigma + \delta\Sigma_\delta + \exp[-4T]\Sigma_T + \Sigma_{\delta,T} \;, \\
\mu_N &= \mu + \delta\mu_\delta + \exp[-2T]\mu_T + \mu_{\delta,T} \;,
\end{aligned}$$

with

$$\begin{aligned}
\Sigma_T &= -(\Sigma - \mathrm{Id})\Sigma^2 \;, \\
\Sigma_\delta &= \mathrm{Id} - (1/2)\Sigma^2(\Sigma - \mathrm{Id})^{-1}\log(\Sigma) \;, \\
\mu_T &= \Sigma\mu, \\
\mu_\delta &= \{-2\Sigma^{-1} - (1/4)\Sigma(\Sigma - \mathrm{Id})^{-1}\log(\Sigma)\}\mu \;.
\end{aligned}$$

In addition, we have $\lim_{\delta\to 0, T\to+\infty} \|\Sigma_{\delta,T}\|/(\delta + \exp[-4T]) = 0$ and $\lim_{\delta\to 0, T\to+\infty} \|\mu_{\delta,T}\|/(\delta + \exp[-2T]) = 0$.

At first sight, it might appear surprising that Σ^{-1} does not appear in Σ_T and μ_T. Note that in the extreme case where $\Sigma = 0$ and $\delta \to 0$, i.e. we only consider the error associated with the fact that $T \neq +\infty$, then we have no error. This is because in this case the associated continuous-time process is an Ornstein-Uhlenbeck bridge which has distribution $\mathrm{N}(\mu, 0)$ at time T.

We will use the following result.

Lemma S8. *Let $\pi_i = \mathrm{N}(\mu_i, \Sigma_i)$ for $i \in \{0, 1\}$, with $\mu_0, \mu_1 \in \mathbb{R}^d$ and $\Sigma_0, \Sigma_1 \in \mathbb{S}_d(\mathbb{R})_+$. Then, we have that*

$$\mathrm{KL}(\pi_0\|\pi_1) = (1/2)\{\log(\det(\Sigma_1)/\det(\Sigma_0)) - d + \mathrm{Tr}(\Sigma_1^{-1}\Sigma_0) + (\mu_1 - \mu_0)^\top\Sigma_1^{-1}(\mu_1 - \mu_0)\}.$$

In particular, applying Lemma S8 we have that for any $\Sigma \in \mathbb{S}_d(\mathbb{R})_+$

$$\mathrm{KL}(\mathrm{N}(0, \Sigma)\|\mathrm{N}(0, \mathrm{Id})) = (1/2)\{-\log(\det(\Sigma)) + \mathrm{Tr}(\Sigma) - d\}. \tag{S14}$$

Proposition S9. *Let $\{\bar{x}_{t_k}\}_{k=0}^N$ the sequence defined by (6). We have that $\bar{x}_{t_N} \sim \mathrm{N}(\mu_N, \Sigma_N)$, with μ_N, Σ_N given by Corollary S7. We have that*

$$\mathrm{KL}(\mathrm{N}(\mu, \Sigma)\|\mathrm{N}(\mu_N, \Sigma_N)) \leq \delta|\,\mathrm{Tr}(\Sigma^{-1}\Sigma_\delta)| + \exp[-4T]|\,\mathrm{Tr}(\Sigma^{-1}\Sigma_T)| + \exp[-4T]\mu^\top\Sigma\mu + E_{T,\delta} \;,$$

with $E_{T,\delta}$ a higher order term such that $\lim_{T\to+\infty,\delta\to 0} E_{T,\delta}/(\delta + \exp[-4T]) = 0$.

We now prove Theorem S6.

Proof. For any k, denote $Y_k = \bar{x}_{t_{N-k}}$. First, we recall that for any $k \in \{0, \dots, N-1\}$ and $x \in \mathbb{R}^d$, $\nabla \log p_{T-k\gamma}(x) = -\Sigma_{T-k\gamma}^{-1} x$ where for any $t \in [0, T]$

$$\Sigma_t = (1 - \exp[-2t])\,\mathrm{Id} + \exp[-2t]\Sigma \ .$$

Hence, we get that for any $k \in \{0, \dots, N-1\}$

$$Y_{k+1} = ((1+\gamma)\,\mathrm{Id} - 2\gamma\Sigma_{T-k\gamma}^{-1})Y_k + 2\gamma\Sigma_{T-k\gamma}^{-1} M_{T-k\gamma} + \sqrt{2\gamma} Z_{k+1} \ , \tag{S15}$$

where for any $t \in [0, T]$, $M_t = \exp[-t]\mu$. Therefore, we get that for any $k \in \{0, \dots, N\}$, Y_k is a Gaussian random variable. Using (S23), we have that for any $k \in \{0, \dots, N-1\}$

$$\mathbb{E}[\hat{Y}_{k+1}\hat{Y}_{k+1}^\top] = ((1+\gamma)\,\mathrm{Id} - 2\gamma\Sigma_{T-k\gamma}^{-1})\mathbb{E}[\hat{Y}_k\hat{Y}_k^\top]((1+\gamma)\,\mathrm{Id} - 2\gamma\Sigma_{T-k\gamma}^{-1}) + 2\gamma\,\mathrm{Id} \ , \tag{S16}$$

where for any $k \in \{0, \dots, N\}$, $\hat{Y}_k = Y_k - \mathbb{E}[Y_k]$. There exists $\mathrm{P} \in \mathbb{R}^{d\times d}$ orthogonal such that $\mathrm{D} = \mathrm{P}\Sigma\mathrm{P}^\top$ is diagonal. Note that for any $k \in \{0, \dots, N-1\}$, we have that $\Lambda_k = \mathrm{P}((1+\gamma)\,\mathrm{Id} - 2\gamma\Sigma_{T-k\gamma}^{-1})\mathrm{P}^\top$ is diagonal. For any $k \in \{0, \dots, N\}$, define $\mathrm{H}_k = \mathrm{P}\mathbb{E}[\hat{Y}_k\hat{Y}_k^\top]\mathrm{P}^\top$. Note that $\mathrm{H}_0 = \mathrm{Id}$. Using (S16), we have that for any $k \in \{0, \dots, N-1\}$

$$\mathrm{H}_{k+1} = \Lambda_k^2 \mathrm{H}_k + 2\gamma\,\mathrm{Id} \ . \tag{S17}$$

Hence, for any $k \in \{0, \dots, N\}$, H_k is diagonal. For any diagonal matrix $C \in \mathbb{R}^{d\times d}$ denote $\{c^1, \dots, c^d\}$ its diagonal elements. Let $i \in \{1, \dots, d\}$. Using (S17), we have that for any $k \in \{0, \dots, N-1\}$

$$h_{k+1}^i = (\lambda_k^i)^2 h_k^i + 2\gamma \ .$$

Using this result we have that for any $k \in \{0, \dots, N\}$

$$h_k^i = (\textstyle\prod_{\ell=0}^{k-1} \lambda_\ell^i)^2 + 2\gamma \sum_{\ell=0}^{k-1} (\prod_{j=0}^{\ell-1} \lambda_{k-1-j}^i)^2 = (\prod_{\ell=0}^{k-1} \lambda_\ell^i)^2 + 2\gamma \sum_{\ell=0}^{k-1} (\prod_{j=k-\ell}^{k-1} \lambda_j^i)^2 \ .$$

Let $k_1, k_2 \in \{0, \dots, N\}$ with $k_1 < k_2$. In what follows, we derive an expansion of $I_{k_1,k_2} = \prod_{k=k_1}^{k_2} \lambda_k^i$ w.r.t. $\gamma > 0$. We have that

$$I_{k_1,k_2} = \textstyle\prod_{k=k_1}^{k_2} \lambda_k^i = \exp[\sum_{k=k_1}^{k_2} \log(\lambda_k^i)] = \exp[\sum_{k=k_1}^{k_2} \log(1+\gamma a_k^i)] \ , \tag{S18}$$

where for any $k \in \{0, \dots, N\}$, $a_k^i = 1 - 2/d_{(N-k)\gamma}^i$, with $d_{(N-k)\gamma}^i = 1 + \exp[-2(N-k)\gamma](d^i - 1)$. Hence, there exist $(b_{k,\gamma}^i)_{k\in\{0,\dots,N\}}$ bounded such that for any $k \in \{0, \dots, N\}$ we have

$$\log(1+\gamma a_k^i) = \gamma a_k^i - (\gamma^2/2)(a_k^i)^2 + \gamma^3 b_{k,\gamma}^i \ .$$

In addition, using Proposition S10, there exists $C_{k_1,k_2}^\gamma \geq 0$ such that $\gamma C_{k_1,k_2}^\gamma \leq C$ with $C \geq 0$ not dependent on $k_2, k_2 \in \{0, \dots, N\}$, $\gamma > 0$ and

$$\textstyle\sum_{k=k_1}^{k_2} \log(1+\gamma a_k^i) = \int_{t_1}^{t_2^+} a^i(t)\mathrm{d}t - (\gamma/2)[\int_{t_1}^{t_2^+} a^i(t)^2\mathrm{d}t + a^i(t_2^+) - a^i(t_1)] + C_{k_1,k_2}^\gamma \gamma^3 \ ,$$

with $t_1 = k_1\gamma$, $t_2^+ = (k_2+1)\gamma$ and for any $t \in [0, T]$, $a_t = 1 - 2/d_{T-t}^i$ with $d_{T-t}^i = 1 + \exp[-2(T-t)](d^i - 1)$. Hence, using this result and (S18), we get that there exists $D_{k_1,k_2}^\gamma \geq 0$ such that $\gamma D_{k_1,k_2}^\gamma \leq D$ with $D \geq 0$ not dependent on $k_2, k_2 \in \{0, \dots, N\}$, $\gamma > 0$ and

$$I_{k_1,k_2} = \exp[\textstyle\int_{t_1}^{t_2^+} a^i(t)\mathrm{d}t] - \exp[\int_{t_1}^{t_2^+} a^i(t)](\gamma/2)[\int_{t_1}^{t_2^+} a^i(t)^2\mathrm{d}t + a^i(t_2^+) - a^i(t_1)] + \gamma^3 D_{k_1,k_2}^\gamma \ . \tag{S19}$$

Using this result, we get that there exists $E_1^\gamma \geq 0$ such that $\gamma E_1^\gamma \leq E$ with $E \geq 0$ not dependent on γ such that

$$(\textstyle\prod_{\ell=0}^{N-1} \lambda_\ell^i)^2 = \exp[2\int_0^T a^i(t)\mathrm{d}t] - \gamma \exp[2\int_0^T a^i(t)\mathrm{d}t][\int_0^T a^i(t)^2\mathrm{d}t + a^i(T) - a^i(0)] + \gamma^3 E_1^\gamma \ . \tag{S20}$$

Similarly, using (S19), there exist $E \geq 0$ and $(E_{2,\ell}^\gamma)_{\ell\in\{0,\dots,N\}}$ such that for any $\ell \in \{0, \dots, N\}$, $E_{2,\ell}^\gamma \geq 0$ and $\gamma E_{2,\ell}^\gamma \leq E$ with $E \geq 0$ not dependent on γ and ℓ such that

$$\begin{aligned}
2\gamma \textstyle\sum_{\ell=0}^{N-1} (\prod_{j=N-\ell}^{N-1} \lambda_j^i)^2 &= (2\gamma) \textstyle\sum_{\ell=0}^{N-1} \exp[2\int_{T-\ell\gamma}^T a^i(t)\mathrm{d}t]\} \\
&\quad -2\gamma^2 \textstyle\sum_{\ell=0}^{N-1} \{\exp[2\int_{T-\ell\gamma}^T a^i(t)\mathrm{d}t][\int_{T-\ell\gamma}^T a^i(t)^2\mathrm{d}t + a^i(T) - a^i(T-\ell\gamma)]\} \\
&\quad + \gamma^4 \textstyle\sum_{\ell=0}^{N-1} E_{2,\ell}^\gamma \ .
\end{aligned}$$

Therefore, using Proposition S10, there exists E_3^γ such that $\gamma E_3^\gamma \leq E$ with $E \geq 0$ not dependent on γ and

$$2\gamma \sum_{\ell=0}^{N-1} (\prod_{j=N-\ell}^{N-1} \lambda_j^i)^2 = 2\int_0^T \exp[2\int_{T-t}^T a^i(s)\mathrm{d}s]\mathrm{d}t + \gamma(1 - \exp[2\int_0^T a^i(t)\mathrm{d}t]) \\ -2\gamma \int_0^T \{\exp[2\int_{T-t}^T a^i(s)\mathrm{d}s][\int_{T-t}^T a^i(s)^2\mathrm{d}t + a^i(T) - a^i(T-t)]\}\mathrm{d}t \\ + \gamma^3 E_3^\gamma \ . \tag{S21}$$

Hence, combining (S20) and (S21) we get that

$$h_N^i = c_T^i - \gamma e_T^i + \gamma^3 E^\gamma \ ,$$

with

$$c_T^i = \exp[2\int_0^T a^i(t)\mathrm{d}t] + 2\int_0^T \exp[2\int_{T-t}^T a^i(s)\mathrm{d}s]\mathrm{d}t \ . \tag{S22}$$

and

$$e_T^i = -\exp[2\int_0^T a^i(t)\mathrm{d}t][\int_0^T a^i(t)^2\mathrm{d}t + a^i(T) - a^i(0)] + 1 - \exp[2\int_0^T a^i(t)\mathrm{d}t] \\ -2\int_0^T \exp[2\int_{T-t}^T a^i(s)\mathrm{d}s][\int_{T-t}^T a^i(s)^2\mathrm{d}s + a^i(T) - a^i(T-t)]\mathrm{d}t \ .$$

In what follows, we compute c_T^i and e_T^i.

(i) Using Lemma S11 we have

$$\exp[2\int_0^T a^i(t)\mathrm{d}t] = d^2 \exp[-2T]/(1 + \exp[-2T](d-1))^2 \ .$$

In addition, using Lemma S12 we have

$$\int_0^T \exp[2\int_{T-t}^T a^i(s)\mathrm{d}s] = (d/2)(1 - \exp[-2T])/(1 + \exp[-2T](d-1)) \ .$$

Combining these results and (S22), we get that

$$c_T^i = d + d^2 \exp[-2T](1 - (1 + \exp[-2T](d-1))^{-1})/(1 + \exp[-2T](d-1)) \\ = d + d^2(d-1)\exp[-4T]/(1 + \exp[-2T](d-1))^2 \ .$$

(ii) We conclude for e_T^i using Proposition S20 with $\lambda = d^i - 1$.

This concludes the proof of (S13). Next, we compute the evolution of the mean. Using (S23), we have

$$\mathbb{E}[Y_{k+1}] = ((1+\gamma)\,\mathrm{Id} - 2\gamma\Sigma_{T-k\gamma}^{-1})\mathbb{E}[Y_k] + 2\gamma\mathbb{E}[\Sigma_{T-k\gamma}^{-1} M_{T-k\gamma}] \ , \tag{S23}$$

Note that for any $k \in \{0, \ldots, N-1\}$, we have that $\Lambda_k = \mathrm{P}((1+\gamma)\,\mathrm{Id} - 2\gamma\Sigma_{T-k\gamma}^{-1})\mathrm{P}^\top$ is diagonal. For any $k \in \{0, \ldots, N\}$, define $\mathrm{H}_k = \mathrm{P}\mathbb{E}[Y_k]\mathrm{P}^\top$. Note that $\mathrm{H}_0 = 0$. For any $k \in \{0, \ldots, N-1\}$ we have that

$$\mathrm{H}_{k+1} = \Lambda_k \mathrm{H}_k + 2\gamma \mathrm{D}_{T-k\gamma}^{-1} \mathrm{V}_{T-k\gamma} \ , \tag{S24}$$

where for any $t \in [0,T]$, $\mathrm{D}_t = \mathrm{P}\Sigma_t\mathrm{P}^\top$ and $\mathrm{V}_t = \mathrm{P}M_t$. Let $i \in \{1, \ldots, d\}$. Using (S24), we have for any $k \in \{0, \ldots, N-1\}$

$$h_{k+1}^i = \lambda_k^i h_k^i + 2\gamma v_{T-k\gamma}^i / d_{T-k\gamma}^i \ . \tag{S25}$$

In what follows, we define for any $t \in [0,T]$, $r(t)^i = v_{T-t}^i / d_{T-t}^i$ and note that for any $t \in [0,T]$

$$r(t)^i = \exp[-(T-t)]/(1 + \exp[-2(T-t)](d^i - 1))(\mathrm{P}\mu)^i \ . \tag{S26}$$

Using (S25) and that $h_0^i = 0$, we have that for any $k \in \{0, \ldots, N\}$

$$h_k^i = 2\gamma \sum_{\ell=0}^{k-1} r((k-\ell-1)\gamma) \prod_{j=0}^{\ell-1} \lambda_{k-1-j}^i = 2\gamma \sum_{\ell=0}^{k-1} r((k-\ell-1)\gamma) \prod_{j=k-\ell}^{k-1} \lambda_j^i \ .$$

Using (S19), we get that there exists $D^\gamma \geq 0$ such that $\gamma D^\gamma \leq D$ not dependent on γ and

$$\begin{aligned}
h_N^i &= 2\gamma \textstyle\sum_{k=0}^{N-1} r(T-(k+1)\gamma) \exp[\int_{T-k\gamma}^T a^i(t)\mathrm{d}t] \\
&\quad -\gamma^2 \textstyle\sum_{k=0}^{N-1} r(T-(k+1)\gamma) \exp[\int_{T-k\gamma}^T a^i(t)\mathrm{d}t][\int_{T-k\gamma}^T a^i(t)^2\mathrm{d}t + a^i(T) - a^i(T-k\gamma)] \\
&\quad + \textstyle\sum_{k=0}^{N-1} \gamma^4 D_{k,N}^\gamma \\
&= 2\gamma \textstyle\sum_{k=0}^{N-1} r(T-(k+1)\gamma) \exp[\int_{T-k\gamma}^T a^i(t)\mathrm{d}t] \\
&\quad -\gamma^2 \textstyle\sum_{k=0}^{N-1} r(T-(k+1)\gamma) \exp[\int_{T-k\gamma}^T a^i(t)\mathrm{d}t][\int_{T-k\gamma}^T a^i(t)^2\mathrm{d}t + a^i(T) - a^i(T-k\gamma)] \\
&\quad +\gamma^3 D^\gamma \, .
\end{aligned}$$

Using Proposition S10, we get that there exists $E^\gamma \geq 0$ such that $\gamma E^\gamma \leq E$ not dependent on γ and

$$\begin{aligned}
h_N^i &= 2\gamma \textstyle\sum_{k=0}^{N-1} r(T-(k+1)\gamma) \exp[\int_{T-k\gamma}^T a^i(t)\mathrm{d}t] \\
&\quad -\gamma \textstyle\int_0^T r(T-t) \exp[\int_{T-t}^T a^i(s)\mathrm{d}s][\int_{T-t}^T a^i(t)^2\mathrm{d}t + a^i(T) - a^i(T-t)]\mathrm{d}t \\
&\quad +\gamma^3 E^\gamma \, .
\end{aligned}$$

In addition, for any $k \in \{0, \ldots, N\}$, there exists $u_k \geq 0$ with $u_k \leq u$ and $u \geq 0$ not dependent on k and

$$r(T-(k+1)\gamma) = r(T-k\gamma) - r'(T-k\gamma)\gamma + u_k\gamma^2 \, .$$

Using this result, we get that exists $F^\gamma \geq 0$ such that $\gamma F^\gamma \leq F$ not dependent on γ and

$$\begin{aligned}
h_N^i &= 2\gamma \textstyle\sum_{k=0}^{N-1} r(T-k\gamma) \exp[\int_{T-k\gamma}^T a^i(t)\mathrm{d}t] \\
&\quad -2\gamma^2 \textstyle\sum_{k=0}^{N-1} r'(T-k\gamma) \exp[\int_{T-k\gamma}^T a^i(t)\mathrm{d}t] \\
&\quad -\gamma \textstyle\int_0^T r(T-t) \exp[\int_{T-t}^T a^i(s)\mathrm{d}s][\int_{T-t}^T a^i(t)^2\mathrm{d}t + a^i(T) - a^i(T-t)]\mathrm{d}t \\
&\quad +\gamma^3 F^\gamma \, .
\end{aligned}$$

Using Proposition S10, we get that there exists $G^\gamma \geq 0$ such that $\gamma G^\gamma \leq G$ not dependent on γ and

$$\begin{aligned}
h_N^i &= 2\gamma \textstyle\sum_{k=0}^{N-1} r(T-k\gamma) \exp[\int_{T-k\gamma}^T a^i(t)\mathrm{d}t] \\
&\quad -2\gamma \textstyle\int_0^T r'(T-t) \exp[\int_{T-t}^T a^i(t)\mathrm{d}s]\mathrm{d}t \\
&\quad -\gamma \textstyle\int_0^T r(T-t) \exp[\int_{T-t}^T a^i(s)\mathrm{d}s][\int_{T-t}^T a^i(t)^2\mathrm{d}t + a^i(T) - a^i(T-t)]\mathrm{d}t \\
&\quad +\gamma^3 G^\gamma \, .
\end{aligned}$$

In addition, using Proposition S10, we get that there exists $H^\gamma \geq 0$ such that $\gamma H^\gamma \leq H$ not dependent on γ and

$$\begin{aligned}
h_N^i &= 2 \textstyle\int_0^T r(T-t) \exp[\int_{T-t}^T a^i(s)\mathrm{d}s]\mathrm{d}t \\
&\quad -\gamma\{r(0)\exp[\textstyle\int_0^T a^i(t)\mathrm{d}t] - r(T)\} - 2\gamma \textstyle\int_0^T r'(T-t) \exp[\int_{T-t}^T a^i(s)\mathrm{d}s]\mathrm{d}t \\
&\quad -\gamma \textstyle\int_0^T r(T-t) \exp[\int_{T-t}^T a^i(s)\mathrm{d}s][\int_{T-t}^T a^i(t)^2\mathrm{d}t + a^i(T) - a^i(T-t)]\mathrm{d}t \\
&\quad +\gamma^3 H^\gamma \, .
\end{aligned} \tag{S27}$$

In addition, we have by integration by part

$$\begin{aligned}
&\textstyle\int_0^T r'(T-t) \exp[\int_{T-t}^T a^i(s)\mathrm{d}s]\mathrm{d}t \\
&\qquad = -\{r(0)\exp[\textstyle\int_0^T a^i(t)\mathrm{d}t] - r(T)\} - \textstyle\int_0^T r(T-t)a^i(T-t) \exp[\int_{T-t}^T a^i(s)\mathrm{d}s]\mathrm{d}t \, .
\end{aligned}$$

Combining this result and (S27) we get that

$$\begin{aligned}
h_N^i &= 2 \textstyle\int_0^T r(T-t) \exp[\int_{T-t}^T a^i(s)\mathrm{d}s]\mathrm{d}t \\
&\quad +\gamma\{r(0)\exp[\textstyle\int_0^T a^i(t)\mathrm{d}t] - r(T)\} \\
&\quad -\gamma \textstyle\int_0^T r(T-t) \exp[\int_{T-t}^T a^i(s)\mathrm{d}s][\int_{T-t}^T a^i(t)^2\mathrm{d}t + a^i(T) - 3a^i(T-t)]\mathrm{d}t \\
&\quad +\gamma^3 H^\gamma \, .
\end{aligned} \tag{S28}$$

In what follows, we assume that $d^i \neq 0$. The case where $d^i = 0$ is left to the reader. Finally using (S26) and Lemma S11 we have that for any $t \in [0,T]$

$$\begin{aligned}\exp[\textstyle\int_{T-t}^T a^i(s)\mathrm{d}s]r(T-t)^i &= \exp[-2t]/(1+\exp[-2t](d^i-1))^2(\mathrm{P}\mu)^i d^i \\ &= \exp[2\textstyle\int_{T-t}^T a^i(s)\mathrm{d}s](\mathrm{P}\mu)^i/d^i \ .\end{aligned}$$

Therefore, combining this result and (S28), we get that

$$\begin{aligned}h_N^i = (\mathrm{P}\mu)^i/d^i[2\textstyle\int_0^T \exp[2\int_{T-t}^T a^i(s)\mathrm{d}s]\mathrm{d}t \\ +\gamma\{\exp[2\textstyle\int_0^T a^i(t)\mathrm{d}t]-1\} \\ -\gamma\textstyle\int_0^T \exp[2\int_{T-t}^T a^i(s)\mathrm{d}s][\int_{T-t}^T a^i(t)^2\mathrm{d}t + a^i(T) - 3a^i(T-t)]\mathrm{d}t] \\ +\gamma^3 H^\gamma \ ,\end{aligned}$$

which concludes the proof upon using Lemma S12 and Proposition S21. □

S5.3 Technical lemmas

We are going to make use of the following lemma which is a direct consequence of the Euler-MacLaurin formula.

Proposition S10. *Let $f \in \mathrm{C}^\infty([0,T])$, and $(u_k^\gamma)_{k\in\{0,\dots,N-1\}}$ with $N \in \mathbb{N}$ and $\gamma = T/N > 0$ such that for any $k \in \{0,\dots,N-1\}$, $u_k^\gamma = f(k\gamma)$. Then, there exists $C \geq 0$ such that*

$$\textstyle\int_0^T f(t)\mathrm{d}t - \gamma\sum_{k=0}^{N-1} u_k^\gamma - (\gamma/2)\{f(T)-f(0)\} = C\gamma^2 \ .$$

Proof. Apply the classical Euler-MacLaurin formula to $t \mapsto f(t\gamma)$. □

We will also use the following lemmas.

Lemma S11. *Let $\lambda \in (-1,+\infty)$ and $a : [0,T] \to \mathbb{R}$ such that for any $t \in [0,T]$,*

$$a(t) = 1 - 2/(1+\exp[-2(T-t)]\lambda) \ .$$

Then, we have that for any $t \in [0,T]$,

$$\textstyle\int_{T-t}^T a(s)\mathrm{d}s = t + \log((1+\lambda)/(\exp[2t]+\lambda)) \ .$$

In particular, we have that for any $t \in [0,T]$

$$\exp[2\textstyle\int_{T-t}^T a(s)\mathrm{d}s] = \exp[-2t](1+\lambda)^2/(1+\lambda\exp[-2t])^2 \ .$$

Proof. Let $t \in [0,T]$. We have that $\int_{T-t}^T a(s)\mathrm{d}s = \int_0^t a(T-s)\mathrm{d}s$. Define b such that for any $t \in [0,T]$, $b(t) = a(T-t)$. In particular, we have that for any $t \in [0,T]$

$$b(t) = 1 - 2/(1+\lambda\exp[-2t]) \ .$$

Hence, we have

$$\begin{aligned}\textstyle\int_0^t b(s)\mathrm{d}s &= t - 2\int_0^t (1+\lambda\exp[-2s])^{-1}\mathrm{d}s \\ &= t - \textstyle\int_0^t 2\exp[2s]/(\exp[2s]+\lambda)\mathrm{d}s \\ &= t + \log((1+\lambda)/(\exp[2t]+\lambda)) \ ,\end{aligned}$$

which concludes the proof. □

Lemma S12. *Let $\lambda \in (-1,+\infty)$ and $a : [0,T] \to \mathbb{R}$ such that for any $t \in [0,T]$,*

$$a(t) = 1 - 2/(1+\exp[-2(T-t)]\lambda) \ .$$

Then, we have that for any $t \in [0,T]$,

$$\begin{aligned}\textstyle\int_0^t \exp[2\int_{T-s}^T a(u)\mathrm{d}u]\mathrm{d}s &= (1/2)(1+\lambda)^2[(1+\lambda\exp[-2t])^{-1} - 1/(1+\lambda)]/\lambda \\ &= (1/2)(1+\lambda)(1-\exp[-2t])/(1+\lambda\exp[-2t]) \ .\end{aligned}$$

Proof. Let $t \in [0,T]$. Using Lemma S11 we have that for any $s \in [0,T]$

$$\exp[2\int_{T-s}^{T} a(u)\mathrm{d}u] = (1+\lambda)^2 \exp[2s]/(\lambda + \exp[2s])^2 = (1+\lambda)^2 \exp[-2s]/(1+\lambda\exp[-2s])^2 \ .$$

Assume that $\lambda \neq 0$. Then, we have that

$$\begin{aligned}\int_0^t \exp[2\int_{T-s}^{T} a(u)\mathrm{d}u]\mathrm{d}s &= (1/2)(1+\lambda)^2/\lambda \int_0^t 2\lambda \exp[-2t]/(1+\lambda\exp[-2t])^2 \mathrm{d}s \\ &= (1/2)(1+\lambda)^2[(1+\lambda\exp[-2t])^{-1} - 1/(1+\lambda)]/\lambda \\ &= (1/2)(1+\lambda)(1-\exp[-2t])/(1+\lambda\exp[-2t]) \ .\end{aligned}$$

We conclude the proof upon remarking that his result still holds in the case where $\lambda = 0$. □

Lemma S13. *Let $\lambda \in (-1,+\infty)$ and $a : [0,T] \to \mathbb{R}$ such that for any $t \in [0,T]$,*

$$a(t) = 1 - 2/(1+\exp[-2(T-t)]\lambda) \ .$$

Then, if $\lambda \neq 0$, we have that for any $t \in [0,T]$,

$$\begin{aligned}&\int_0^t \exp[2\int_{T-s}^{T} a(u)\mathrm{d}u]/(1+\lambda\exp[-2s])\mathrm{d}s \\ &\qquad = (1/4)(1+\lambda)^2[(1+\lambda\exp[-2t])^{-2} - 1/(1+\lambda)^2]/\lambda \\ &\qquad = (1/4)(1-\exp[-2t])(2+\lambda(1+\exp[-2t]))/(1+\lambda\exp[-2t])^2 \ .\end{aligned}$$

If $\lambda = 0$ we have

$$\int_0^t \exp[2\int_{T-s}^{T} a(u)\mathrm{d}u]/(1+\lambda\exp[-2s])\mathrm{d}s = (1/2)(1-\exp[-2t]) \ .$$

Proof. Let $t \in [0,T]$. Using Lemma S11 we have that for any $s \in [0,T]$

$$\exp[\int_{T-s}^{T} a(u)\mathrm{d}u]/(1+\lambda\exp[-2s]) = (1+\lambda)^2 \exp[-2s]/(1+\lambda\exp[-2s])^3 \ .$$

Assume that $\lambda \neq 0$. Then, we have that

$$\begin{aligned}\int_0^t \exp[\int_{T-s}^{T} a(u)\mathrm{d}u]/(1+\lambda\exp[-2s])\mathrm{d}s &= (1/2)(1+\lambda)^2/\lambda \int_0^t 2\lambda \exp[-2t]/(1+\lambda\exp[-2t])^3 \mathrm{d}s \\ &= (1/4)(1+\lambda)^2[(1+\lambda\exp[-2t])^{-2} - 1/(1+\lambda)^2]/\lambda \\ &= (1/4)(1-\exp[-2t])(2+\lambda(1+\exp[-2t]))/(1+\lambda\exp[-2t])^2 \ .\end{aligned}$$

We conclude the proof upon remarking that his result still holds in the case where $\lambda = 0$. □

Lemma S14. *Let $\lambda \in (-1,+\infty)$ and $a : [0,T] \to \mathbb{R}$ such that for any $t \in [0,T]$,*

$$a(t) = 1 - 2/(1+\exp[-2(T-t)]\lambda) \ .$$

Then, we have that for any $t \in [0,T]$

$$\begin{aligned}&\int_0^t \exp[2\int_{T-s}^{T} a(u)\mathrm{d}u]a(T-s)\mathrm{d}s \\ &\qquad = -(1/2)(1-\exp[-2t])(1-\lambda^2\exp[-2t])/(1+\lambda\exp[-2t])^2 \ .\end{aligned}$$

Proof. Let $t \in [0,T]$. We have that

$$\begin{aligned}&\int_0^t \exp[2\int_{T-s}^{T} a(u)\mathrm{d}u]a(T-s)\mathrm{d}s \\ &\quad = \int_0^t \exp[2\int_{T-s}^{T} a(u)\mathrm{d}u]\mathrm{d}s - 2\int_0^t \exp[2\int_{T-s}^{T} a(u)\mathrm{d}u]/(1+\lambda\exp[-2s])\mathrm{d}s \ . \qquad \text{(S29)}\end{aligned}$$

Using Lemma S12, we have that

$$\int_0^t \exp[2\int_{T-s}^{T} a(u)\mathrm{d}u]\mathrm{d}t = (1/2)(1+\lambda)(1-\exp[-2t])/(1+\lambda\exp[-2t]) \ . \qquad \text{(S30)}$$

In addition, using Lemma S13, we have

$$\begin{aligned}&\int_0^t \exp[2\int_{T-s}^{T} a(u)\mathrm{d}u]/(1+\lambda\exp[-2s])\mathrm{d}s \\ &\qquad = (1/4)(1-\exp[-2t])(2+\lambda(1+\exp[-2t]))/(1+\lambda\exp[-2t])^2 \ . \qquad \text{(S31)}\end{aligned}$$

Combining (S30) and (S31) in (S29) we have that

$$\begin{aligned}
&\int_0^t \exp[2\int_{T-s}^T a(u)\mathrm{d}u]a(T-s)\mathrm{d}s \\
&\quad = (1/2)(1-\exp[-2t])[(1+\lambda)(1+\lambda\exp[-2t])]/(1+\lambda\exp[-2t])^2 \\
&\qquad - (1/2)(1-\exp[-2t])(2+\lambda(1+\exp[-2t]))/(1+\lambda\exp[-2t])^2 \\
&\quad = -(1/2)(1-\exp[-2t])(1-\lambda^2\exp[-2t])/(1+\lambda\exp[-2t])^2 \;,
\end{aligned}$$

which concludes the proof. □

Lemma S15. *Let $\lambda \in (-1, +\infty)$ we have that for any $t \in [0, T]$*

$$\int_0^t (1+\lambda\exp[-2s])^{-1}\mathrm{d}s = (1/2)\log((\lambda+\exp[2t])/(\lambda+1)) \;.$$

In addition, we have for any $t \in [0, T]$

$$\int_0^t (1+\lambda\exp[-2s])^{-2}\mathrm{d}s = (1/2)\log((\lambda+\exp[2t])/(\lambda+1)) + (\lambda/2)[(\exp[2t]+\lambda)^{-1} - (\lambda+1)^{-1}] \;.$$

Finally, we have that for any $t \in [0, T]$

$$\begin{aligned}
\int_0^t (1+\lambda\exp[-2s])^{-3}\mathrm{d}s &= (1/2)\log((\lambda+\exp[2t])/(\lambda+1)) + \lambda[(\exp[2t]+\lambda)^{-1} - (\lambda+1)^{-1}] \\
&\quad - (\lambda^2/4)[(\exp[2t]+\lambda)^{-2} - (\lambda+1)^{-2}] \;.
\end{aligned}$$

Proof. Let $k \in \{1, 2, 3\}$. Using the change of variable $u \mapsto \exp[2u]$ we have that

$$\int_0^t (1+\lambda\exp[-2s])^{-k}\mathrm{d}s = (1/2)\int_1^{\exp[2t]} u^{k-1}/(u+\lambda)\mathrm{d}u \;.$$

Therefore, we have that

$$\int_0^t (1+\lambda\exp[-2s])^{-1}\mathrm{d}s = (1/2)\int_1^{\exp[2t]} (u+\lambda)^{-1}\mathrm{d}u = (1/2)\log((\lambda+\exp[2t])/(\lambda+1)) \;.$$

In addition, using that for any $u \in [0, T]$, $u = (u+\lambda) - \lambda$ we have that

$$\begin{aligned}
&\int_0^t (1+\lambda\exp[-2s])^{-2}\mathrm{d}s = (1/2)\int_1^{\exp[2t]} u(u+\lambda)^{-2}\mathrm{d}u \\
&\quad = (1/2)\int_1^{\exp[2t]} (u+\lambda)^{-1}\mathrm{d}u - (\lambda/2)\int_1^{\exp[2t]} (u+\lambda)^{-2}\mathrm{d}u \\
&\quad = (1/2)\log((\lambda+\exp[2t])/(\lambda+1)) + (\lambda/2)[(\exp[2t]+\lambda)^{-1} - (\lambda+1)^{-1}] \;.
\end{aligned}$$

Finally, using that for any $u \in [0, T]$, $u \in [0, T]$, $u^2 = (u+\lambda)^2 - 2\lambda(u+\lambda) + \lambda^2$ we have that

$$\begin{aligned}
&\int_0^t (1+\lambda\exp[-2s])^{-3}\mathrm{d}s = (1/2)\int_1^{\exp[2t]} u^2(u+\lambda)^{-2}\mathrm{d}u \\
&\quad = (1/2)\int_1^{\exp[2t]} (u+\lambda)^{-1}\mathrm{d}u - \lambda\int_1^{\exp[2t]} (u+\lambda)^{-2}\mathrm{d}u + (\lambda^2/2)\int_1^{\exp[2t]} (u+\lambda)^{-3}\mathrm{d}u \\
&\quad = (1/2)\log((\lambda+\exp[2t])/(\lambda+1)) + \lambda[(\exp[2t]+\lambda)^{-1} - (\lambda+1)^{-1}] \\
&\qquad - (\lambda^2/4)[(\exp[2t]+\lambda)^{-2} - (\lambda+1)^{-2}] \;,
\end{aligned}$$

which concludes the proof. □

Lemma S16. *Let $\lambda \in (-1, +\infty)$ and $a : [0, T] \to \mathbb{R}$ such that for any $t \in [0, T]$,*

$$a(t) = 1 - 2/(1+\exp[-2(T-t)]\lambda) \;.$$

Then, we have that for any $t \in [0, T]$,

$$\int_{T-t}^T a(s)^2\mathrm{d}s = t - 2\lambda(1-\exp[-2t])/[(1+\lambda)(1+\lambda\exp[-2t])] \;.$$

Proof. Let $t \in [0, T]$. Similarly to the proof of Lemma S11, we have that $\int_{T-t}^T a(s)\mathrm{d}s = \int_0^t a(T-s)\mathrm{d}s$. Define b such that for any $t \in [0, T]$, $b(t) = a(T-t)$. In particular, we have that for any $t \in [0, T]$

$$b(t) = 1 - 2/(1+\lambda\exp[-2t]) \;.$$

We have that

$$\int_{T-t}^{T} a(s)^2 \mathrm{d}s = \int_0^t b(s)^2 \mathrm{d}s = \int_0^t (1 - 4/(1 + \lambda \exp[-2s]) + 4/(1 + \lambda \exp[-2s])^2) \mathrm{d}s \; .$$

Combining this result and Lemma S15, we have

$$\begin{aligned} \int_{T-t}^{T} a(s)^2 \mathrm{d}s &= t + 2\lambda[(\lambda + \exp[2t])^{-1} - (\lambda + 1)^{-1}] \\ &= t - 2\lambda(1 - \exp[-2t])/[(1 + \lambda)(1 + \lambda \exp[-2t])] \; . \end{aligned}$$

□

Lemma S17. *Let $\lambda \in (-1, +\infty)$ and $a : [0, T] \to \mathbb{R}$ such that for any $t \in [0, T]$,*

$$a(t) = 1 - 2/(1 + \exp[-2(T - t)]\lambda) \; .$$

Then, if $\lambda \neq 0$, we have that

$$\begin{aligned} \int_0^T \exp[2 \int_{T-t}^{T} a(s) \mathrm{d}s] (\int_{T-t}^{T} a(s)^2 \mathrm{d}s) \mathrm{d}t &= -(T/2)(1 + \lambda)^2 \exp[-2T]/(1 + \lambda \exp[-2T]) \\ &+ (1 + \lambda)^2/(4\lambda) \log((1 + \lambda)/(1 + \lambda \exp[-2T])) \\ &- (\lambda/2)(1 - \exp[-2T])^2/(1 + \lambda \exp[-2T])^2 \; . \end{aligned} \tag{S32}$$

If $\lambda = 0$, we have that

$$\int_0^T \exp[2 \int_{T-t}^{T} a(s) \mathrm{d}s] (\int_{T-t}^{T} a(s)^2 \mathrm{d}s) \mathrm{d}t = -(T/2) \exp[-2T] + (1/4)(1 - \exp[-2T]) \; . \tag{S33}$$

Note that taking $\lambda \to 0$ in (S32) we recover (S33), using that for any $u > 0$, $\lim_{\lambda \to 0} \log(1 + \lambda u)/\lambda = u$.

Proof. We first start with the case $\lambda \neq 0$. Similarly to the proof of Lemma S11, we have that $\int_{T-t}^{T} a(s) \mathrm{d}s = \int_0^t a(T - s) \mathrm{d}s$. Define b such that for any $t \in [0, T]$, $b(t) = a(T - t)$. We have that

$$\int_0^T \exp[2 \int_{T-t}^{T} a(s) \mathrm{d}s] (\int_{T-t}^{T} a(s)^2 \mathrm{d}s) \mathrm{d}t = \int_0^T \exp[2 \int_{T-t}^{T} a(s) \mathrm{d}s] (\int_0^t b(s)^2 \mathrm{d}s) \mathrm{d}t \; .$$

Let $A : [0, T] \to \mathbb{R}$ such that for any $t \in [0, T]$,

$$A(t) = \int_0^t \exp[2 \int_{T-s}^{T} a(u) \mathrm{d}u] \mathrm{d}s \; .$$

Note that $A(0) = 0$. Hence, by integration by parts, we have

$$\int_0^T \exp[2 \int_{T-t}^{T} a(s) \mathrm{d}s] (\int_0^t b(s)^2 \mathrm{d}s) \mathrm{d}t = A(T) \int_0^T b(t)^2 \mathrm{d}t - \int_0^T A(t) b(t)^2 \mathrm{d}t \; .$$

In what follows, we compute $\int_0^T A(t) b(t)^2 \mathrm{d}t$. First, we recall that for any $t \in [0, T]$

$$b(t)^2 = (1 - 2/(1 + \lambda \exp[-2t]))^2 = 1 - 4/(1 + \lambda \exp[-2t]) + 4/(1 + \lambda \exp[-2t])^2 \; . \tag{S34}$$

In addition, using Lemma S12, we have that for any $t \in [0, T]$

$$A(t) = (1/2)\{(1 + \lambda)^2/(\lambda(1 + \lambda \exp[-2t])) - (1 + \lambda)/\lambda\} \; . \tag{S35}$$

Using (S34) and (S35) we have that for any $t \in [0, T]$

$$\begin{aligned} 2A(t)b(t)^2 &= -(1 + \lambda)/\lambda + [4(1 + \lambda)/\lambda + (1 + \lambda)^2/\lambda] u_1(t) \\ &\quad - [4(1 + \lambda)^2/\lambda + 4(1 + \lambda)/\lambda] u_2(t) + [4(1 + \lambda)^2/\lambda] u_3(t) \\ &= -(1 + \lambda)/\lambda + [(1 + \lambda)(5 + \lambda)/\lambda] u_1(t) \\ &\quad - [4(1 + \lambda)(2 + \lambda)/\lambda] u_2(t) + [4(1 + \lambda)^2/\lambda] u_3(t) \; , \end{aligned} \tag{S36}$$

where for any $k \in \{1, 2, 3\}$ and $t \in [0, T]$ we have

$$u_k(t) = (1 + \lambda \exp[-2t])^{-k} \; .$$

For any $k \in \{0, 1, 2\}$ denote $v_k : [0, T] \to \mathbb{R}$ such that for any $t \in [0, T]$ and $k \in \{1, 2\}$

$$v_0(t) = \log((\lambda + \exp[2t])/(\lambda + 1)) \; , \qquad v_k(t) = (\exp[2t] + \lambda)^{-k} - (1 + \lambda)^{-k} \; .$$

Combining (S36) and Lemma S15, we get that for any $t \in [0, T]$

$$\begin{aligned}
2\int_0^t A(s)b(s)^2\mathrm{d}s &= -[(1+\lambda)/\lambda]t \\
&\quad + (1/2)\{[(1+\lambda)(5+\lambda)/\lambda] - [4(1+\lambda)(2+\lambda)/\lambda] + [4(1+\lambda)^2/\lambda]\}v_0(t) \\
&\quad + \{-(\lambda/2)[4(1+\lambda)(2+\lambda)/\lambda] + \lambda[4(1+\lambda)^2/\lambda]\}v_1(t) \\
&\quad - (\lambda^2/4)[4(1+\lambda)^2/\lambda]v_2(t) \\
&= -[(1+\lambda)/\lambda]t + (1+\lambda)^2/(2\lambda)v_0(t) + 2(1+\lambda)\lambda v_1(t) - \lambda(1+\lambda)^2 v_2(t) \; .
\end{aligned}$$

In addition, we have that

$$\begin{aligned}
-[(1+\lambda)/\lambda]t + (1+\lambda)^2/(2\lambda)v_0(t) &= -[(1+\lambda)/\lambda]t + [(1+\lambda)^2/\lambda]t \\
&\quad + (1+\lambda)^2/(2\lambda)\log((1+\lambda\exp[-2t])/(1+\lambda)) \\
&= (1+\lambda)t + (1+\lambda)^2/(2\lambda)\log((1+\lambda\exp[-2t])/(1+\lambda)) \; .
\end{aligned}$$

Therefore, we get that

$$\begin{aligned}
2\int_0^t A(s)b(s)^2\mathrm{d}s &= (1+\lambda)t + (1+\lambda)^2/(2\lambda)\log((1+\lambda\exp[-2t])/(1+\lambda)) \\
&\quad + 2(1+\lambda)\lambda v_1(t) + \lambda(1+\lambda)^2 v_2(t) \; .
\end{aligned} \tag{S37}$$

In addition, we have that

$$(1+\lambda)\lambda v_1(t) = -\lambda(1-\exp[-2T])/(1+\lambda\exp[-2T]) \; . \tag{S38}$$

We also have that

$$\begin{aligned}
\lambda(1+\lambda)^2 v_2(t) &= \lambda(2\lambda + 1 - 2\lambda\exp[2T] - \exp[4T])/(\exp[2T]+\lambda)^2 \\
&= \lambda(1-\exp[2T])(1+2\lambda+\exp[2T])/(\exp[2T]+\lambda)^2 \\
&= -\lambda(1-\exp[-2T])(1+(1+2\lambda)\exp[-2T])/(1+\lambda\exp[-2T])^2 \; .
\end{aligned} \tag{S39}$$

Finally, using Lemma S12 and Lemma S16 we have

$$\begin{aligned}
A(T)\int_0^T b(t)^2\mathrm{d}t &= (1/2)(1+\lambda)(1-\exp[-2T])/(1+\lambda\exp[-2T]) \\
&\quad \times (T - 2\lambda(1-\exp[-2T])/[(1+\lambda)(1+\lambda\exp[-2T])]) \\
&= (T/2)(1+\lambda)(1-\exp[-2T])/(1+\lambda\exp[-2T]) \\
&\quad - \lambda(1-\exp[-2T])^2/(1+\lambda\exp[-2T])^2 \; .
\end{aligned} \tag{S40}$$

Combining (S37), (S38), (S39) and (S40) we get

$$\begin{aligned}
\int_0^T \exp[2\int_{T-t}^T a(s)\mathrm{d}s](\int_{T-t}^T a(s)^2\mathrm{d}s)\mathrm{d}t &= (T/2)(1+\lambda)(1-\exp[-2T])/(1+\lambda\exp[-2T]) \\
&\quad - \lambda(1-\exp[-2T])^2/(1+\lambda\exp[-2T])^2 \\
&\quad - (1+\lambda)(T/2) + (1+\lambda)^2/(4\lambda)\log((1+\lambda)/(1+\lambda\exp[-2T])) \\
&\quad + \lambda(1-\exp[-2T])/(1+\lambda\exp[-2T]) \\
&\quad - (\lambda/2)(1-\exp[-2T])((1+2\lambda)\exp[-2T]+1)/(1+\lambda\exp[-2T])^2 \; .
\end{aligned} \tag{S41}$$

In addition, we have that

$$\begin{aligned}
&-(\lambda/2)(1-\exp[-2T])^2/(1+\lambda\exp[-2T])^2 \\
&\quad = -\lambda(1-\exp[-2T])^2/(1+\lambda\exp[-2T])^2 \\
&\qquad + \lambda(1-\exp[-2T])/(1+\lambda\exp[-2T]) \\
&\qquad - (\lambda/2)(1-\exp[-2T])((1+2\lambda)\exp[-2T]+1)/(1+\lambda\exp[-2T])^2 \; .
\end{aligned}$$

Combining this result and (S41), we get

$$\begin{aligned}
\int_0^T \exp[2\int_{T-t}^T a(s)\mathrm{d}s](\int_{T-t}^T a(s)^2\mathrm{d}s)\mathrm{d}t &= (T/2)(1+\lambda)(1-\exp[-2T])/(1+\lambda\exp[-2T]) \\
&\quad - (1+\lambda)(T/2) + (1+\lambda)^2/(4\lambda)\log((1+\lambda)/(1+\lambda\exp[-2T])) \\
&\quad - (1/2)(1-\exp[-2T])^2/(1+\lambda\exp[-2T])^2 \; .
\end{aligned} \tag{S42}$$

Finally, we have

$$(T/2)(1+\lambda)(1-\exp[-2T])/(1+\lambda\exp[-2T]) - (T/2)(1+\lambda)$$
$$= -(T/2)(1+\lambda)^2\exp[-2T]/(1+\lambda\exp[-2T]) ,$$

which concludes the proof in the case $\lambda \neq 0$ upon combining this result and (S42). In the case $\lambda = 0$, we have that for any $t \in [0,T]$, $a(t) = -1$ and therefore by integration by part we have

$$\int_0^T \exp[2\int_{T-t}^T a(s)\mathrm{d}s](\int_{T-t}^T a(s)^2\mathrm{d}s)\mathrm{d}t = -(T/2)\exp[-2T] + (1/4)(1-\exp[-2T]) ,$$

which concludes the proof. □

We are now ready to prove the following results.

Proposition S18. *Let $\lambda \in (-1,+\infty)$ and $a : [0,T] \to \mathbb{R}$ such that for any $t \in [0,T]$,*

$$a(t) = 1 - 2/(1+\exp[-2(T-t)]\lambda) .$$

Then, we have that for any $t \in [0,T]$,

$$\exp[2\int_0^T a(t)\mathrm{d}t]\{\int_0^T a(t)^2\mathrm{d}t + a(T) - a(0) + 1\}$$
$$= (T+1)\exp[-2T](\lambda+1)^2/(1+\lambda\exp[-2T])^2 .$$

Proof. First, we have that

$$a(T) - a(0) = 1 - 2/(1+\lambda) - 1 + 2/(1+\lambda\exp[-2T])$$
$$= 2\lambda(1-\exp[-2T])/[(1+\lambda)(1+\lambda\exp[-2T])] . \tag{S43}$$

In addition, using Lemma S16 we have

$$\int_0^T a(s)^2\mathrm{d}s = T - 2\lambda(1-\exp[-2T])/[(1+\lambda)(1+\lambda\exp[-2T])] . \tag{S44}$$

Finally, using Lemma S11 we have that

$$\exp[2\int_0^T a(s)\mathrm{d}s] = \exp[-2T](\lambda+1)^2/(1+\lambda\exp[-2T])^2 . \tag{S45}$$

We conclude the proof upon combining (S43), (S44) and (S45). □

Finally, we have the following proposition.

Proposition S19. *Let $\lambda \in (-1,+\infty)$ and $a : [0,T] \to \mathbb{R}$ such that for any $t \in [0,T]$,*

$$a(t) = 1 - 2/(1+\exp[-2(T-t)]\lambda) .$$

Then, if $\lambda \neq 0$, we have that for any $t \in [0,T]$,

$$\int_0^T \exp[2\int_{T-t}^T a(s)\mathrm{d}s][\int_{T-t}^T a(s)^2\mathrm{d}s + a(T) - a(T-t)]\mathrm{d}t$$
$$= -(T/2)(1+\lambda)^2\exp[-2T]/(1+\lambda\exp[-2T])$$
$$+ (1+\lambda)^2/(4\lambda)\log((1+\lambda)/(1+\lambda\exp[-2T]))$$
$$+ (\lambda/2)\exp[-2T]/(1+\lambda\exp[-2T])^2 .$$

If $\lambda = 0$, we have that

$$\int_0^T \exp[2\int_{T-t}^T a(s)\mathrm{d}s][\int_{T-t}^T a(s)^2\mathrm{d}s + a(T) - a(T-t)]\mathrm{d}t$$
$$= -(T/2)\exp[-2T] + (1/4)(1-\exp[-2T]) .$$

Proof. We assume that $\lambda \neq 0$. The case where $\lambda = 0$ is left to the reader. First, using Lemma S17, we have that

$$\int_0^T \exp[2\int_{T-t}^T a(s)\mathrm{d}s](\int_{T-t}^T a(s)^2\mathrm{d}s)\mathrm{d}t = -(T/2)(1+\lambda)^2\exp[-2T]/(1+\lambda\exp[-2T])$$
$$+ (1+\lambda)^2/(4\lambda)\log((1+\lambda)/(1+\lambda\exp[-2T]))$$
$$+ (3\lambda/2)\exp[-2T](1-\exp[-2T])(1+\lambda)/(1+\lambda\exp[-2T])^2 . \tag{S46}$$

Second, using Lemma S14, we have that

$$\begin{aligned}&\int_0^T \exp[2\int_{T-t}^T a(u)\mathrm{d}u]a(T-t)\mathrm{d}t\\&\quad= -(1/2)(1-\exp[-2T])(1-\lambda^2\exp[-2T])/(1+\lambda\exp[-2T])^2\ .\end{aligned}\tag{S47}$$

Third, using Lemma S12 and that $a(T) = 1 - 2/(1+\lambda)$, we have that

$$\begin{aligned}a(T)\int_0^T \exp[2\int_{T-t}^T a(s)\mathrm{d}s]\mathrm{d}t &= a(T)(1/2)(1+\lambda)(1-\exp[-2T])/(1+\lambda\exp[-2T])\\&= (1/2)(1+\lambda)(1-\exp[-2T])/(1+\lambda\exp[-2T])\\&\quad-(1-\exp[-2T])/(1+\lambda\exp[-2T])\ .\end{aligned}\tag{S48}$$

Combining (S46), (S47) and (S48) we get

$$\begin{aligned}&\int_0^T \exp[2\int_{T-t}^T a(s)\mathrm{d}s][\int_{T-t}^T a(s)^2\mathrm{d}s + a(T) - a(T-t)]\mathrm{d}t\\&\quad= -(T/2)(1+\lambda)^2\exp[-2T]/(1+\lambda\exp[-2T])\\&\qquad+(1+\lambda)^2/(4\lambda)\log((1+\lambda)/(1+\lambda\exp[-2T]))\\&\qquad+(3\lambda/2)\exp[-2T](1-\exp[-2T])(1+\lambda)/(1+\lambda\exp[-2T])^2\\&\qquad+(1/2)(1-\exp[-2T])(1-\lambda^2\exp[-2T])/(1+\lambda\exp[-2T])^2\\&\qquad+(1/2)(1+\lambda)(1-\exp[-2T])/(1+\lambda\exp[-2T])\\&\qquad-(1-\exp[-2T])/(1+\lambda\exp[-2T])\end{aligned}$$

In addition, we have

$$\begin{aligned}&(\lambda/2)(1-\exp[-2T])/(1+\lambda\exp[-2T])^2\\&\quad=(1/2)(1-\exp[-2T])(1-\lambda^2\exp[-2T])/(1+\lambda\exp[-2T])^2\\&\qquad+(1/2)(1+\lambda)(1-\exp[-2T])/(1+\lambda\exp[-2T])\\&\qquad-(1-\exp[-2T])/(1+\lambda\exp[-2T])\ ,\end{aligned}$$

Finally, we have

$$\begin{aligned}&(\lambda/2)\exp[-2T]/(1+\lambda\exp[-2T])^2\\&\quad=-(\lambda/2)(1-\exp[-2T])^2/(1+\lambda\exp[-2T])^2\\&\qquad+(\lambda/2)(1-\exp[-2T])/(1+\lambda\exp[-2T])^2\ .\end{aligned}$$

which concludes the proof. □

Finally, we have the following result.

Proposition S20. *Let $\lambda \in (-1, +\infty)$ and $a:\ [0,T] \to \mathbb{R}$ such that for any $t \in [0,T]$,*

$$a(t) = 1 - 2/(1+\exp[-2(T-t)]\lambda)\ .$$

Then, if $\lambda \neq 0$, we have that for any $t \in [0,T]$,

$$\begin{aligned}&-\exp[2\int_0^T a(t)\mathrm{d}t]\{\int_0^T a(t)^2\mathrm{d}t + a(T) - a(0)\} + 1 - \exp[2\int_0^T a(t)\mathrm{d}t]\\&\quad-2\int_0^T \exp[2\int_{T-t}^T a(s)\mathrm{d}s][\int_{T-t}^T a(s)^2\mathrm{d}s + a(T) - a(T-t)]\mathrm{d}t\\&\qquad=1-\exp[-2T](1-\lambda T\exp[-2T])(\lambda+1)^2/(1+\lambda\exp[-2T])^2\\&\qquad\quad-(1+\lambda)^2/(2\lambda)\log((1+\lambda)/(1+\lambda\exp[-2T]))\\&\qquad\quad-\lambda\exp[-2T]/(1+\lambda\exp[-2T])^2\ .\end{aligned}$$

In particular, we have that

$$\begin{aligned}&-\exp[2\int_0^T a(t)\mathrm{d}t]\{\int_0^T a(t)^2\mathrm{d}t + a(T) - a(0)\} + 1 - \exp[2\int_0^T a(t)\mathrm{d}t]\\&\quad-2\int_0^T \exp[2\int_{T-t}^T a(s)\mathrm{d}s][\int_{T-t}^T a(s)^2\mathrm{d}s + a(T) - a(T-t)]\mathrm{d}t\\&\qquad=1-(1/2)(1+\lambda)^2\log(1+\lambda)/\lambda + O(\exp[-2T])\ .\end{aligned}$$

If $\lambda = 0$, we have that for any $t \in [0,T]$

$$\begin{aligned}
&-\exp[2\int_0^T a(t)\mathrm{d}t]\{\int_0^T a(t)^2\mathrm{d}t + a(T) - a(0)\} + 1 - \exp[2\int_0^T a(t)\mathrm{d}t] \\
&\quad - 2\int_0^T \exp[2\int_{T-t}^T a(s)\mathrm{d}s][\int_{T-t}^T a(s)^2\mathrm{d}s + a(T) - a(T-t)]\mathrm{d}t \\
&\quad = (1/2)(1-\exp[-2T])\ .
\end{aligned}$$

Proof. The proof is a direct consequence of Proposition S18, Proposition S19 and the fact that

$$\begin{aligned}
&-\exp[-2T](1-\lambda T\exp[-2T])(\lambda+1)^2/(1+\lambda\exp[-2T])^2 \\
&\quad = -(T+1)\exp[-2T](1+\lambda^2)/(1+\lambda\exp[-2T])^2 \\
&\quad\quad + T(1+\lambda)^2\exp[-2T]/(1+\lambda\exp[-2T])\ .
\end{aligned}$$

□

Proposition S21. *Let $\lambda \in (-1,+\infty)$ and $a:\ [0,T] \to \mathbb{R}$ such that for any $t \in [0,T]$,*

$$a(t) = 1 - 2/(1+\exp[-2(T-t)]\lambda)\ .$$

Then, we have that

$$\begin{aligned}
&\exp[2\int_0^T a(t)\mathrm{d}t] - 1 - \int_0^T \exp[2\int_{T-t}^T a(s)\mathrm{d}s]\{\int_{T-t}^T a(s)^2\mathrm{d}s + a(T) - 3a(T-t)\}\mathrm{d}t \\
&\quad = \exp[-2T](1+\lambda)^2/(1+\lambda\exp[-2T])^2 - 1 \\
&\quad\quad - (1/2)(1+\lambda)(1-\exp[-2T])/(1+\lambda\exp[-2T])(1-2/(1+\lambda)) \\
&\quad\quad - (3/2)(1-\exp[-2T])(1-\lambda^2\exp[-2T])/(1+\lambda\exp[-2T])^2 \\
&\quad\quad + (T/2)(1+\lambda)^2\exp[-2T]/(1+\lambda\exp[-2T]) \\
&\quad\quad - (1+\lambda)^2/(4\lambda)\log((1+\lambda)/(1+\lambda\exp[-2T])) \\
&\quad\quad + (\lambda/2)(1-\exp[-2T])^2/(1+\lambda\exp[-2T])^2\ .
\end{aligned}$$

In particular, we have

$$\begin{aligned}
&\exp[2\int_0^T a(t)\mathrm{d}t] - 1 - \int_0^T \exp[2\int_{T-t}^T a(s)\mathrm{d}s]\{\int_{T-t}^T a(s)^2\mathrm{d}s + a(T) - 3a(T-t)\}\mathrm{d}t \\
&\quad = -2 - (1+\lambda)^2/(4\lambda)\log(1+\lambda) + O(\exp[-2T])\ .
\end{aligned}$$

Proof. Using Lemma S11, we have that

$$\exp[2\int_0^T a(t)\mathrm{d}t] = \exp[-2T](1+\lambda)^2/(1+\lambda\exp[-2T])^2\ . \tag{S49}$$

Using Lemma S12, we have

$$\int_0^T \exp[2\int_{T-t}^T a(s)\mathrm{d}s]\mathrm{d}t = (1/2)(1+\lambda)(1-\exp[-2t])/(1+\lambda\exp[-2t])\ . \tag{S50}$$

Using Lemma S14, we have

$$\begin{aligned}
&\int_0^T \exp[2\int_{T-t}^T a(s)\mathrm{d}s]a(T-t)\mathrm{d}t \\
&\quad = -(1/2)(1-\exp[-2T])(1-\lambda^2\exp[-2T])/(1+\lambda\exp[-2T])^2\ .
\end{aligned} \tag{S51}$$

Finally, using Lemma S17, we have

$$\begin{aligned}
\int_0^T \exp[2\int_{T-t}^T a(s)\mathrm{d}s](\int_{T-t}^T a(s)^2\mathrm{d}s)\mathrm{d}t &= -(T/2)(1+\lambda)^2\exp[-2T]/(1+\lambda\exp[-2T]) \\
&\quad + (1+\lambda)^2/(4\lambda)\log((1+\lambda)/(1+\lambda\exp[-2T])) \\
&\quad - (\lambda/2)(1-\exp[-2T])^2/(1+\lambda\exp[-2T])^2\ .
\end{aligned} \tag{S52}$$

We conclude upon combining (S49), (S50), (S51), (S52) and that $a(T) = 1 - 2/(1+\lambda)$. □

S5.4 General setting

In this section, we prove Theorem 2. In order to compare our results with [5, Theorem 1], we redefine a few processes. Let $p \in \mathscr{P}(\mathbb{R}^d)$ be the target distribution. Consider the Ornstein-Ulhenbeck forward dynamics $(x_t)_{t\in[0,T]}$ such that $\mathrm{d}x_t = -x_t\mathrm{d}t + \sqrt{2}\mathrm{d}w_t$ and x_0 has distribution p_0. We consider the backward chain $(X_k)_{k\in\{0,\dots,N\}}$ such that for any $k \in \{0,\dots,N-1\}$,

$$X_k = X_{k+1} + \gamma_{k+1}\{X_{k+1} + 2\nabla \log p_{t_{k+1}}(X_{k+1})\} + \sqrt{2\gamma_{k+1}}Z_{k+1}, \tag{S53}$$

with $\{Z_k\}_{k\in\mathbb{N}}$ a family of i.i.d. Gaussian random variables with zero mean and identity covariance matrix, $t_k = \sum_{\ell=1}^{k}\gamma_\ell$, $\sum_{\ell=1}^{N}\gamma_\ell = T$ and X_N has distribution $p_0 = \mathrm{N}(0,\mathrm{Id})$ (independent from $\{Z_k\}_{k\in\mathbb{N}}$). Notice that here we do not consider a score approximation in the recursion in order to clarify our approximation results. We recall the following result from [5, Theorem 1].

Theorem S22. *Assume that p_0 admits a bounded density (w.r.t. the Lebesgue measure) $p_0 \in \mathrm{C}^3(\mathbb{R}^d,(0,+\infty))$ and that there exist $d_1, A_1, A_2, A_3 \geq 0$, $\beta_1,\beta_2,\beta_3 \in \mathbb{N}$ and $\mathtt{m}_1 > 0$ such that for any $x \in \mathbb{R}^d$ and $i \in \{1,2,3\}$*

$$\|\nabla^i \log p_0(x)\| \leq A_i(1+\|x\|^{\beta_i}), \quad \langle \nabla \log p_0(x), x\rangle \leq -\mathtt{m}_1\|x\|^2 + d_1\|x\|,$$

with $\beta_1 = 1$. Then there exist $B, C, D \geq 0$ such that for any $N \in \mathbb{N}$ and $\{\gamma_k\}_{k=1}^N$ with $\gamma_k > 0$ for any $k \in \{1,\dots,N\}$ we have

$$\|\mathcal{L}(X_0) - p_0\|_{\mathrm{TV}} \leq C\exp[DT]\sqrt{\gamma^\star} + B\exp[-T]. \tag{S54}$$

where $\gamma^\star = \sup_{k\in\{1,\dots,N\}}\gamma_k$ and $\mathcal{L}(X_0)$ is the distribution of X_0 given in (S53).

In the rest of this note we improve the theorem in the following way:

(a) We remove the exponential dependency w.r.t. the time in the first term of the RHS of (S54).

(b) We provide explicit bounds $B, C, D \geq 0$ depending on the parameters of p_0.

Lemma S23. *Assume*

$$\sup_{x,t}\|\nabla^2 \log p_t(x)\| \leq K \quad \textit{and} \quad \|\partial_t \nabla \log p_t(x)\| \leq M\,\mathrm{e}^{-\alpha t}\,\|x\|.$$

Then there exists $D \geq 0$ such that for any $x \in \mathbb{R}^d$ and $t \in [0,T]$, $\|\nabla \log p_t(x)\| \leq D(1+\|x\|)$ with $D = \|\nabla \log p_0(0)\| + K + CT$.

Proof. Let $x \in \mathbb{R}^d$ and $t \in [0,T]$. Since $(t,x) \mapsto \log p_t(x) \in \mathrm{C}^2([0,T]\times\mathbb{R}^d,(0,+\infty))$, we have that

$$\begin{aligned}\nabla \log p_t(x) &= \nabla \log p_0(x) + \textstyle\int_0^t \partial_s \nabla \log p_s(x)\mathrm{d}s \\ &= \nabla \log p_0(0) + \textstyle\int_0^1 \nabla^2 \log p_0(ux)(x)\mathrm{d}u + \int_0^t \partial_s \nabla \log p_s(x)\mathrm{d}s.\end{aligned}$$

Therefore, we have that

$$\begin{aligned}\|\nabla \log p_t(x)\| &\leq \|\nabla \log p_0(0)\| + K\|x\| + \textstyle\int_0^t \|\partial_s \nabla \log p_s(x)\|\mathrm{d}s \\ &\leq \|\nabla \log p_0(0)\| + K\|x\| + M\textstyle\sum_{k=0}^{N-1}(t_k - t_{k-1})\exp[-\alpha t_k]\|x\| \\ &\leq \|\nabla \log p_0(0)\| + K\|x\| + MT\|x\|,\end{aligned}$$

which concludes the proof. □

Note that in the previous proposition we can derive a tighter bound for D which does not depend on the limiting time $T > 0$. However, we do not use the bound $D > 0$ in our quantitative result and therefore our simple bound suffices.

We also have the following useful lemma.

Lemma S24. *Let $T \geq \log(2\mathbb{E}[\|X_0\|^2]) + \log(2)/2$ and assume that there exists $\eta > 0$ such that aaa Then, we have*

$$\textstyle\int_{\mathbb{R}^d} p_\infty(x_T)^2/p_T(x_T)\mathrm{d}x_T \leq \exp[4] + E_T\ ,$$

with $E_T \sim C\exp[-T]$ when $T \to +\infty$ and $C \geq 0$.

If p_∞ satisfies the following Φ-entropy inequality for any $f : \mathbb{R}_d \to (0, \infty)$ measurable

$$\int_{\mathbb{R}^d} \|\nabla f(x)\|^2 / f(x)^3 p_\infty(x) \mathrm{d}x \leq C[\int_{\mathbb{R}^d} (1/f(x)) p_\infty(x) \mathrm{d}x - 1/(\int_{\mathbb{R}^d} f(x) p_\infty(x) \mathrm{d}x)] \,, \tag{S55}$$

with $C \geq 0$. Then, we have as in [1, Proposition 7.6.1]

$$\chi^2(p_\infty || p_t) = \int_{\mathbb{R}^d} p_\infty^2(x)/p_T(x) \mathrm{d}x - 1 \leq \mathrm{e}^{-Ct} \,,$$

which immediately concludes the proof of Lemma S24. However, to the best of our knowledge, establishing (S55) remains an open problem. Note that controlling $\chi^2(p_t || p_\infty)$ is much easier as the exponential decay of this divergence is linked with the Poincaré inequality which is satisfied in our Gaussian setting. In what follows, we consider another approach which relies on the structure of the Ornstein-Ulhenbeck transition kernel and provide non-tight upper bounds.

Proof. Let $T \geq 0$, $\varepsilon > 0$ and $x_T \in \mathbb{R}^d$

$$\|x_T - \mathrm{e}^{-T} x_0\|^2 \leq (1+\varepsilon)\|x_T\|^2 + (1 + 1/\varepsilon)\mathrm{e}^{-2T}\|x_0\|^2 \,.$$

Let $\varepsilon > 0$ and $x_T \in \mathbb{R}^d$, we have

$$p_T(x_T)^{-2} \leq \exp[(1+\varepsilon)/\sigma_T^2 \|x_T\|^2] \times (\int_{\mathbb{R}^d} p(x_0) \exp[-\mathrm{e}^{-2T}(1 + 1/\varepsilon)/(2\sigma_T^2)\|x_0\|^2] \mathrm{d}x_0)^{-2} (2\pi\sigma_T^2)^d \,.$$

For any $x_T \in \mathbb{R}^d$, we have

$$p_\infty(x_T)^2 / p_T(x_T) \leq \exp[\{-1 + (1+\varepsilon)/(2\sigma_T^2)\}\|x_T\|^2](2\pi/\sigma_T^2)^{-d/2} (\int_{\mathbb{R}^d} p(x_0) \exp[-\mathrm{e}^{-2T}(1 + 1/\varepsilon)/(2\sigma_T^2)\|x_0\|^2] \mathrm{d}x_0)^{-1} \,.$$

In what follows, we set $\varepsilon = \mathrm{e}^{-T}$. We have that

$$-1 + (1+\varepsilon)/(2\sigma_T^2) = (2\sigma_T^2)^{-1}(-2\sigma_T^2 + 1 + \varepsilon) = -(1 - 2\mathrm{e}^{-T} + \varepsilon)/(2\sigma_T^2) = -(1 - \mathrm{e}^{-T})/(2\sigma_T^2) \,.$$

Therefore, we get that

$$\int_{\mathbb{R}^d} \exp[\{-1 + (1+\varepsilon)/(2\sigma_T^2)\}\|x_T\|^2](2\pi/\sigma_T^2)^{-d/2} \mathrm{d}x_T = (1 - \mathrm{e}^{-T})^{-d/2} \,. \tag{S56}$$

In addition, we have that for any $R \geq 0$ using that $\sigma_T^2 \geq 1/2$ since $T \geq \log(2)/2$

$$\begin{aligned} &\int_{\mathbb{R}^d} p(x_0) \exp[-\mathrm{e}^{-2T}(1 + 1/\varepsilon)/\sigma_T^2 \|x_0\|^2] \mathrm{d}x_0 \\ &\quad \geq \mathbb{P}(X_0 \in \bar{\mathrm{B}}(0, R)) \exp[-\mathrm{e}^{-2T}(1 + 1/\varepsilon)/\sigma_T^2 R^2] \\ &\quad \geq \mathbb{P}(X_0 \in \bar{\mathrm{B}}(0, R)) \exp[-4\mathrm{e}^{-T} R^2] \end{aligned} \tag{S57}$$

Now let $R^2 = \mathrm{e}^T$. We obtain

$$\int_{\mathbb{R}^d} p(x_0) \exp[-\mathrm{e}^{-2T}(1 + 1/\varepsilon)/\sigma_T^2 \|x_0\|^2] \mathrm{d}x_0 \geq \mathbb{P}(X_0 \in \bar{\mathrm{B}}(0, \mathrm{e}^{T/2})) \exp[-4] \,.$$

In addition, using Markov inequality, we have

$$\mathbb{P}(X_0 \in \bar{\mathrm{B}}(0, \mathrm{e}^{T/2})) = 1 - \mathbb{P}(\|X_0\|^2 \geq \mathrm{e}^T) \geq 1 - \mathbb{E}[\|X_0\|^2]\mathrm{e}^{-T} \geq 0 \,.$$

Therefore, combining this result and (S57), we have

$$\int_{\mathbb{R}^d} p(x_0) \exp[-\mathrm{e}^{-2T}(1 + 1/\varepsilon)/\sigma_T^2 \|x_0\|^2] \mathrm{d}x_0 \geq \exp[-4](1 - \mathbb{E}[\|X_0\|^2]\mathrm{e}^{-T}) > 0 \,. \tag{S58}$$

We conclude upon combining (S56) and (S58). □

We are now ready to state the following lemma.

Lemma S25. *There exists a unique strong solution to the SDE* $\mathrm{d}y_t = \{y_t + 2\nabla \log p_{T-t}(y_t)\}\mathrm{d}t + \sqrt{2}\mathrm{d}w_t$ *with initial condition* $\mathcal{L}(y_0) = p_\infty$. *In addition, we have that* $\mathbb{E}[\sup_{t \in [0,T]} \|y_t\|^\alpha] < +\infty$ *for any* $\alpha > 0$.

Proof. Let $b : [0,T] \times \mathbb{R}^d$ given for any $t \in [0,T]$ and $x \in \mathbb{R}^d$ by $b(t,x) = x + 2\nabla \log p_t(x)$. We have that $b \in \mathrm{C}^1([0,T] \times \mathbb{R}^d, \mathbb{R}^d)$ and in particular is locally Lipschitz. In addition, using Lemma S23 we have that for any $t \in [0,T]$ and $x \in \mathbb{R}^d$, $\|b(t,x)\| \leq (1+D)\|x\|$. Hence using [14, Theorem 2.3, Theorem 3.1] and [35, Theorem 2.1] (with $V(x) = (1/2)\|x\|^2$) there exists a unique strong solution to the SDE $\mathrm{d}y_t = \{y_t + 2\nabla \log p_{T-t}(y_t)\}\mathrm{d}t + \sqrt{2}\mathrm{d}w_t$ with initial condition $\mathcal{L}(y_0) = p_\infty$. Let $\alpha > 1$, then we have for any $t \in [0,T]$

$$\sup_{s\in[0,t]} \|y_t\|^\alpha \leq 3^{\alpha-1}[\|y_0\|^\alpha + t^{\alpha-1}(1+D)^\alpha \int_0^t \sup_{u\in[0,s]} \|y_u\|^\alpha \mathrm{d}u + 2^{\alpha/2} \sup_{s\in[0,t]} \|w_u\|^\alpha].$$

Using that $\mathbb{E}[\sup_{s\in[0,T]} \|w_u\|^\alpha]$ and Grönwall's lemma, we get that $\mathbb{E}[\sup_{t\in[0,T]} \|y_t\|^\alpha] < +\infty$ for any $\alpha > 1$. The result is extended to any $\alpha > 0$ since for any $\alpha \in (0,1]$ we have that

$$\mathbb{E}[\sup_{t\in[0,T]} \|y_t\|^\alpha] \leq \mathbb{E}[\sup_{t\in[0,T]} \|y_t\|]^\alpha < +\infty.$$

□

We are now ready to prove Theorem 2.

Proof. The beginning of the proof is similar to the one of [5, Theorem 1]. For any $k \in \{1,\dots,N\}$, denote R_k the Markov kernel such that for any $x \in \mathbb{R}^d$, $\mathsf{A} \in \mathcal{B}(\mathbb{R}^d)$ and $k \in \{0,\dots,N-1\}$ we have

$$\mathrm{R}_{k+1}(x,\mathsf{A}) = (4\pi\gamma_{k+1})^{-d/2} \int_{\mathsf{A}} \exp[-\|\tilde{x} - \mathcal{T}_{k+1}(x)\|^2/(4\gamma_{k+1})]\mathrm{d}\tilde{x},$$

where for any $x \in \mathbb{R}^d$, $\mathcal{T}_{k+1}(x) = x + \gamma_{k+1}\{x + 2\nabla \log p_{t_{k+1}}(x)\}$. Define for any $k_0, k_1 \in \{1,\dots,N\}$ with $k_1 \geq k_0$ $\mathrm{Q}_{k_0,k_1} = \prod_{\ell=k_0}^{k_1} \mathrm{R}_{k_1+k_0-\ell}$. Finally, for ease of notation, we also define for any $k \in \{1,\dots,N\}$, $\mathrm{Q}_k = \mathrm{Q}_{k+1,N}$. Note that for any $k \in \{1,\dots,N\}$, X_k has distribution $p_\infty \mathrm{Q}_k$, where $p_\infty \in \mathscr{P}(\mathbb{R}^d)$ with density w.r.t. the Lebesgue measure p_∞. Let $\mathbb{P} \in \mathscr{P}(\mathcal{C})$ be the probability measure associated with the diffusion

$$\mathrm{d}x_t = -x_t\mathrm{d}t + \sqrt{2}\mathrm{d}w_t, \quad x_0 \sim p_0,$$

First, we have for any $\mathsf{A} \in \mathcal{B}(\mathbb{R}^d)$

$$p_0\mathbb{P}_{T|0}(\mathbb{P}^R)_{T|0}(\mathsf{A}) = \mathbb{P}_T(\mathbb{P}^R)_{T|0}(\mathsf{A}) = (\mathbb{P}^R)_0(\mathbb{P}^R)_{T|0}(\mathsf{A}) = (\mathbb{P}^R)_T(\mathsf{A}) = p_0(\mathsf{A}).$$

Hence $p_0 = p_0\mathbb{P}_{T|0}(\mathbb{P}^R)_{T|0}$. Using this result we have

$$\begin{aligned}
\|p_0 - p_\infty \mathrm{Q}_0\|_{\mathrm{TV}} &= \|p_0\mathbb{P}_{T|0}(\mathbb{P}^R)_{T|0} - p_\infty \mathrm{Q}_0\|_{\mathrm{TV}} \\
&\leq \|p_0\mathbb{P}_{T|0}(\mathbb{P}^R)_{T|0} - p_\infty(\mathbb{P}^R)_{T|0}\|_{\mathrm{TV}} + \|p_\infty(\mathbb{P}^R)_{T|0} - p_\infty \mathrm{Q}_0\|_{\mathrm{TV}} \\
&\leq \|p_0\mathbb{P}_{T|0} - p_\infty\|_{\mathrm{TV}} + \|p_\infty(\mathbb{P}^R)_{T|0} - p_\infty \mathrm{Q}_0\|_{\mathrm{TV}}.
\end{aligned}$$

Note that $\mathcal{L}(X_0) = p_\infty \mathrm{Q}_0$ and therefore

$$\|\mathcal{L}(X_0) - p_0\|_{\mathrm{TV}} \leq \|p_0\mathbb{P}_{T|0} - p_\infty\|_{\mathrm{TV}} + \|p_\infty(\mathbb{P}^R)_{T|0} - p_\infty \mathrm{Q}_0\|_{\mathrm{TV}}.$$

We now bound each one of these terms.

(a) First, we bound $\|p_0\mathbb{P}_{T|0} - p_\infty\|_{\mathrm{TV}}$. Using the Pinsker inequality [1, Equation 5.2.2] we have that

$$\|p_0\mathbb{P}_{T|0} - p_\infty\|_{\mathrm{TV}} \leq \sqrt{2}\,\mathrm{KL}(p_0\mathbb{P}_{T|0}\|p_\infty)^{1/2}. \tag{S59}$$

In addition, p_∞ satisfies the log-Sobolev inequality with constant $C = 1$, [8]. Namely, for any $f \in \mathrm{C}^1(\mathbb{R}^d, (0,+\infty))$ such that $f \in \mathrm{L}^1(p_\infty)$ and $\int_{\mathbb{R}^d} \|\nabla \log f(x)\|^2 f(x)\mathrm{d}p_\infty(x) < +\infty$ we have

$$\begin{aligned}
&\int_{\mathbb{R}^d} f(x)\log f(x)\mathrm{d}p_\infty(x) - (\int_{\mathbb{R}^d} f(x)\mathrm{d}p_\infty(x))(\log \int_{\mathbb{R}^d} f(x)\mathrm{d}p_\infty(x)) \\
&\qquad \leq (C/2)\int_{\mathbb{R}^d} \|\nabla \log f(x)\|^2 f(x)\mathrm{d}p_\infty(x),
\end{aligned}$$

with $C = 1$. Therefore, using [1, Theorem 5.2.1] we have that for any $f \in \mathrm{L}^1(p_\infty)$ with $\int_{\mathbb{R}^d} |f(x)||\log f(x)| \mathrm{d}p_\infty(x) < +\infty$

$$\mathrm{Ent}_{p_\infty}\left(\mathbb{P}_{T|0}[f]\right) \leq \exp[-2T]\mathrm{Ent}_{p_\infty}(f), \tag{S60}$$

where for any $g \in \mathrm{L}^1(p_\infty)$ with $\int_{\mathbb{R}^d} |g(x)||\log g(x)| \mathrm{d}p_\infty(x) < +\infty$ we define

$$\mathrm{Ent}_{p_\infty}(g) = \int_{\mathbb{R}^d} g(x) \log g(x) \mathrm{d}p_\infty(x) - \left(\int_{\mathbb{R}^d} g(x) \mathrm{d}p_\infty(x)\right)\left(\log \int_{\mathbb{R}^d} g(x) \mathrm{d}p_\infty(x)\right).$$

Note that $(\mathrm{d}p_T/\mathrm{d}p_\infty) = \mathbb{P}_{T|0}[\mathrm{d}p_0/\mathrm{d}p_\infty]$ and that for any $\mu \in \mathscr{P}(\mathbb{R}^d)$ with $\mathrm{KL}(\mu\|p_\infty) < +\infty$ we have $\mathrm{Ent}_{p_\infty}(\mathrm{d}\mu/\mathrm{d}p_\infty) = \mathrm{KL}(\mu\|p_\infty)$. Using these results, (S59) and (S60) we get that

$$\|p_0\mathbb{P}_{T|0} - p_\infty\|_{\mathrm{TV}} \leq \sqrt{2}\exp[-T]\,\mathrm{KL}(p_0\|p_\infty)^{1/2}. \tag{S61}$$

In addition, we have that

$$\mathrm{KL}(p_0\|p_\infty) = (d/2)\log(2\pi) + \int_{\mathbb{R}^d} \|x\|^2 \mathrm{d}p_0(x) - \mathrm{H}(p_0),$$

where $\mathrm{H}(p_0) = -\int_{\mathbb{R}^d} \log(p_0(x))p_0(x)\mathrm{d}x$. Combining this result and (S61) we get that

$$\|p_0\mathbb{P}_{T|0} - p_\infty\|_{\mathrm{TV}} \leq \sqrt{2}\exp[-T]((d/2)\log(2\pi) + \int_{\mathbb{R}^d} \|x\|^2 \mathrm{d}p_0(x) - \mathrm{H}(p_0))^{1/2},$$

which concludes the first part of the proof.

(b) First, let $\mathbb{Q} \in \mathscr{P}(\mathcal{C})$ such that $\mathbb{Q} = p_\infty \mathbb{P}^R_{|0}$, where $\mathbb{P}^R_{|0}$ is the disintegration of $\mathbb{P}^R$ w.r.t. $\phi : \mathcal{C} \to \mathbb{R}^d$ given for any $\omega \in \mathcal{C}$ by $\phi(\omega) = \omega_T$, see [25] for instance. Note that for any $f \in \mathrm{C}(\mathcal{C})$ with f bounded we have

$$\begin{aligned}\mathbb{Q}[f] = \int_{\mathbb{R}^d}\int_{\mathcal{C}} f(\omega)\mathbb{P}^R_{|0}(\omega_0, \mathrm{d}\omega)\mathrm{d}p_\infty(\omega_0) &= \int_{\mathbb{R}^d}\int_{\mathcal{C}} f(\omega)\mathbb{P}^R_{|0}(\omega_0, \mathrm{d}\omega)(\mathrm{d}p_\infty/\mathrm{d}p_T)(\omega_0)\mathrm{d}p_T(\omega_0) \\ &= \int_{\mathcal{C}} f(\omega)(\mathrm{d}p_\infty/\mathrm{d}p_T)(\omega_0)\mathrm{d}\mathbb{P}^R(\omega).\end{aligned}$$

Therefore, we get that for any $\omega \in \mathcal{C}$, $(\mathrm{d}\mathbb{Q}/\mathrm{d}\mathbb{P}^R)(\omega) = (\mathrm{d}p_\infty/\mathrm{d}p_T)(\omega_0)$. Let $\mathbb{R} = p_\infty \mathbb{P}_{|0}$. Note that for any $t \in [0, T]$, $\mathbb{R}_t = p_\infty$ and that $\mathbb{R}$ is associated with the process $\mathrm{d}x_t = -x_t\mathrm{d}t + \sqrt{2}\mathrm{d}w_t$ with $\mathcal{L}(x_0) = p_\infty$. In particular, $\mathbb{R}$ satisfies [2, Hypothesis 1.8]. Using [25, Theorem 2.4] we have that

$$\mathrm{KL}(\mathbb{P}\|\mathbb{R}) = \mathrm{KL}(p_0\|p_\infty) + \int_{\mathbb{R}^d} \mathrm{KL}(\mathbb{P}_{|0}(x_0)\|\mathbb{P}_{|0}(x_0))\mathrm{d}p_0(x_0) = \mathrm{KL}(p_0\|p_\infty) < +\infty.$$

Therefore, we can apply [2, Theorem 4.9]. Let $u \in \mathrm{C}^\infty_c(\mathbb{R}^d, \mathbb{R})$, we have that $(\mathbf{M}^u_t(y))_{t\in[0,T]}$ is a local martingale, where we have for any $t \in [0, T]$

$$\mathbf{M}^u_t(y) = u(y_t) - u(y_0) - \int_0^t \{\langle \nabla u(y_s), y_s + 2\nabla \log p_{T-s}(y_s)\rangle + \Delta u(y_s)\}\mathrm{d}s,$$

where $\mathcal{L}(y) = \mathbb{P}^R$. Since u is compactly supported we have that $\sup_{\omega\in\mathcal{C}} \sup_{t\in[0,T]} |\mathbf{M}^u_t(\omega)| < +\infty$ and therefore $(\mathbf{M}^u_t(y))_{t\in[0,T]}$ is a martingale. We now show that $(\mathbf{M}^u_t(y))_{t\in[0,T]}$ is a martingale, with $\mathcal{L}(y) = \mathbb{Q}$. Since $\sup_{\omega\in\mathcal{C}} \sup_{t\in[0,T]} |\mathbf{M}^u_t(\omega)| < +\infty$, we have that for any $t \in [0, T]$, $\mathbb{E}[|\mathbf{M}^u_t|] < +\infty$. Let $t, s \in [0, T]$ with $t > s$ and $g : \mathcal{C} \to \mathbb{R}^d$ bounded. We have that $\mathbb{E}[|g(\{x_{T-s}\}_{s\in[0,t]})|^2(\mathrm{d}p_\infty/\mathrm{d}p_T)(x_T)^2] < +\infty$. Hence, we have that

$$\mathbb{E}[(\mathbf{M}^u_t(x_{T-\cdot}) - \mathbf{M}^u_s(x_{T-\cdot}))g(\{x_{T-s}\}_{s\in[0,t]})(\mathrm{d}p_\infty/\mathrm{d}p_T)(x_T)] = 0.$$

Using this result and that for any $\omega \in \mathcal{C}$, $(\mathrm{d}\mathbb{Q}/\mathrm{d}\mathbb{P}^R)(\omega) = (\mathrm{d}p_\infty/\mathrm{d}p_T)(\omega_0)$ we get

$$\mathbb{E}[(\mathbf{M}^u_t(y) - \mathbf{M}^u_s(y))g(\{y_s\}_{s\in[0,t]})] = 0.$$

Hence, for any $u \in \mathrm{C}^2_c(\mathbb{R}^d, \mathbb{R})$, $(\mathbf{M}^u_t(y))_{t\in[0,T]}$ is a martingale. In addition, $(\mathbf{M}^u_t(\mathbf{Z}))_{t\in[0,T]}$ is a martingale using Lemma S25 and Itô's lemma, where $\mathbf{Z}$ is the solution to the SDE in Lemma S25. In addition, we have that $\mathcal{L}(\mathbf{Z}_0) = \mathcal{L}(y_0) = p_\infty$. Using Lemma S23 and the remark following [2, Hypothesis 1.8], we get that $\mathcal{L}(\mathbf{Z}) = \mathcal{L}(y) = \mathbb{Q}$. We have just shown that the time-reversed process with initialisation p_∞ can be obtained as a strong solution of an SDE. Using Lemma S23 and Lemma S25, we have that for any $t \in [0, T]$

$$\mathbb{E}[\int_0^t \|x_s + 2\nabla \log p_s(x_s)\|^2\mathrm{d}s + \int_0^t \|w_s + 2\nabla \log p_s(w_s)\|^2\mathrm{d}s] < +\infty.$$

Combining this result and [5, Lemma S13] we have that

$$\|p_\infty \mathbb{P}^R_{T|0} - p_\infty \mathrm{Q}_0\|^2_{\mathrm{TV}} \leq (1/2) \int_0^T \mathbb{E}[\|b_1(t,(y_s)_{s\in[0,T]}) - b_2(t,(y_s)_{s\in[0,T]})\|^2]\mathrm{d}t, \tag{S62}$$

where for any $t \in [0,T]$ and $\omega \in \mathcal{C}$ we have that

$$b_1(t,\omega) = \omega_t + 2\nabla \log p_{T-t}(\omega_t), \qquad b_2(t,\omega) = \omega_{t_\gamma} + 2\nabla \log p_{T-t_\gamma}(\omega_{t_\gamma}),$$

where $t_\gamma = \sum_{k=0}^{N-1} \mathbb{1}_{[T-t_{k+1},T-t_k)}(t)(T-t_{k+1})$. Noting that $(y_t)_{t\in[0,T]}$ is distributed according to $\mathbb{Q}$ and using that $(\mathrm{d}\mathbb{Q}/\mathrm{d}\mathbb{P}^R)(\omega) = (\mathrm{d}p_\infty/\mathrm{d}p_T)(\omega_0)$, (S62) and the Cauchy-Schwarz inequality we have

$$\begin{aligned}
&\|p_\infty \mathbb{P}^R_{T|0} - p_\infty \mathrm{Q}_0\|^2_{\mathrm{TV}} \\
&\leq (1/2)\mathbb{E}[(\mathrm{d}p_\infty/\mathrm{d}p_T)(x_T)^2]^{1/2} \int_0^T \mathbb{E}^{1/2}[\|b_1(t,(x_{T-s})_{s\in[0,T]}) - b_2(t,(x_{T-s})_{s\in[0,T]})\|^4]\mathrm{d}t \\
&\leq (1/2)\mathbb{E}[(\mathrm{d}p_\infty/\mathrm{d}p_T)(x_T)^2]^{1/2} \\
&\quad \times \int_0^T \mathbb{E}^{1/2}[\|b_1(T-t,(x_{T-s})_{s\in[0,T]}) - b_2(T-t,(x_{T-s})_{s\in[0,T]})\|^4]\mathrm{d}t.
\end{aligned} \tag{S63}$$

In addition, we have that for any $t \in [0,T]$ and $\omega \in \mathcal{C}$ we have

$$\begin{aligned}
&\|b_1(t,\omega) - b_2(t,\omega)\| \\
&\leq \|\omega_t - \omega_{t_\gamma}\| + 2\|\nabla \log p_{T-t}(\omega_t) - \nabla \log p_{T-t_\gamma}(\omega_t)\| \\
&\qquad + 2\|\nabla \log p_{T-t_\gamma}(\omega_t) - \nabla \log p_{T-t_\gamma}(\omega_{t_\gamma})\| \\
&\leq (1 + 2\sup_{s\in[0,T]} \sup_{x\in\mathbb{R}^d} \|\nabla^2 \log p_s(x)\|)\|\omega_t - \omega_{t_\gamma}\| \\
&\qquad + 2\sup_{s\in[T-t,T-t_\gamma]} \|\partial_t \nabla \log p_t(\omega_t)\|(t - t_\gamma) \\
&\leq (1+2K)\|\omega_t - \omega_{t_\gamma}\| + 2\sup_{s\in[T-t,T-t_\gamma]} \|\partial_s \nabla \log p_s(\omega_t)\|(t - t_\gamma).
\end{aligned}$$

Note that

$$T - (T-t)_\gamma = T - \sum_{k=0}^{N-1} \mathbb{1}_{[T-t_{k+1},T-t_k)}(T-t)(T-t_{k+1}) = \sum_{k=0}^{N-1} \mathbb{1}_{(t_k,t_{k+1}]}(t)t_{k+1}.$$

For any $t \in [0,T]$, denote $t^\gamma = T - (T-t)_\gamma = \sum_{k=0}^{N-1} \mathbb{1}_{(t_k,t_{k+1}]}(t)t_{k+1}$. Therefore, we get that for any $t \in (t_k, t_{k+1}]$

$$\begin{aligned}
&\|b_1(T-t,\omega) - b_2(T-t,\omega)\| \\
&\quad \leq (1+2K)\|\omega_{T-t} - \omega_{(T-t)_\gamma}\| + 2\sup_{s\in[t,t^\gamma]} \|\partial_s \nabla \log p_s(\omega_{T-t})\|(t^\gamma - t) \\
&\quad \leq (1+2K)\|\omega_{T-t} - \omega_{(T-t)_\gamma}\| + 2\sup_{s\in[t_k,t_{k+1}]} \|\partial_s \nabla \log p_s(\omega_{T-t})\|\gamma_{k+1} \\
&\quad \leq (1+2K)\|\omega_{T-t} - \omega_{(T-t)_\gamma}\| + 2\mathrm{S}_{t_k}(\omega_{T-t})\gamma_{k+1}.
\end{aligned}$$

Combining this result and that for any $a, b \geq 0$, $(a+b)^4 \leq 8a^4 + 8b^4$ we get that for any $t \in (t_k, t_{k+1}]$

$$\begin{aligned}
&\mathbb{E}[\|b_1(T-t,(x_{T-s})_{s\in[0,T]}) - b_2(T-t,(x_{T-s})_{s\in[0,T]})\|^4] \\
&\qquad \leq 8(1+2K)^4\mathbb{E}[\|x_t - x_{t_k}\|^4] + 16\mathbb{E}[\mathrm{S}_{t_k}(x_t)^4]\gamma_{k+1}^4.
\end{aligned} \tag{S64}$$

In addition, we have that for any $t \in [0,T]$, $x_t = \exp[-t]x_0 + w_{(1-\exp[-2t])^{1/2}}$. Hence, for any $s, t \in [0,T]$ with $t > s$ we have

$$\|x_t - x_s\| \leq \exp[-s](\exp[t-s] - 1)\|x_0\| + \|w_{(1-\exp[-2t])} - w_{(1-\exp[-2s])}\|.$$

Therefore, we have that for any $s, t \in [0,T]$ with $t > s$

$$\begin{aligned}
\mathbb{E}[\|x_t - x_s\|^4] &\leq 8\exp[-4s](1-\exp[-t+s])^4\mathbb{E}[\|x_0\|^4] + 8\mathbb{E}[\|w_{(1-\exp[-2t])} - w_{(1-\exp[-2s])}\|^4] \\
&\leq 8\exp[-4s](1-\exp[-t+s])^4\mathbb{E}[\|x_0\|^4] + 24(\exp[-t] - \exp[-s])^2 \\
&\leq 8\exp[-4s](1-\exp[-t+s])^4\mathbb{E}[\|x_0\|^4] + 24\exp[-2s](1-\exp[-t+s])^2 \\
&\leq 8\mathbb{E}[\|x_0\|^4]\exp[-4s](t-s)^4 + 24\exp[-2s](t-s)^2.
\end{aligned} \tag{S65}$$

In addition, using that that for any $k \in \{0, \dots, N-1\}$ and $x \in \mathbb{R}^d$, $\mathtt{S}_{t_k}(x) \leq M \exp[-\alpha t_k]\|x\|$ we get that

$$\mathbb{E}[\mathtt{S}_{t_k}(x_t)^4] \leq 24 M^4 \exp[-4\alpha t_k]\{1 + \mathbb{E}[\|x_0\|^4]\}.$$

Combining this result, (S64) and (S65) we get that for any $t \in (t_k, t_{k+1}]$

$$\begin{aligned}
&\mathbb{E}[\|b_1(T-t, (x_{T-s})_{s\in[0,T]}) - b_2(T-t, (x_{T-s})_{s\in[0,T]})\|^4] \\
&\qquad \leq 64(1+2K)^4 \mathbb{E}[\|x_0\|^4] \exp[-4t_k]\gamma_{k+1}^4 \\
&\qquad\quad + 192(1+2K)^4 \exp[-2t_k]\gamma_{k+1}^2 + 384 M^4 \exp[-4\alpha t_k]\{1 + \mathbb{E}[\|x_0\|^4]\}\gamma_{k+1}^4.
\end{aligned}$$

Using this result and that for any $a, b \geq 0$, $(a+b)^{1/2} \leq a^{1/2} + b^{1/2}$, we have for any $t \in (t_k, t_{k+1}]$

$$\begin{aligned}
&\mathbb{E}^{1/2}[\|b_1(T-t, (x_{T-s})_{s\in[0,T]}) - b_2(T-t, (x_{T-s})_{s\in[0,T]})\|^4] \\
&\qquad \leq 8(1+2K)^2 \mathbb{E}^{1/2}[\|x_0\|^4] \exp[-2t_k]\gamma_{k+1}^2 \\
&\qquad\quad + 14(1+2K)^2 \exp[-t_k]\gamma_{k+1} + 20 M^2 \exp[-2\alpha t_k]\{1 + \mathbb{E}^{1/2}[\|x_0\|^4]\}\gamma_{k+1}^2.
\end{aligned} \tag{S66}$$

We have that for any $\beta > 0$,

$$\textstyle\sum_{k=0}^{N-1} \exp[-\beta t_k] \leq \sum_{k\in\mathbb{N}} \exp[-\beta\gamma_\star k] \leq (1 - \exp[-\beta\gamma_\star])^{-1} \leq 1 + \beta/\gamma_\star.$$

Then using this result, (S66) and (S63) we get that

$$\begin{aligned}
\|p_\infty \mathbb{P}^R_{T|0} - p_\infty \mathrm{Q}_0\|_{\mathrm{TV}}^2 &\leq \mathbb{E}[(\mathrm{d}p_\infty/\mathrm{d}p_T)(x_T)^2]^{1/2}[4(1+2K)^2 \mathbb{E}^{1/2}[\|x_0\|^4](1 + /(2\gamma_\star))(\gamma^\star)^3 \\
&\quad + 7(1+2K)^2(1+1/\gamma_\star)(\gamma^\star)^2 + 10M^2\{1 + \mathbb{E}^{1/2}[\|x_0\|^4]\}(1 + 1/(2\alpha\gamma_\star))(\gamma^\star)^3].
\end{aligned}$$

Therefore, we get that

$$\begin{aligned}
\|p_\infty \mathbb{P}^R_{T|0} - p_\infty \mathrm{Q}_0\|_{\mathrm{TV}} &\leq \mathbb{E}[(\mathrm{d}p_\infty/\mathrm{d}p_T)(x_T)^2]^{1/4}[2(1+2K)\mathbb{E}^{1/4}[\|x_0\|^4](1 + /(2\gamma_\star)^{1/2})(\gamma^\star)^{3/2} \\
&\quad + 3(1+2K)(1 + 1/\gamma_\star^{1/2})\gamma^\star + 4M\{1 + \mathbb{E}^{1/4}[\|x_0\|^4]\}(1 + 1/(2\alpha\gamma_\star)^{1/2})(\gamma^\star)^{3/2}] \\
&\leq \mathbb{E}[(\mathrm{d}p_\infty/\mathrm{d}p_T)(x_T)^2]^{1/4}[6(1+2K)(1 + \mathbb{E}^{1/4}[\|x_0\|^4]) \\
&\quad + 4M\{1 + \mathbb{E}^{1/4}[\|x_0\|^4]\}(1 + 1/(2\alpha)^{1/2})](\gamma^\star)^2/\gamma_\star)^{1/2} \\
&\leq 6(1 + \mathbb{E}^{1/4}[\|x_0\|^4])\mathbb{E}[(\mathrm{d}p_\infty/\mathrm{d}p_T)(x_T)^2]^{1/4}[1 + K + M(1 + 1/(2\alpha)^{1/2})](\gamma^\star)^2/\gamma_\star)^{1/2},
\end{aligned}$$

which concludes the proof upon using Lemma S24.

□

We now check that the assumption of Theorem 2 are satisfied in a Gaussian setting.

Proposition S26. *Assume that $p_0 = \mathrm{N}(0, \Sigma)$ and that $T \geq 1 + (1/2)[\log^+(\|\Sigma\|) + \log(d+1)]$ then we have that for any $t \in [0, T]$ and $x \in \mathbb{R}^d$*

$$\|\nabla^2 \log p_t(x)\| \leq \max(1, \|\Sigma^{-1}\|), \qquad \|\partial_t \nabla \log p_t(x)\| \leq 2\exp[-2t]\max(1, \|\Sigma^{-1}\|)^2 \|\Sigma - \mathrm{Id}\|\|x\|.$$

In addition, we have that $\int_{\mathbb{R}^d} p_\infty(x)^2/p_T(x)\mathrm{d}x \leq \sqrt{2}$.

Proof. Recall that for any $t \in [0, T]$, $x_t = \exp[-t]x_0 + w_{1-\exp[-2t]}$. Therefore, we have that for any $t \in [0, T]$, $p_t = \mathrm{N}(0, \Sigma_t)$ with $\Sigma_t = \exp[-2t]\Sigma + (1 - \exp[-2t])\,\mathrm{Id}$. Hence, we get that for any $t \in [0, T]$ and $x \in \mathbb{R}^d$, $\nabla^2 \log p_t(x) = (\exp[-2t]\Sigma + (1 - \exp[-2t]\,\mathrm{Id})^{-1}$. Using this result, we have that for any $t \in [0, T]$ and $x \in \mathbb{R}^d$, $\|\nabla^2 \log p_t(x)\| \leq \max(1, \|\Sigma^{-1}\|)$. Similarly, for any $t \in [0, T]$ and $x \in \mathbb{R}^d$ we have

$$\partial_t \nabla \log p_t(x) = \partial_t \Sigma_t^{-1} x = -\Sigma_t^{-1}(\partial_t \Sigma_t)\Sigma_t^{-1} x.$$

Hence, for any $t \in [0,T]$ and $x \in \mathbb{R}^d$ we have $\|\partial_t \nabla \log p_t(x)\| \leq 2\exp[-2t]\max(1, \|\Sigma^{-1}\|)^2 \|\Sigma - \mathrm{Id}\,\| \|x\|$. Finally, we have that for any $t \in [0,T]$ and $x \in \mathbb{R}^d$

$$\langle x, [2\,\mathrm{Id} - (\exp[-2t]\Sigma + (1-\exp[-2t])\,\mathrm{Id})^{-1}]x\rangle \geq (2 - (\exp[-2t]\|\Sigma^{-1}\|^{-1} + (1-\exp[-2t]))^{-1})\|x\|^2.$$

Let $\varepsilon \in (0, 1/2]$. For any $t \in [0,T]$, we have that $2 - (\exp[-2t]\|\Sigma^{-1}\|^{-1} + (1-\exp[-2t]))^{-1} \geq 1 - \varepsilon$ if and only if $\exp[-2t](1 - \|\Sigma^{-1}\|^{-1}) \leq 1 - (1+\varepsilon)^{-1}$. Using that $-\log(1-(1+\varepsilon)^{-1}) = \log(1+\varepsilon^{-1})$ we have that for any $t \geq (1/2)\log(1+\varepsilon^{-1})$ and $x \in \mathbb{R}^d$

$$p_\infty(x)^2 / p_t(x) \leq \exp[-\|x\|^2/4](2\pi)^{-d/2}\det(\Sigma_t).$$

Combining this result and the fact that $\int_{\mathbb{R}^d} \exp[-\|x\|^2/2(1-\varepsilon)]\mathrm{d}x = (2(1-\varepsilon)\pi)^{d/2}$, we get that for any $t \geq (1/2)\log(1+\varepsilon^{-1})$

$$\int_{\mathbb{R}^d} p_\infty(x)^2 / p_t(x)\mathrm{d}x \leq \int_{\mathbb{R}^d} \exp[-\|x\|^2/2(1-\varepsilon)](2\pi)^{-d/2}\det(\Sigma_t)^{1/2}\mathrm{d}x \leq (1-\varepsilon)^{d/2}\det(\Sigma_t)^{1/2}.$$

Let $\varepsilon = 1/(2d) \leq 1/2$. Note that $T \geq (1/2)\{-\log(|\|\Sigma^{-1}\|^{-1} - 1|) + \log(1+2d)\}$. Hence, we have that

$$\int_{\mathbb{R}^d} p_\infty(x)^2 / p_T(x)\mathrm{d}x \leq \exp[-\log(1-1/(2d))(d/2)]\det(\Sigma_T)^{1/2}.$$

Since for any $t \in [0, 1/2)$, $-\log(1-t) \leq \log(2)t$ we get that

$$\int_{\mathbb{R}^d} p_\infty(x)^2 / p_T(x)\mathrm{d}x \leq 2^{1/4}\det(\Sigma_T)^{1/2}. \tag{S67}$$

Finally, using that $\Sigma_T = \exp[-2T]\Sigma + (1-\exp[-2T])\,\mathrm{Id}$ we have that

$$\det(\Sigma_T)^{1/2} \leq (\exp[-2T]\|\Sigma\| + 1 - \exp[-2T])^{d/2} \leq (1 + \exp[-2T]\|\Sigma\|)^{d/2}.$$

Hence, using that result and that for any $t \geq 0$, $\log(1+t) \leq t$ we have

$$\det(\Sigma_T)^{1/2} \leq \exp[\exp[-2T]\|\Sigma\|(d/2)]\ .$$

Since, $T \geq (1/2)\{\log(\|\Sigma\|) + \log(d) + \log(2) - \log(\log(2^{1/4}))\}$, we get that $\det(\Sigma_T)^{1/2} \leq 2$, which concludes the proof upon combining this result and (S67). □

Therefore, we get the following simplified result in the Gaussian setting.

Corollary S27. *Assume that* $p = \mathrm{N}(0, \Sigma)$, *with* $\|\Sigma^{-1}\| \geq 1$, $\gamma^\star = \gamma_\star = \gamma > 0$ *and* $T \geq 1 + (1/2)[\log^+(\|\Sigma\|) + \log(d+1)]$, *then we have*

$$\begin{aligned}\|\mathcal{L}(X_0) - p_0\|_{\mathrm{TV}} \leq \exp[-T/2](\log^+(\|\Sigma^{-1}\|) + \|\Sigma - \mathrm{Id}\,\|)^{1/2} \\ +48(1 + \|\Sigma\|^{1/2}d^{1/2})\|\Sigma^{-1}\|^2[1 + \|\Sigma - \mathrm{Id}\,\|]\sqrt{\gamma}.\end{aligned}$$

Proof. Using (S14) and Proposition S26 we have

$$\begin{aligned}\|\mathcal{L}(X_0) - p_0\|_{\mathrm{TV}} &\leq \exp[-T/2](-\log(\det(\Sigma)) + \mathrm{Tr}(\Sigma) - d)^{1/2} \\ &\quad +12(1 + (\textstyle\int_{\mathbb{R}^d}\|x\|^4\mathrm{d}p_0(x))^{1/4})[1 + K + 2C]\sqrt{(\gamma^\star)^2/\gamma_\star} \\ &\leq \exp[-T/2](-\log(\det(\Sigma)) + \mathrm{Tr}(\Sigma) - d)^{1/2} \\ &\quad +12(1 + (\textstyle\int_{\mathbb{R}^d}\|x\|^4\mathrm{d}p_0(x))^{1/4})[1 + \|\Sigma^{-1}\| + 2\|\Sigma^{-1}\|^2\|\Sigma - \mathrm{Id}\,\|]\sqrt{(\gamma^\star)^2/\gamma_\star} \\ &\leq \exp[-T/2](-\log(\det(\Sigma)) + \mathrm{Tr}(\Sigma) - d)^{1/2} \\ &\quad +12(1 + 3^{1/4}\|\Sigma\|^{1/2}d^{1/2})[1 + \|\Sigma^{-1}\| + 2\|\Sigma^{-1}\|^2\|\Sigma - \mathrm{Id}\,\|]\sqrt{(\gamma^\star)^2/\gamma_\star} \\ &\leq \exp[-T/2](-\log(\det(\Sigma)) + \mathrm{Tr}(\Sigma) - d)^{1/2} \\ &\quad +48(1 + \|\Sigma\|^{1/2}d^{1/2})\|\Sigma^{-1}\|^2[1 + \|\Sigma - \mathrm{Id}\,\|]\sqrt{(\gamma^\star)^2/\gamma_\star} \\ &\leq \exp[-T/2](\log^+(\|\Sigma^{-1}\|) + \|\Sigma - \mathrm{Id}\,\|)^{1/2} \\ &\quad +48(1 + \|\Sigma\|^{1/2}d^{1/2})\|\Sigma^{-1}\|^2[1 + \|\Sigma - \mathrm{Id}\,\|]\sqrt{(\gamma^\star)^2/\gamma_\star}.\end{aligned}$$

□

S6 Proof of Theorem 3

Proof. For any x and j, denote $\bar{p}_{j,0}(\cdot|x)$ the distribution of $\bar{x}_{j,0}$ given $x_j = x$ and $p_{j,0}$ the distribution of $\tilde{x}_{j,0}$. For any j we have

$$\mathrm{KL}(p_j \| p_{j,0}) = \mathrm{KL}(p_{j+1} \| p_{j+1,0}) + \mathbb{E}[\mathrm{KL}(\bar{p}_{j+1}(\cdot|x_{j+1}) \| \bar{p}_{j+1,0}(\cdot|x_{j+1}))].$$

By recursion, we have that

$$\mathrm{KL}(p \| p_0) = \mathrm{KL}(p_J \| p_{j,0}) + \textstyle\sum_{j=1}^{J} \mathbb{E}[\mathrm{KL}(\bar{p}_j(\cdot|x_j) \| \bar{p}_{j,0}(\cdot|x_j))].$$

Combining Proposition S9 and Lemma S4, we get that

$$\mathrm{KL}(p \| p_0) \leq (\delta + \exp[-4T])(2^{-J}L)^n + \textstyle\sum_{j=1}^{J} (\delta + \exp[-4T])(2^{-j}L)^n (2^n - 1) + E_{T,\delta}.$$

Therefore, $\mathrm{KL}(p \| p_0) \leq (\delta + \exp[-4T])L^n + E_{T,\delta}$, which concludes the proof. □

S7 Experimental Details on Gaussian Experiments

We now give some details on the experiments in Section 3.2 (Figure 2). We use the exact formulas for the Stein score of p_t in this case: if $x_0 \sim \mathcal{N}(M, \Sigma)$, then $x_t \sim N(M_t, \Sigma_t)$ with $M_t = e^{-t}M$ and

$$\Sigma_t = \mathrm{e}^{-2t}\Sigma + (1 - \mathrm{e}^{-2t})\,\mathrm{Id}\,.$$

Under an ideal situation where there is no score error, the discretization of the (backward) generative process is given by equation (S23):

$$x_{k+1} = ((1+\delta)\,\mathrm{Id} - 2\delta\Sigma_{T-k\delta}^{-1})x_k + 2\delta\Sigma_{T-k\delta}^{-1}M_{T-k\delta} + \sqrt{2\delta}z_{k+1}\ ,$$

where δ is the uniform step size and z_k are iid white Gaussian random variables. For the SGM case, $M = 0$. The starting step of this discretization is itself $x_0 \sim \mathcal{N}(0, \mathrm{Id})$. From this formula, the covariance matrix $\hat{\Sigma}_k$ of x_k satisfies the recursion (S16):

$$\hat{\Sigma}_{k+1} = ((1+\delta)\,\mathrm{Id} - 2\delta\Sigma_{T-k\delta}^{-1})\hat{\Sigma}_k((1+\delta)\,\mathrm{Id} - 2\delta\Sigma_{T-k\delta}^{-1}) + 2\delta\,\mathrm{Id}\ ,$$

from which we can exactly compute $\hat{\Sigma}_k$ for very k, and especially for $k = N = T/\delta$, as a function of Σ, the final time T, and the step size δ. In all our experiments, we choose stationary processes: their covariance Σ is diagonal in a Fourier basis, with eigenvalues (*power spectrum*) noted $\hat{P}_k$. All the x_k remain stationary so $\hat{\Sigma}_k$ is still diagonal in a Fourier basis, with power spectrum noted $\hat{P}_k$. The error displayed in the left panel of figure 2 is:

$$\|\hat{P}_N - P\| = \max_{\omega} |\hat{P}_N(\omega) - P(\omega)| / \max_{\omega} |P(\omega)|,$$

normalized by the operator norm of Σ.

The illustration in the middle panel of Figure 2, for WSGM, is done for simplicity only at one scale (ie, at $j = 1$ in Algorithm 1): instead of stacking the full cascade of conditional distributions for all $j = J, \dots, 1$, we use the true low-frequencies $x_{j,0} = x_1$. Here, we use Daubechies-4 wavelets. We sample $\bar{x}_{j,0}$ using the Euler-Maruyama recursion (S23)-(S16) for the conditional distribution. We recall that in the Gaussian case, $\bar{x}_1$ and x_1 are jointly Gaussian. The conditional distribution of $\bar{x}_1$ given x_1 is known to be $\mathcal{N}(Ax_1, \Gamma)$, where:

$$A = -\mathrm{Cov}(\bar{x}_1, x_1)\mathrm{Var}(x_1)^{-1}, \quad \Gamma = \mathrm{Var}(\bar{x}_1) - \mathrm{Cov}(\bar{x}_1, x_1)\mathrm{Var}(x_1)^{-1}\mathrm{Cov}(\bar{x}_1, x_1)^\top.$$

We solve the recursion (S16) with a step size δ and $N = T/\delta$ steps; the sampled conditional wavelet coefficients $\bar{x}_{j,0}$ have conditional distribution noted $\mathcal{N}(\hat{A}_N x, \hat{\Gamma}_N)$. The full covariance of $(\tilde{x}_{j,0}, \bar{x}_{j,0})$, written in the basis given by the high/low frequencies, is now given by

$$\hat{\Sigma}_N = \begin{bmatrix} \hat{\Gamma}_N & \mathrm{Cov}(x_1, \bar{x}_1)\hat{A}_N^\top \\ \hat{A}_N \mathrm{Cov}(x_1, \bar{x}_1)^\top & \mathrm{Cov}(x_1, x_1) \end{bmatrix}.$$

Figure 2, middle panel compares the eigenvalues (power spectrum) of these covariances, as a function of δ, with the ones of Σ.

The right panel of 2 gives the smallest N needed to reach $\|\hat{P}_N - P\| = 0.1$ in both cases (SGM and WSGM), based on a power law extrapolation of the curves $N \mapsto \hat{P}_N$.

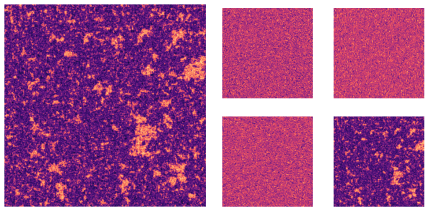


Figure S1: Example of a realization of a φ^4 critical field ($L = 256$) with its wavelet decomposition on the left (lower-frequencies are on bottom right panel).

S8 Experimental Details on the φ^4 Model

In this section, we develop and and make more precise the results in Section 4.1.

S8.1 The Critical φ^4 Process and its Stein Score Regularity

The macroscopic energy of non-Gaussian distributions can be specified as shown in (20), where K is a coupling matrix and V is non-quadratic potential. The φ^4-model over the $L \times L$ periodic grid is the special case defined by $C = -\Delta$ (the negative two-dimensional discrete Laplacian) and V is a quartic potential:

$$E(x) = \frac{\beta}{2} \sum_{|u-v|=1} (x(u) - x(v))^2 + \sum_u (x(u)^2 - 1)^2.$$

Here, β is a parameter proportional to an inverse temperature.

In physics, the φ^4 model is a typical example of second-order phase transitions: the quadratic part reduces spatial fluctuations, and V favors configurations whose entries remain close to ± 1 (in physics, this is often called a *double-well potential*). In the thermodynamic limit $L \to \infty$, both term compete according to the value of β.

- For $\beta \ll 1$, the quadratic term becomes negligible and the marginals of the field become independent; this is the disordered state.
- For $\beta \gg 1$, the quadratic term favors configuration which are spatially smooth and the potential term drives the values towards ± 1, resulting in an ordered state, where all values of the field are simultaneously close to either $+1$ or to -1.

A phase transition occurs between these two regimes at a critical temperature $\beta_c \sim 0.68$ [36, 20]. At this point, the φ^4 field display very long-range correlations and an ill-conditioned Hessian $\nabla^2 \log p$. The sampling of φ^4 at this critical point becomes very difficult. This "critical slowing down" phenomenon is why, from a machine learning point of view, the critical φ^4 field is an excellent example of hard-to-learn and hard-to-sample distribution, yet still accessible for mathematical analysis.

Our wavelet diffusion considers the sampling of the conditional probability $p(\bar{x}_1|x_1)$ instead of $p(x_0)$, by inverting the noise diffusion projected on the wavelet coefficients. Theorem 2 indicates that the loss obtained with any SGM-type method depends on the regularity parameters of $\nabla \log p_t$ in (10).

Strictly speaking, to get a bound on K we should control the norm of $\nabla^2 \log p_t$ over all x and t. However, a look at the proof of the theorem indicates that this control does not have to be uniform in x; for instance, there is no need to control this Hessian in domains which have an extremely small probability under p_t. Moreover, since p_t is a convolution between p_0 and a Gaussian, we expect that a control over $\nabla^2 \log p_0(x)$ will actually be sufficient to control $\nabla^2 \log p_t(x)$ for all $t > 0$; these facts are non-rigorous for the moment. The distribution of some spectral statistics of $\nabla^2 \log p_0$ over samples drawn from the φ^4-model are shown in Figure S2 (blue).

Considering conditional probabilities $\bar{p}$ instead of p acts on the Hessian of the φ^4-energy as a projection over the wavelet field: in the general context of (20),

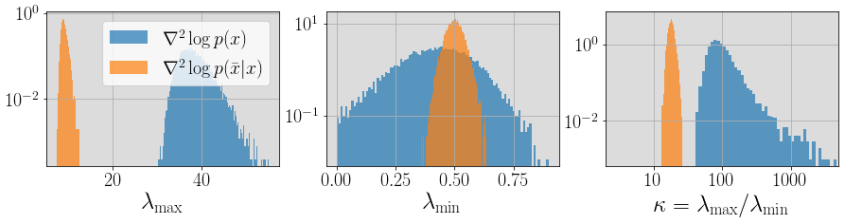


Figure S2: Histograms of 10^5 realizations of $\lambda_{\min}, \lambda_{\max}$ and $\kappa = \lambda_{\max}/\lambda_{\min}$ of the Hessian matrices in (S68) for the critical φ^4 model in dimension $L = 32$. The mean values of κ are respectively $\mu = 18.32$ and $\bar{\mu} = 210.53$; standard deviations are $\sigma = 1.78$ and $\bar{\sigma} = 9451.37$.

$$-\nabla_x^2 \log p(x_0) = K + \nabla^2 V(x_0), \qquad -\nabla_{\bar{x}_1}^2 \log p(\bar{x}_1|x_1) = \gamma^2 \bar{G}(K + \nabla^2 V(x_0))\bar{G}^\top. \quad \text{(S68)}$$

The proof is in Appendix S8. The distribution of the conditioning number of $\nabla_x^2 \log p$ and $\nabla_{\bar{x}}^2 \log p$ over samples drawn from the φ^4 model is shown at Figure S2: the Hessian of the wavelet log-probability is orders-of-magnitude better conditioned than its single-scale counterpart, with a very concentrated distribution. The same phenomenon occurs at each scale j, and the same is true for $\lambda_{\min}, \lambda_{\max}$. It turns out that considering wavelet coefficient not only concentrates these eigenvalues, but also drives $\lambda_{\min}$ away from 0. In the context of multiscale Gaussian processes, Theorem S4 gives a rigorous proof of this phenomenon. In the general case, $\nabla^2 \log p_t$ is not reduced to the inverse of a covariance matrix, but we expect the same phenomenon to be true.

S8.2 Score Models and Details on our Numerical Experiments of φ^4

In this section, we give some details on our numerical experiments from Section 4.1.

Training Data and Wavelets

We used samples from the φ^4 model generated using a classical MCMC algorithm — the sampling script will be publicly available in our repository.

The wavelet decompositions of our fields were performed using Python's `pywavelets` package and `Pytorch Wavelets` package. For synthetic experiments, we used the Daubechies wavelets with $p = 4$ vanishing moments (see [31, Section 7.2.3]).

Score Model

At the first scale $j = 0$, the distribution of the φ^4 model falls into the general form given in (20), and it is assumed that at each scale j, the distribution of the field at scale j still assumes this shape — with modified constants and coupling parameters. The score model we use at each scale is given by:

$$s_{K,\theta}(x) = \tfrac{1}{2} x^\top K x + \textstyle\sum_u (\theta_1 v_1(x(u)) + \cdots + \theta_m v_m(x(u))),$$

where the parameters are $K, \theta_1, \ldots, \theta_m$ and v_i are a family of smooth functions. One can also represent this score as $s_{K,\theta} = K \cdot xx^\top + \theta^\top U(x)$ where $U_i(x) = \sum_u v_i(x(u))$.

Learning

We trained our various algorithms using SGM or WSGM up to a time $T = 5$ with $n_{\text{train}} = 2000$ steps of forward diffusion. At each step t, the parameters were learned by minimizing the score loss:

$$\ell(K, \theta) = \mathbb{E}[|\nabla s_{K,\theta}(x_t)|^2 + 2\Delta_x s_{K,\theta}(x_t)]$$

using the Adam optimiser with learning rate $\texttt{lr} = 0.01$ and default parameters α, β. At the start of the diffusion ($t = 0$) we use 10000 steps of gradient descent. For $t > 1$, we use only 100 steps of gradient descent, but initialized at (K_{t-1}, θ_{t-1}).

Sampling

For the sampling, we used uniform steps of discretization.

For the error metric, we first measure the L^2-norm between the power spectra $P, \hat{P}$ of the true φ^4 samples and our synthesized examples; more precisely, we set:

$$D_1 = \|P - \hat{P}\|^2.$$

This error on second-order statistics is perfectly suitable for Gaussian processes, but must be refined for non-Gaussian processes. We also consider the total variation distance between the histograms of the marginal distributions (in the case of two-dimensions, pixel-wise histograms). We note this error D_2; our final error measure is $D_1 + D_2$. This is the error used in Figure S2.

S8.3 Proofs of (S68)

In the sequel, ∇f is the gradient of a function f, and ∇^2 is the Hessian matrix of f. The *Laplacian* of f is the trace of the Hessian.

Lemma S28. *Let $U : \mathbb{R}^n \to \mathbb{R}$ be smooth and M be a $n \times m$ matrix. We set $F(x) = U(Mx)$ where $x \in \mathbb{R}^m$. Then, $\nabla^2 F(x) = M^\top \nabla^2 U(x) M$.*

Proof. Let $U : \mathbb{R}^n \to \mathbb{R}$ be smooth and M be a $n \times m$ matrix. Then,

$$\partial_k F(x) = \sum_{i=1}^{n} M_{i,k} (\partial_i U)(Mx).$$

Similarly,

$$\partial_{k,\ell} F(x) = \sum_{i=1}^{n} \sum_{j=1}^{n} M_{i,k} M_{j,\ell} \partial_j (\partial_i U)(Mx). \tag{S69}$$

This is equal to $(M^\top \nabla^2 U M)_{k,\ell}$. □

Lemma S29. *Under the setting of the preceding lemma, if $U(x) = \sum_{i=1}^n f(x_i)$, then (i) $\nabla^2 U(x) = \mathrm{diag}(u''(x_1), \dots, u''(x_n))$ and (ii) the Laplacian of $F(x) = U(Mx)$ is given by*

$$\Delta F(x) = \sum_{i=1}^{n} (M^\top M)_{i,i} u''(x_i).$$

Proof. The proof of (i) comes from the fact that $\partial_i U(x) = u'(x_i)$, hence $\partial_j \partial_i U(x) = u''(x_i)$ if $i = j$, zero otherwise. The proof of (ii) consists in summing the $k = \ell$ terms in (S69) and using (i). □

For simplicity, let us note $p(x) = \mathrm{e}^{-H(x)}/Z$ where Z_0 is a normalization constant and $H(x) = x^\top K x/2 + V(x)$. Then,

$$\nabla_x p(x) = -\nabla_x H(x), \qquad \nabla_x^2 p(x) = -\nabla_x^2 H(x),$$

and the formula in the left of (S68) comes from the fact that the Hessian of $x^\top K x$ is $2K$.

For the second term, let us first recall that if $\bar{x}_1$ and x_1 are the wavelet coefficients and low-frequencies of x, they are linked by (18). Consequently, the joint density of $(\bar{x}_1, x_1)$ is:

$$q(\bar{x}_1, x_1) = \mathrm{e}^{-H(\gamma G^\top x_1 + \gamma \bar{G}^\top \bar{x}_1)}/Z_1$$

where Z_1 is another normalization constant. The conditional distribution of $\bar{x}_1$ given x_1 is:

$$q(\bar{x}_1 | x_1) = \frac{q(\bar{x}_1, x_1)}{Z_1(x_1)}$$

where $Z_1(x) = \int q(\bar{x}_1, u)\mathrm{d}u$. Consequently,

$$\begin{aligned}\nabla_{\bar{x}_1} \log q(\bar{x}_1|x_1) &= \nabla_{\bar{x}_1}(-H(\gamma G^\top x_1 + \gamma \bar{G}^\top \bar{x}_1) - \log Z_1) - \nabla_{\bar{x}_1} Z_1(x_1) \\ &= -\nabla_{\bar{x}_1} H(\gamma G^\top x_1 + \gamma \bar{G}^\top \bar{x}_1)\end{aligned}$$

and additionally:

$$\nabla^2_{\bar{x}_1} q(\bar{x}_1|x_1) = -\nabla^2_{\bar{x}_1} H(\gamma G^\top x_1 + \gamma \bar{G}^\top \bar{x}_1).$$

The RHS of (S68) then follows from the lemmas in the preceding section.

S9 Experimental Details on CelebA-HQ

Data We use Haar wavelets. The 128×128 original images are thus successively brought to the 64×64 and 32×32 resolutions, separately for each color channel. Each of the 3 channels of x_j and 9 channels of $\bar{x}_j$ are normalized to have zero mean and unit variance.

Architecture Following [38], both the conditional and unconditional scores are parameterized by a neural network with a U-Net architecture. It has 3 residual blocks at each scale, with a base number of channels of $C = 128$. The number of channels at the k-th scale is $a_k C$, where the multipliers $(a_k)_k$ depend on the resolution of the generated images. These multipliers are $(1, 2, 2, 4, 4)$ for models at the 128×128 resolution, $(2, 2, 4, 4)$ for models at the 64×64 resolution, $(4, 4)$ for the conditional model at the 32×32 resolution, and $(1, 2, 2, 2)$ for the unconditional model at the 32×32 resolution. All models include multi-head attention layers in blocks operating on images at resolutions 16×16 and 8×8. The conditioning on the low frequencies x_j is done with a simple input concatenation along channels, while conditioning on time is done through affine rescalings with learned time embeddings at each GroupNorm layer [38, 40].

Training The networks are trained with the (conditional) denoising score matching losses:

$$\ell(\theta_J) = \mathbb{E}_{x_J, t, z}\left[||s_{\theta_J}(t, \mathrm{e}^{-t} x_J + \sqrt{1 - \mathrm{e}^{-2t}} z) - \frac{z}{\sqrt{1 - \mathrm{e}^{-2t}}}||^2\right]$$

$$\ell(\bar{\theta}_j) = \mathbb{E}_{\bar{x}_j, x_j, t, z}\left[||\bar{s}_{\bar{\theta}_j}(t, \mathrm{e}^{-t} \bar{x}_j + \sqrt{1 - \mathrm{e}^{-2t}} z \,|\, x_j) - \frac{z}{\sqrt{1 - \mathrm{e}^{-2t}}}||^2\right]$$

where $z \sim \mathcal{N}(0, \mathrm{Id})$ and the time t is distributed as Tu^2 with $u \sim \mathcal{U}([0, 1])$. We fix the maximum time $T = 5$ for all scales. Networks are trained for 5×10^5 gradient steps with a batch size of 128 at the 32×32 resolution and 64 otherwise. We use the Adam [21] optimizer with a learning rate of 10^{-4} and no weight decay.

Sampling For sampling, we use model parameters from an exponential moving average with a rate of 0.9999. For each number of discretization steps N, we use the Euler-Maruyama discretization with a uniform step size $\delta_k = T/N$ starting from $T = 5$. This discretization scheme is used at all scales. For FID computations, we generate $30,000$ samples in each setting.